

AD/A-002 820

METHOD OF MOMENTS APPLICATIONS.  
VOLUME I - AN INTRODUCTION TO THE METHOD  
OF MOMENTS

A. T. Adams

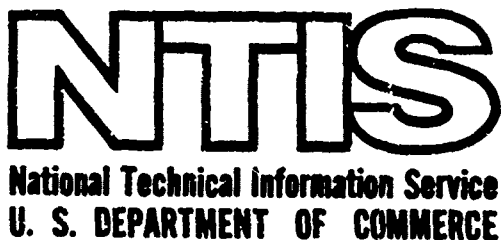
Syracuse University

Prepared for:

Rome Air Development Center

November 1974

DISTRIBUTED BY:



## UNCLASSIFIED

SECURITY CLASSIFICATION OF THIS PAGE (When Data Entered)

REPORT DOCUMENTATION PAGE		READ INSTRUCTIONS BEFORE COMPLETING FORM
1. REPORT NUMBER RADC-TR-73-217, Vol. I (of nine)	2. GOVT ACCESSION NO.	3. RECIPIENT'S CATALOG NUMBER AD/A-002820
4. TITLE (and Subtitle) <b>METHOD OF MOMENTS APPLICATIONS</b> Volume I - An Introduction to the Method of Moments		5. TYPE OF REPORT & PERIOD COVERED Technical (Phase) Report P 73 - Jun 74
7. AUTHOR(s) A.T. Adams		6. PERFORMING ORG. REPORT NUMBER None
9. PERFORMING ORGANIZATION NAME AND ADDRESS Syracuse University Dept. of Electrical and Computer Engineering Syracuse, New York 13210		10. PROGRAM ELEMENT, PROJECT, TASK AREA & WORK UNIT NUMBERS JO 45400132 PE 62702F
11. CONTROLLING OFFICE NAME - ADDRESS Rome Air Development Center (RBCT) Griffiss Air Force Base, New York 13441		12. REPORT DATE November 1974
14. MONITORING AGENCY NAME & ADDRESS (if different from Controlling Office) Same		13. NUMBER OF PAGES 120
16. DISTRIBUTION STATEMENT (of this Report)  Approved for Public Release. Distribution Unlimited.		15. SECURITY CLASS. (of this report) Unclassified
17. DISTRIBUTION STATEMENT (of the abstract entered in Block 20, if different from Report) Same		15a. DECLASSIFICATION/DOWNGRADING SCHEDULE N/A
18. SUPPLEMENTARY NOTES None		
19. KEY WORDS (Continue on reverse side if necessary and identify by block number) Method of Moments Electromagnetic Fields Electrostatics Antennas		
20. ABSTRACT (Continue on reverse side if necessary and identify by block number)  This report is the first volume of the RADC Method of Moments Applications Series. The volumes of this series deal with the application of the method of moments to various practical problems such as antenna coupling, near field prediction, aperture coupling, feedline interference, etc. These problems are of particular interest to antenna system designers and those in the area of electromagnetic compatibility. There is an emphasis in the Applications Series upon experimental verification of effects noted and cross checking of results. (more)		

DD FORM 1 JAN 73 EDITION OF 1 NOV 65 IS OBSOLETE

UNCLASSIFIED

SECURITY CLASSIFICATION OF THIS PAGE (When Data Entered)

UNCLASSIFIED

SECURITY CLASSIFICATION OF THIS PAGE(When Data Entered)

20. ABSTRACT (continued)

This first volume serves the purpose of an introduction to the Method of Moments Applications Series. The basis of the method of moments is outlined and the notation and conventions used throughout the series are introduced. Illustrative examples are presented.

The following volumes of the series have been completed at this time; several other volumes are in preparation:

- Volume I - An Introduction to the Method of Moments
- Volume II - Near Fields of Thin-Wire Antennas
- Volume III - Thin Wire Analysis Program (TWAP) User Manual
- Volume IV - Feedline Interference with Dipole Performance-Theory and Experiment
- Volume V - Thin-Wire Antenna Analysis Computer Codes Compared with Measured Data
- Volume VI - Matrix Methods for Static Microstrip Problems
- Volume VII - Internal Syracuse University Memoranda
- Volume VIII - Aperture Coupling Through Long Slots
- Volume IX - Near and Far Field Thin-Wire Coupling

UNCLASSIFIED

SECURITY CLASSIFICATION OF THIS PAGE(When Data Entered)

ia

METHOD OF MOMENTS APPLICATIONS

Volume I  
An Introduction to the  
Method of Moments

A.T. Adams  
Syracuse University

Approved for Public Release.  
Distribution Unlimited.

## FOREWORD

This is Volume I of a nine-volume technical report prepared by the Department of Electrical and Computer Engineering, Syracuse University, Syracuse, New York, under Contract F30602-72-C-0360, Job Order 45400132, for Rome Air Development Center, Griffiss Air Force Base, New York. Mr. Kenneth R. Siarkiewicz (RBCT) was the RADC Project Engineer.

The report describes work accomplished between February 1973 and June 1974.

This report has been reviewed by the RADC Information Office (OI) and is releasable to the National Technical Information Service (NTIS). At NTIS it will be available to the general public, including foreign nations.

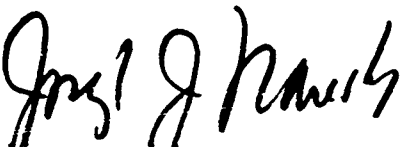
This report has been reviewed and approved for publication.

APPROVED:



KENNETH R. SIARKIEWICZ  
Project Engineer

APPROVED:



JOSEPH J. NARESKY  
Chief, Reliability & Compatibility Division

FOR THE COMMANDER:



CARLO P. CROCETTI  
Chief, Plans Office

## ABSTRACT

This report is the first volume of the RADC Method of Moments Applications Series. The volumes of this series deal with the application of the method of moments [1]-[2] to various practical problems such as antenna coupling, near field prediction, aperture coupling, feedline interference, etc. These problems are of particular interest to antenna system designers and those in the area of electromagnetic compatibility [3]-[4]. There is an emphasis in the Applications Series upon experimental verification of effects noted and cross checking of results.

This first volume serves the purpose of an introduction to the Method of Moments Applications Series. The basis of the method of moments is outlined and the notation and conventions used throughout the series are introduced. Illustrative examples are presented.

The following volumes of the series have been completed at this time; several other volumes are in preparation:

VOLUME 1 - AN INTRODUCTION TO THE METHOD OF MOMENTS

VOLUME 2 - NEAR FIELDS OF THIN-WIRE ANTENNAS

VOLUME 3 - THIN WIRE ANALYSIS PROGRAM (TWAP) USER MANUAL

VOLUME 4 - FEEDLINE INTERFERENCE WITH DIPOLE PERFORMANCE - THEORY AND EXPERIMENT

VOLUME 5 - THIN-WIRE ANTENNA ANALYSIS COMPUTER CODES COMPARED WITH MEASURED DATA

VOLUME 6 - MATRIX METHODS FOR STATIC MICROSTRIP PROBLEMS

VOLUME 7 - INTERNAL SYRACUSE UNIVERSITY MEMORANDA

VOLUME 8 - APERTURE COUPLING THROUGH LONG SLOTS

VOLUME 9 - NEAR AND FAR FIELD THIN-WIRE COUPLING

## TABLE OF CONTENTS

	<b>PAGE</b>
<b>I. THE BASIS OF THE METHOD OF MOMENTS -----</b>	<b>1</b>
1.1. Introduction -----	1
1.2. The Method of Moments for Parallel Straight Thin-Wire Radiators and Scatterers -----	5
1.2.1. General Formulation -----	5
1.2.2. Determination of $Z_{ij}$ For Pulse Expansion Functions and Impulsive Weighting Functions -----	12
1.2.3. The Scattering Problem -----	17
1.2.4. Arbitrary Weighting and Expansion Functions -----	20
1.3 The Method of Moments For Non-Parallel Thin Wires -----	21
<b>II. LOADING AND EXCITATION IN THE METHOD OF MOMENTS -----</b>	<b>24</b>
2.1. Subsection (n-Port) Parameters -----	24
2.2. N-Port Parameters of the Driven or Loaded Subsections -----	27
2.3. The Dual Analysis For Loading -----	29
<b>III. SUMMARY OF METHODS FOR THE DETERMINATION OF AUXILIARY QUANTITIES -----</b>	<b>33</b>
3.1. Introduction -----	33
3.2. Impedance and Admittance Quantities -----	33
3.3. Near and Far Fields -----	34
3.3.1. Radiation Hazards -----	35
3.3.2. Near Field Ellipses -----	35
3.4. Beam Pattern Synthesis -----	35
3.5. Optimization of Radiation Characteristics -----	35
3.6. Aperture Coupling -----	36
3.7. Antenna-to-Antenna Coupling -----	36
3.8. Electrostatic Applications -----	36
<b>IV. SOME APPLICATIONS OF THE METHOD OF MOMENTS FOR THIN WIRES -----</b>	<b>38</b>
4.1. Dipole to Dipole Coupling -----	38
4.2. Near Field Prediction -----	43
4.3. Transmission Line Interference with Dipole Performance -----	56
4.4. Microstrip Applications -----	60
4.5. Aperture Coupling -----	63

TABLE OF CONTENTS (Continued)

	PAGE
V. CONCLUSIONS -----	72
APPENDIX A - JUSTIFICATION OF THE THIN WIRE MODEL-----	73
APPENDIX B - $z_{1j}$ FOR STRAIGHT PARALLEL WIRES WITH PULSE EXPANSION FUNCTIONS AND IMPULSIVE WEIGHTS -----	87
APPENDIX C - SYMMETRY ABOUT THE MAIN DIAGONAL FOR THE MATRICES [z] AND [D]. -----	93
ACKNOWLEDGEMENT -----	98
REFERENCES -----	99

## LIST OF ILLUSTRATIONS

Figure	PAGE
1 - 1 Thin-Wire Antennas -----	6
(a) A Collection of Straight, Parallel, Thin-wire Antennas -----	-----
(b) Fat Dipole Model -----	-----
(c) Filamentary Model -----	-----
(d) Filamentary, Subsectional Model of Antennas in 1-1a -----	-----
1 - 2 Typical Subsections of the Thin-wire Model -----	8
1 - 3 Typical Expansion Functions and Resultant Current Representations -----	9
1 - 4 The Scattering Problem -----	18
1 - 5 Skewed Wires (a) Typical Subsections (b) Skew Angle -----	22
2 - 1 'Typica' Driven, Loaded Subsection (Series Model) -----	25
2 - 2 Typical Driven, Loaded Subsection (Parallel Model) -----	30
4 - 1 Coupling Between Resonant Dipoles Oriented End-to-End -----	39
4 - 2 Coupling Between Quarter-wave Dipoles Oriented End-to-End ----- and Broadside	40
4 - 3 Coupling Between Resonant Dipoles Oriented End-to-End in the Presence of a Parasitic Wire -----	41
4 - 4 Near Fields of a Halfwave Dipole ( $a/\lambda = 0.005$ , $\Delta\ell/\lambda = 0.05$ , $v = 1$ volt, $\lambda = 3m$ .) (a) $E_p$ (b) $E_z$ (c) $H_\phi$ -----	44,45,46
4 - 5 Near Fields of a Resonant Dipole - Theory and Experiment ( $a/\lambda = 0.00503$ , $\ell/\lambda = 0.4484$ , $\Delta\ell/\lambda = 0.02242$ , $\lambda = 3m$ ) (a) $E_p$ (b) $E_z$ -----	48,49
4 - 6 Near Electric Field of an Eight-Element Linear Array of Dipoles ( $\ell/\lambda = 0.5$ , $d/\lambda = 0.5$ , $z = 0$ )-Polar Coordinate Plot (a) Broadside Excitation (b) Endfire Excitation -----	50,51
4 - 7 Near Electric Field of a Uniformly Excited Eight-Element Linear Array of Dipoles ( $d/\lambda = 0.5$ , $z = 0$ )-Rectangular Plot (a) Halfwave Dipoles (b) Hertzian Dipoles -----	53,54
4 - 8 Radiation Hazard Contours in the Principal H-Plane of a Uniformly Excited Eight-Element Linear Array of Dipoles ( $v = 1$ volt, $\ell/\lambda = 0.5$ , $d/\lambda = 0.5$ , $z = 0$ ) -----	55

LIST OF ILLUSTRATION (Continued)

Figure	Page
4 - 9 Near Electric Field of a Two-Element Endfire Array of Resonant Dipoles ( $\ell/\lambda = 0.4484$ , $d/\lambda = 0.5$ , $a/\lambda = 0.00503$ , $\Delta\ell/\lambda = 0.02242$ , $\lambda = 3m$ , $v = + 1$ volt) (a) $y/\lambda = 0.05$ (b) $y/\lambda = 0.03$ -----	57,58
4 - 10 Dipole and Transmission Line -----	59
4 - 11 Cross Polarization Ratio of a Transmission Line and Dipole -----	61
4 - 12 Cross Polarization Ratio of a Transmission Line and Dipole - Theory and Experiment -----	62
4 - 13 Capacitance of a Square Dielectric-Loaded Parallel-Plate Capacitor -----	64
4 - 14 Discontinuity Capacitance for a Sudden Change in Microstrip Width (a) Geometry (b) Capacitance -----	65,66
4 - 15 Characteristic Impedance of a Three-Layer Microstrip -----	67
4 - 16 Equivalent Disk Currents on a Rectangular Grid, Due to a Plane Wave Normally Incident upon a Rectangular Aperture In a Plane Screen, Polarized Parallel to the Short Side ( $E^1 = 1$ volt/meter, $f = 100$ Mhz) -----	69
4 - 17 Fields in a Rectangular Aperture in a Plane Screen, Due to a Plane Wave Normally Incident, Polarized Parallel to the Short side -----	70
4 - 18 Near Fields Beyond a Rectangular Aperture in a Plane Screen, Due To A Plane Wave Normally Incident, Polarized Parallel to the Short Side -----	71
A - 1 A Fat Dipole -----	74
A - 2 A Plane Wave Incident Upon A Conducting Cylinder of Radius "a" and Infinite Length -----	75
A - 3 Two Parallel Conducting Cylinders -----	80
A - 4 $A_1/A_0$ For The Two Wire Problem As A Function Of Spacing -----	82
A - 5 Fourier Coefficients Of The Two Wire Problem (a) $D/2a = 1.05$ , (b) $D/2a = 1.5$ , (c) $D/2a = 5.0$ -----	83,84,85

LIST OF ILLUSTRATIONS (Continued)

Figure	Page
B - 1 Typical Parallel Subsections For Thin-wire Antenna Problems (a) General Location (b) Translation To The Origin -----	88
B - 2 Distance Elements For Parallel Subsections -----	91
C - 1 Two Perpendicular, Thin, Charged Wires -----	94
C - 2 Ratio R ( $D_{ij}/D_{ji}$ ) As A Function Of b/a -----	97

## I - THE BASIS OF THE METHOD OF MOMENTS

### 1.1 INTRODUCTION

There have been several dramatic shifts in the direction of technical fields over the last few decades. This is especially true of the field of electromagnetic theory and its application to radiation and scattering problems. During the last few decades, this field has evolved continuously from one based solidly on the classical theory, but applicable to a narrow range of problems, to one based on the classical theory, but formulated in terms suitable to the computer age and applicable to a wide variety of practical problems.

Electromagnetic problems can be formulated in two alternative ways either as (1) a partial differential equation with boundary conditions, or as (2) an integral equation. During the 1930's and 1940's, emphasis was placed upon the corresponding classical methods of separation of variables and the classical integral equation solutions. A high degree of ingenuity was used to apply these classical methods to practical problems. However, only a narrow range of problems could be treated by these methods. In the method of separation of variables only geometries which coincided with the separable coordinate systems could be treated. One often had to drastically modify a practical problem in order to fit it to a separable geometry. Some of the separable systems were extremely complex mathematically. It is not an exaggeration to say that in some cases years of experience were required for an engineer to effectively utilize a particular coordinate system. However, considering the techniques available, the only practical

approach was to push these limited methods to their utmost, and this was done most effectively during the decades of the 1930's and 1940's.

For the practicing engineer, the classical methods were not, for the most part, completely within his grasp; and furthermore, his problems were much too complex to be reduced to the simple mathematical forms which could be handled by the classical methods. As a result, he had recourse to a "bag of tricks" developed over the years for each particular area of application. In other words, there was a severe "gap" between the simple applications of the classical methods used by researchers and the complex applications confronting the practicing engineer.

During the 1940's and 1950's the gap was closed somewhat by the advent of the variational techniques which were applied first to waveguide and then to radiation problems. Restrictions on the geometry were partially removed. Variational expressions could be found for a wide variety of quantities of interest. However, the evaluation of these expressions was often quite difficult because of the multiple integrals involved.

During the decades of the 1960's and 1970's a new method has emerged which is capable of treating a wide variety of problems. This is the method of moments as outlined by Harrington [1], [2]. This method has proven especially useful because of its wide applicability. The method is conceptually simple, although the detailed methodology may be quite complex. In each case, the defining integral equation is replaced with a matrix equation. The matrix equation may then be solved by any one of a number of techniques, such as matrix inversion.

In the method of moments, prior knowledge of the induced source distribution (charge distribution for static problems and current distribution for

time-varying problems) is not required, and, as a result, complex structures can be treated almost as easily as simple ones. The structure of the antenna or scatterer may be very complex, but the basic method does not change.

Methods of matrix inversion for the solution of problems in electromagnetic theory date back almost a century to Maxwell [5] who used such a method to calculate approximate values of capacitance, and who called the technique "the method of subareas". In the 1950's, Reitan and Higgins [6]-[10] applied the same method to a number of capacitance problems. In the early 1960's, several investigators [11]-[38] applied the method to time-harmonic radiation, scattering and waveguide problems. Harrington [1], [2] unified the subject material and gave it the name "the method of moments".

In the late 1960's and early 1970's there has been a tremendous outpouring of literature on the subject of moment methods. The methods have been applied to an extremely wide variety of problems in electromagnetic theory, including thin-wire radiation and scattering problems, scattering from dielectrics, analysis of waveguides of arbitrary cross section, discontinuity problems in waveguides and microstrip, analysis of lossy structures, propagation over an inhomogeneous earth, antenna beam pattern synthesis, analysis of near fields, analysis of radiation and scattering from bodies of revolution and bodies of arbitrary shape, etc. Many of these were problems which could not be adequately treated heretofore.

The literature on the method of moments is already so large as to preclude a comprehensive bibliography. References [39]-[115] include a partial bibliography of the work done at Syracuse University. Short courses in the method of moments have been offered at the University of Mississippi [116], [117],

the University of Illinois [118], Ohio State University [119], UCLA [120], the University of Naples [121] and the University of Trondheim [122]. The course notes from the University of Illinois are now available in book form [123].

The method of moments permits us to model problems realistically. The boundary conditions are imposed directly and the matrix inversion procedure yields the current distribution which fits the boundary conditions imposed. The principal advantages of the moment methods are flexibility, completeness, accuracy and conceptual simplicity. Arbitrary radiation shapes and arbitrary excitation and loading are permitted. Currents are not assumed but are computed and all mutuals are taken into account. The moment methods have proven to be highly accurate for a wide variety of problems associated with radiation and scattering from thin wires. Since the methods are simple in concept, they are accessible to persons with a wide variety of backgrounds. The principal limitation of the method of moments is associated with the number of unknowns ( $n$ ). Problems of moderate size ( $n \approx 200$  or 300) may be readily treated, but significantly larger systems cannot be adequately treated at present, due to computer core and CPU requirements.

Clearly, the method of moments has taken the antenna/electromagnetic communities by storm. For the first time, we can treat problems "as they exist", with realistic modeling of actual structures. For the first time, we have a single method, capable of being applied to the full range of electromagnetic problems, and capable of being simplified or extended according to requirements of accuracy.

## 1.2 THE METHOD OF MOMENTS FOR PARALLEL STRAIGHT THIN-WIRE RADIATORS AND SCATTERERS

### 1.2.1 GENERAL FORMULATION

In this section the method of moments is introduced for the case of parallel straight thin-wire radiators. Fig. 1-1a shows a collection of  $N$  straight, parallel,  $z$ -directed antennas, excited at arbitrary locations by ideal voltage generators at radian frequency  $\omega$ . First it is desired to compute the current distributions on the antennas. Then, once the unknown currents are determined, other parameters of interest, such as impedances, far fields, near fields, etc. may be determined by further calculation. The currents are, of course, affected by interactions (mutuals) among the various radiators and these must be taken fully into account.

Fig. 1-1b shows a dipole antenna of length  $l$  and radius  $a$ , with surface currents  $J_z$  (longitudinal current),  $J_\phi$  (azimuthal current) and  $J_\rho$  (radial current). In the general radiation or scattering problem the three components of current are all present. Furthermore  $J_z$  and  $J_\phi$  vary with both  $z$  and  $\phi$  and  $J_\rho$  varies with  $\rho$  and  $\phi$ . For thin-wire radiators ( $l \gg a$  and  $a \ll \lambda$ ), circumferential ( $J_\phi$ ) and radial ( $J_\rho$ ) currents may be neglected, the azimuthal variations of  $J_z$  may be neglected, and the surface current  $J_z$  may be replaced with a filamentary model (Fig. 1-1c). The justification of these simplifying assumptions is discussed in Appendix A. It should be noted that the boundary conditions are applied at finite radius "a" so that the finite thickness of the dipole may be taken into account. The voltage source is replaced with an equivalent current source (filament) in the gap region. These foregoing

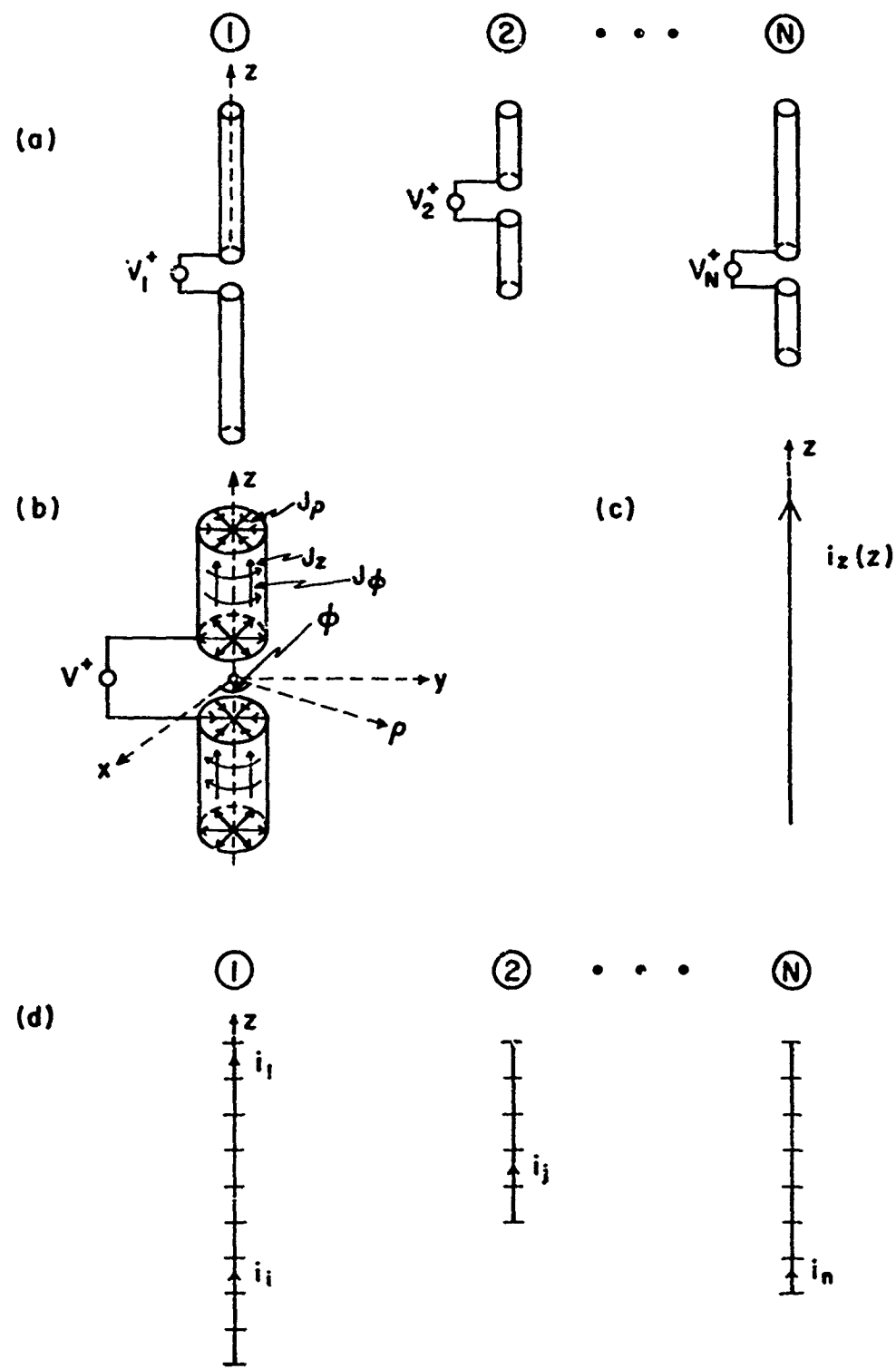


Figure 1-1 Thin-wire Antennas

- (a) A collection of straight, parallel, thin wire antennas
- (b) Fat dipole model
- (c) Filamentary model
- (d) Filamentary, subsectioned model of antennas in 1-1a ....

simplifying assumptions are used throughout this volume.

The rigorous treatment of fat dipoles is considerably more complex. The isolated fat dipole as a radiator or scatterer may be treated by the body-of-revolution methods outlined by Mautz and Harrington [79], [93], [96], [97], [100]. Recently that method has been extended to permit the treatment of parallel fat dipoles [24] as well as the general problem of parallel bodies of revolution.

Thus, the thin-wire antennas of Fig. 1-1a may be represented as filaments, as shown in Fig. 1-1d. The antennas are divided into subsections. The current is unknown, but it is assumed in this section that it is constant over each electrically small subsection. The current on a typical subsection is represented by  $i_j$  where  $i_j$  is a complex number. Fig. 1-2 shows typical subsections  $\Delta l_i$  and  $\Delta l_j$ , with currents  $i_i$  and  $i_j$ , voltages  $v_i$  and  $v_j$ , tangential electric fields  $E_{zi}$  and  $E_{zj}$ , midpoints  $i(x_i, y_i, z_i)$  and  $j(x_j, y_j, z_j)$ , endpoints  $i \pm$  and  $j \pm$ , and with current, voltage, and electric field polarities as indicated.

In general the unknown filamentary current may be designated as  $i(l)$  where  $l$  is a coordinate spanning the filaments. The current  $i(l)$  may be expressed in terms of arbitrary expansion functions as follows:

$$i(l) = \sum_{j=1}^n i_j f_j(l) \quad (1-1)$$

where  $i_j$  are unknown complex numbers and  $f_j$  are known expansion functions. Typical expansion functions and typical resultant current representations are shown in Fig. 1-3. For purposes of this section the  $f_j$  are chosen as pulse functions:

$$f_j(l) = p_j(l) \quad 7 \quad (1-2)$$

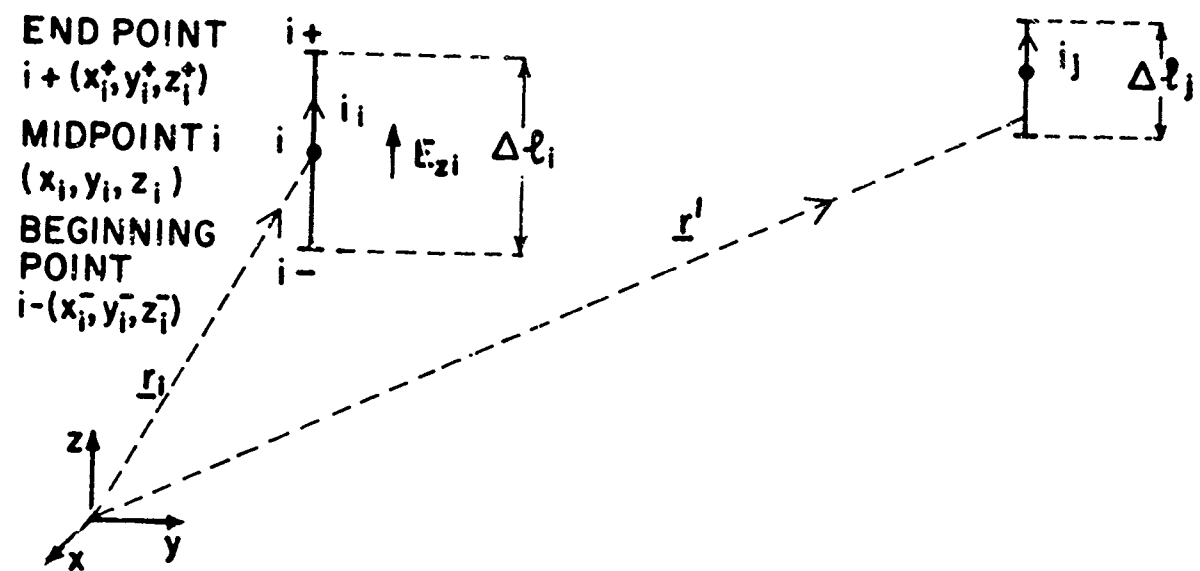


Figure 1-2 Typical subsections of the thin-wire model.

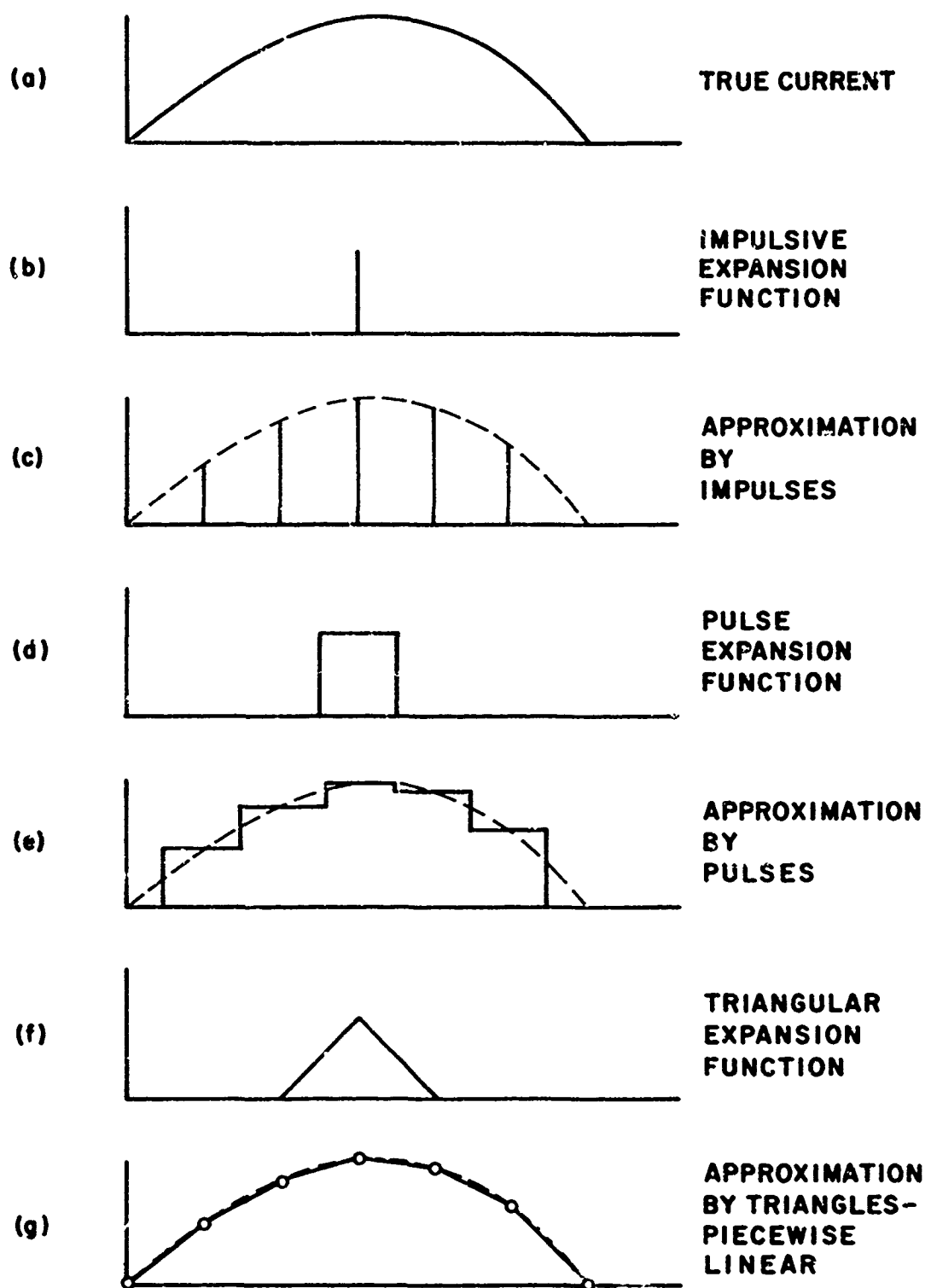


Figure 1-3 Typical expansion functions and resultant current representations

where

$$\begin{aligned} p_j(l) &= 1 && \text{on the } j\text{th subsection} \\ &= 0 && \text{elsewhere} \end{aligned}$$

Note that the antennas need not be center-driven. Antennas with off-center feeds are treated as readily as in the centerfed case. Also, subsection lengths need not be uniform and subsection radii may differ. Note that the gap subsections are represented by current filaments. Essentially the subsections are small enough so that concepts of network theory may be used; any source which applies the proper voltage across the gap is acceptable. The magnitude of the gap currents is unknown, but their effect and the effect of all other currents is to apply the specified voltages across the gaps. We choose current sources rather than voltage sources for simplicity.

Thus, we have reduced the physical problem (Fig. 1-1a) to the model shown in Fig. 1-1d which consists of  $N$  filamentary antennas divided into  $n$  total subsections ( $n > N$ ). For purposes of this section, the current is assumed constant on each subsection. Later in section 1.2.4 the more general representation of the current is discussed in terms of arbitrary expansion and weighting functions.

Now, superposition and linearity may be used to express the relationship between currents and voltages. The voltage across typical subsection  $\Delta l_i$  may be expressed as a sum of the contributions due to all the currents:

$$v_i = i_1 z_{i1} + \dots + i_n z_{in} = \sum_{j=1}^n i_j z_{ij} = 0 \quad (\text{on metallic subsections}) \quad (1-3)$$

$\begin{aligned} &= \text{specified voltages (on driven} \\ &\quad \text{subsections, i.e. gaps)} \end{aligned}$

where  $z_{ij}$  is the voltage\* across subsection  $i$  due to a unit current on subsection  $j$ .

Equation (1-3) is written at each of the  $n$  subsections, leading to a matrix equation

$$[v] = [z][i] \quad (1-4)$$

where  $[v]$  is an  $n$ -element column matrix with zero elements at locations corresponding to metallic subsections and non-zero elements at driven subsections.  $[i]$  is an  $n$ -element column matrix of the complex currents.  $[z]$  is an  $n \times n$  matrix, called the generalized impedance matrix. It represents all the interactions between the  $n$  subsections of the system and may be considered to be the  $n$ -port open-circuit impedance parameters of the system of  $n$  subsections. The impedance matrix  $[z]$  depends only on the geometry of the problem (the locations, orientations, and radii of the various subsections) and the frequency  $\omega$ .

The basic concept of the method of moments is thus very simple involving expansion of the current in subsectional bases, the linearity of the system of Fig. 1-1d and direct application of the boundary conditions. Many other types of problems in electromagnetics also lead to equations of the same general form (Eq. (1-4)). Now it remains to evaluate the typical element  $z_{ij}$  of the matrix  $[z]$ . This is a classical electromagnetic problem, involving the determination of fields due to a given current distribution. In most cases, closed form solutions are not available and  $[z]$  must be determined by approximate methods.

\*The voltage across a subsection may be defined in several different ways corresponding to different weighting functions [1]. The electric field in a given situation is, of course, unique. The simplest definition of voltage would be the product of tangential electric field times subsection length (impulsive weighting function).

### 1.2.2 DETERMINATION OF $z_{ij}$ FOR PULSE EXPANSION FUNCTIONS AND IMPULSIVE WEIGHTING FUNCTIONS.

In this section methods for determining  $z_{ij}$  for parallel wire antennas are outlined and two slightly different computational techniques are described.

Fig. 1-2 shows the basic geometry consisting of two parallel subsections of  $\Delta l_i$  and  $\Delta l_j$ . Note that, from Eq. (1-3),  $z_{ij}$  may be represented as follows

$$z_{ij} = \frac{v_i}{i_j} \quad (\text{with all currents other than } i_j \text{ equal to zero}) \quad (1-5)$$

which corresponds to the usual definition of open-circuit impedance in network theory. Thus,  $z_{ij}$  may be determined from a knowledge of the tangential electric field  $E_{zi}$  and the corresponding voltage  $v_i$  at subsection  $\Delta l_i$ , due to a unit current on subsection  $\Delta l_j$ . Note that

$$v_i = -E_{zi} (\Delta l_i) \quad (1-6)$$

because of the polarities assumed in Fig. 1-2.

The problem is thus the classical one of determining the electric fields due to a filament of current with finite length. Maxwell's equations for the time-harmonic case are:

$$\nabla \times \underline{E} = -j\omega\mu\underline{H} \quad (1-7)$$

$$\nabla \times \underline{H} = j\omega\epsilon\underline{E} + \underline{J} \quad (1-8)$$

The electric and magnetic fields may be expressed in terms of the magnetic vector potential  $\underline{A}$  and the scalar electric potential  $\phi$  where

$$\underline{A} = \mu \iiint_{v'} \frac{\underline{J}(r') e^{-jk|r-r'|}}{4\pi|r-r'|} dv' \quad (1-9)$$

$$\phi = \iiint_v \frac{\rho(\underline{r}') e^{-jk|\underline{r}-\underline{r}'|}}{4\pi\epsilon|\underline{r}-\underline{r}'|} dv' \quad (1-10)$$

where  $\underline{r}$  and  $\underline{r}'$  represent vectors from the origin to field point  $(x, y, z)$  and source point  $(x', y', z')$ , respectively. The volume  $v'$  includes all sources (currents).  $\underline{J}$  is volume current density and  $\rho$  is volume charge density.

Equations (1-9) and (1-10) are obtained from Maxwell's equations and the following assumptions:

$$\underline{B} = \nabla \times \underline{A} \quad (1-11)$$

$$\underline{E} = -j\omega \underline{A} - \nabla \phi \quad (1-12)$$

$$\nabla \cdot \underline{A} = -j\omega \epsilon \mu \phi \quad (1-13)$$

The differential forms of eqs. (1-9) and (1-10) are:

$$(\nabla^2 + k^2) \underline{A} = -\mu \underline{J} \quad (1-14)$$

$$(\nabla^2 + k^2) \phi = -\rho/\epsilon \quad (1-15)$$

The equation of continuity may be represented as

$$\nabla \cdot \underline{J} = -j\omega \rho \quad (1-16)$$

$$\nabla \cdot \underline{J}_s = -j\omega \sigma \quad (1-17)$$

$$\nabla \cdot \underline{I} = -j\omega \lambda \quad (1-18)$$

where  $\underline{J}_s$  and  $\underline{I}$  represent surface and line current density and  $\sigma$  and  $\lambda$  represent surface and line charge density. Note that the subscript  $s$  is omitted in Fig. 1-1b. Eq. (1-17) applies to the actual finite-radius wire model and Eq. (1-18) applies to the filamentary model which is used to compute  $z_{ij}$ . The electric and magnetic fields are now given in terms of  $\underline{A}$  and  $\phi$  by Eqs. (1-11) and (1-12). The electric field may also be expressed in terms of  $\underline{A}$  alone using Eqs. (1-11) and (1-8).

$$\underline{E} = \frac{\nabla \times \underline{V} \times \underline{A}}{j\omega\epsilon\mu} - \frac{\underline{J}}{j\omega\epsilon} \quad (1-19)$$

For straight,  $z$ -directed wires (Fig. 1-1d),  $\underline{J}$  and  $\underline{A}$  are  $z$ -directed and the wave equation (Eq. (1-14)) reduces to

$$(\nabla^2 + k^2)A_z = -\mu J_z \quad (1-20)$$

and the  $z$  component of Eq. (1-19) reduces to

$$E_z = \frac{1}{j\omega\epsilon\mu} \left( -\frac{\partial^2 A_z}{\partial x^2} - \frac{\partial^2 A_z}{\partial y^2} \right) - \frac{J_z}{j\omega\epsilon} \quad (1-21)$$

substituting (1-20) in (1-21) yields

$$E_z = \frac{1}{j\omega\epsilon\mu} \left( \frac{\partial^2}{\partial z^2} + k^2 \right) A_z \quad (1-22)$$

For filamentary currents, Eq. (1-9) reduces to a line integral, i.e.

$$A_z = \mu \int_{\text{wires}} \frac{I_z(z') e^{-jk|\underline{r}-\underline{r}'|}}{4\pi|\underline{r}-\underline{r}'|} dz' \quad (1-23)$$

and the tangential electric field  $E_{zi}$  at arbitrary point  $i$  is

$$E_{zi} = \frac{1}{j\omega\epsilon} \left( \frac{\partial^2}{\partial z_i^2} + k^2 \right) \int_{\text{wires}} \frac{I_z(z') e^{-jk|\underline{r}_i-\underline{r}'|}}{4\pi|\underline{r}_i-\underline{r}'|} dz' \quad (1-24)$$

where  $\underline{r}_i$  is a vector from the origin to the particular field point  $i$  (See Fig. 1-2). Changing the line integral to a summation of integrals over typical subsection  $\Delta l_j$  and substituting Eq. (1-1) with pulse currents (Eq. (1-2)):

$$E_{zi} = \frac{1}{j\omega\epsilon} \left( \frac{\partial^2}{\partial z_i^2} + k^2 \right) \sum_{j=1}^n I_j \int_{\Delta l_j} \frac{e^{-jk|\underline{r}_i-\underline{r}'|}}{4\pi|\underline{r}_i-\underline{r}'|} dz' \quad (1-25)$$

Now if the field point  $i$  is specialized to the center\*  $(x_i, y_i, z_i)$  of typical subsection  $\Delta\ell_i$ , then the voltage  $v_i$  across subsection  $\Delta\ell_i$  may be represented as follows:

$$v_i = -\Delta\ell_i E_{zi} = \sum_{j=1}^n I_j \underbrace{\frac{-\Delta\ell_i}{j\omega\epsilon} \left( \frac{\partial^2}{\partial z_i^2} + k^2 \right) \int_{\Delta\ell_j}^{\Delta\ell_i} \frac{e^{-jk|\underline{r}_i - \underline{r}'|}}{4\pi|\underline{r}_i - \underline{r}'|} dz'}_{z_{ij}} \quad (1-26)$$

and the term in brackets may be identified as the generalized impedance  $z_{ij}$ :

$$v_i = \sum_{j=1}^n z_{ij} I_j \quad (1-27)$$

As index  $i$  assumes values  $1 \dots n$ , the matrix equation

$$[v] = [z][i] \quad (1-28)$$

is obtained.

It is shown in Appendix B (Eq. (B-11)) that  $z_{ij}$  as given in Eq. (1-26) may be represented as follows:

$$z_{ij} = j\omega\mu\Delta\ell_i \Delta\ell_j \psi + \frac{1}{j\omega\epsilon} \frac{\Delta\ell_i \Delta\ell_j}{\Delta z \Delta z} [\psi(\frac{\Delta z'}{2}, \frac{\Delta z}{2}) - \psi(\frac{\Delta z'}{2}, -\frac{\Delta z}{2}) - \psi(-\frac{\Delta z'}{2}, \frac{\Delta z}{2}) + \psi(-\frac{\Delta z'}{2}, -\frac{\Delta z}{2})] \quad (1-29)$$

where

$$\psi = \frac{1}{\Delta\ell_j} \int_{\Delta\ell_j}^{\Delta\ell_i} \frac{e^{-jk|\underline{r}_i - \underline{r}'|}}{4\pi|\underline{r}_i - \underline{r}'|} dz' \quad (1-30)$$

\*As noted previously, boundary conditions are applied at finite radius "a". This is especially important in computing the self impedance  $z_{ii}$  and is less important if subsection  $\Delta\ell_i$  is distant from subsection  $\Delta\ell_j$ . Thus the finite wire radius is taken into account even though a filamentary current model is used.

and  $\psi(+\Delta z'/2, -\Delta z/2)$  represents  $\psi$  of Fig. 1-2 with subsection  $\Delta \ell_j$  shifted as  $\Delta z'/2$  upwards, and subsection  $\Delta \ell_j$  shifted as  $\Delta z/2$  downwards, etc.  $\Delta z'$ ,  $\Delta z$  represent increments used for numerical differentiation. If these increments are chosen equal to corresponding subsection lengths ( $\Delta z' = \Delta \ell_j$ ,  $\Delta z = \Delta \ell_i$ ), then Eq. (1-29) becomes

$$z_{ij} = j\omega\mu\Delta \ell_i \Delta \ell_j \psi + \frac{1}{j\omega\epsilon} [\psi(+,+) - \psi(+,-) - \psi(-,+) + \psi(-,-)] \quad (1-31)$$

where  $\psi(+,-)$  represents  $\psi$  of Fig. 1-2 with subsection  $\Delta \ell_j$  shifted  $\Delta \ell_j/2$  upwards and subsection  $\Delta \ell_i$  shifted  $\Delta \ell_i/2$  downwards, etc.  $\psi$  may be evaluated by methods given in [1], [2]. Eq. (1-31) agrees with Eq. (22) of [3] derived under different assumptions: pulse expansion functions for both charges and currents. Thus the two methods lead to an identical formulation if the increments  $\Delta z$ ,  $\Delta z'$  used for evaluating derivatives are subsection lengths.

Thus the antenna problem of Fig. 1a has been reduced to a set of linear equations which can be solved by standard techniques for such systems. The crux of the problem is to determine the generalized impedance matrix  $[z]$  which represents all the interactions among the current-carrying subsections. Note that  $[z]$  depends only on the geometry of the problem.  $[z]$  is, in effect, the open circuit impedance matrix of an  $n$ -port system consisting of the  $n$  subsections. The matrix  $[z]$  is independent of excitation and loading. Any subsection of the antenna system may be opened up and excited with a voltage generator or loaded with a complex impedance, without changing the matrix  $[z]$ . The effects of loading are explained in more detail in section two.

### 1.2.3 THE SCATTERING PROBLEM

Consider the scattering problem shown in Fig. 1-4 which shows a known field  $\underline{E}^{(inc)}$  incident upon a collection of straight, parallel thin wires which have been replaced with filamentary models. The wires have been divided into  $n$  subsections as before.

The boundary conditions are now applied to the total tangential electric field  $E_{zi}$  at the center of each wire subsection.

$$\text{Let } \underline{E} = \underline{E}^{(s)} + \underline{E}^{(inc)} \quad (1-32)$$

where  $\underline{E}^{(inc)}$  is the known incident field and  $\underline{E}^{(s)}$  is the field radiated by the current-carrying wires.

Taking the  $z$  component of Eq. (1-32) and specializing the field point to the center of subsection  $\Delta\ell_i$ :

$$E_{zi} = E_{zi}^{(s)} + E_{zi}^{(inc)} \quad (1-33)$$

Define incident, scattered, and total voltages as follows:

$$v_i^{(inc)} = -E_{zi}^{(inc)} \Delta\ell_i \quad (1-34a)$$

$$v_i^{(s)} = -E_{zi}^{(s)} \Delta\ell_i \quad (1-34b)$$

$$v_i = -E_{zi} \Delta\ell_i \quad (1-34c)$$

and let  $[v^{(inc)}]$ ,  $[v^{(s)}]$ , and  $[v]$  be the corresponding column matrices of subsection voltages.

The scattered field  $E_{zi}^{(s)}$  may be evaluated by Eqs. (1-29) - (1-31) since the field  $E_{zi}^{(s)}$  desired is that due to radiating wires, as before.

$$E_{zi}^{(s)} = -\frac{1}{\Delta\ell_i} \sum_{j=1}^n i_j z_{ij} \quad (1-35)$$

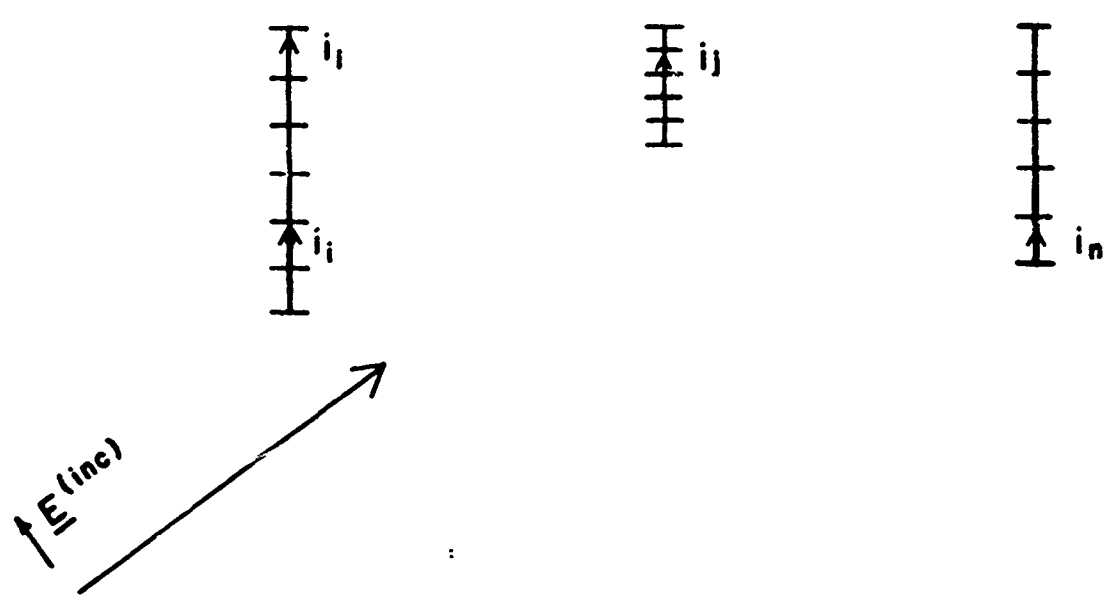


Figure 1-4 The scattering problem

and writing Eq. (1-35) at the center of each subsection yields a matrix equation

$$[v^{(s)}] = [z][i] \quad (1-36)$$

The equivalent of Eq. (1-33) is

$$[v] = [v^{(s)}] + [v^{(inc)}] \quad (1-37)$$

which becomes, for metallic scatterers,

$$[v] = 0 = [v^{(s)}] + [v^{(inc)}] \quad (1-38)$$

or

$$[-v^{(inc)}] = [z][i] \quad (1-39)$$

where the typical element of  $[-v^{(inc)}]$  is  $E_{zi}^{(inc)}(\Delta\ell_i)$ . Eq. (1-39) may be solved by matrix inversion (or other techniques) for the unknown wire currents  $[i]$ .

The scattering problem is thus reduced to the matrix equation (1-39) which is similar in form to the matrix equation (1-28) except that the left hand side of (1-28), the voltage excitation matrix, has been replaced with the negative of the incident voltages. The reason for the sign reversal is, of course, tied in with the distinction between scattered, incident, and total fields.  $[z]$  includes all interactions among subsections of the scatterers and is thus identical to the  $[z]$  matrix which would be used to analyze the radiation properties of this system of conductors (the radiation properties of the system of Fig. 4 excited and loaded at one or more subsections). Note that the incident or impressed field may be that of a plane wave, a spherical wave or any other type of wave. The basic assumption is that the source of the wave is an independent source (not affected by the scattered radiation from the wires).

#### 1.2.4 ARBITRARY WEIGHTING AND EXPANSION FUNCTIONS

In sections 1.2.1 and 1.2.2 the current has been assumed constant over each subsection (pulse expansion function). Fig. 1-3 indicates that better approximations to the current are obtained with more sophisticated expansion functions. Moreover, point-matching has been used in sections 1.2.1 and 1.2.2, i.e., the boundary conditions have been applied at specific points (subsection centers). The tangential electric field is zero at the center of each metallic subsection, but there is no control over its value at intermediate points between subsection centers. A more sophisticated application of the boundary conditions would be to set an average or weighted average of the tangential field equal to zero at metallic subsections in radiation problems.

Consider the electric field  $E_{zi}$  due to currents on the wires of Fig. 1-1 as given by Eq. (1-24):

$$E_{zi} = \frac{1}{j\omega\epsilon} \left( \frac{\partial^2}{\partial z_i^2} + k^2 \right) \int_{\text{wires}} \frac{I_z(z') e^{-jk|\underline{r}_i - \underline{r}'|}}{4\pi|\underline{r}_i - \underline{r}'|} dz'$$

let  $I(z') = \sum I_j f_j(z)$ , as in Eq. (1-1) where the  $f_j$  are arbitrary expansion functions, and let  $w(z)$  be an arbitrary (weighting) function. Substituting in Eq. (1-24):

$$E_{zi} = \sum_{j=1}^n I_j \frac{1}{j\omega\epsilon} \left( \frac{\partial^2}{\partial z_i^2} + k^2 \right) \int_{\Delta \ell_j} \frac{f_j(z') e^{-jk|\underline{r}_i - \underline{r}'|}}{4\pi|\underline{r}_i - \underline{r}'|} dz' \quad (1-40)$$

Multiplying both sides of Eq. (1-40) by  $w(z)$  and integrating over subsection

$\Delta \ell_i$ :

$$\int_{\Delta \ell_i} E_{zi} w(z) dz = \sum_{j=1}^n I_j \int_{\Delta \ell_i} \frac{w(z)}{j\omega\epsilon} \left( \frac{\partial^2}{\partial z_i^2} + k^2 \right) dz \int_{\Delta \ell_j} \frac{f_j(z') e^{-jk|\underline{r}_i - \underline{r}'|}}{4\pi|\underline{r}_i - \underline{r}'|} dz' \quad (1-41)$$

Interchanging the order of differentiation and integration:

$$\int_{\Delta l_i} E_{zi} w(z) dz = \sum_{j=1}^n I_j \int_{\Delta l_i} \int_{\Delta l_j} \frac{1}{j\omega\epsilon} \left( \frac{\partial^2}{\partial z_i^2} + k^2 \right) \frac{f_j(z') w(z) e^{-jk|\underline{r}_i - \underline{r}'|}}{4\pi |\underline{r}_i - \underline{r}'|} dz' dz \quad (1-42)$$

$z_{ij}$

now  $\int_{\Delta l_i} E_{zi} w(z) dz$  is defined as voltage  $v_i$ , the double integral on the right hand side of Eq. (1-42) is defined as the generalized impedance  $z_{ij}$ , and

Eq. (1-42) becomes

$$v_i = \sum_{j=1}^n z_{ij} I_j$$

which in turn becomes

$$[v] = [z][i] \quad (1-43)$$

as  $i$  runs through the indices  $1 - n$ .

Note that the voltage definition has been generalized and now represents a weighted integral of the electric field. If  $w(z)$  is an impulse and  $f_j(z')$  is a pulse function, then Eq. (1-42) reduces to Eq. (1-26). A further generalization of Eq. (1-42) may be made by replacing the integrals with inner products [1].

### 1.3 THE METHOD OF MOMENTS FOR NON-PARALLEL THIN WIRES

The development of sections 1.2.1 and 1.2.2 may be extended to non-parallel (skewed) wires (Fig. 1-5). This involves replacement of  $(\partial^2/\partial z^2 + k^2)$  with the operator  $(\nabla \times \nabla \times)$  and the use of various trigonometric relationships. The development is laborious but straightforward. Details of the development for pulse expansion functions are given in the literature [110].

The result for  $z_{ij}$  is

$$z_{ij} = -\frac{1}{j\omega\epsilon} \left[ (k^2 \Delta l_i \Delta l_j) \cos \theta_{ij} \psi - [\psi(+,+) - \psi(-,+) - \psi(+,-) + \psi(-,-)] \right] \quad (1-44)$$

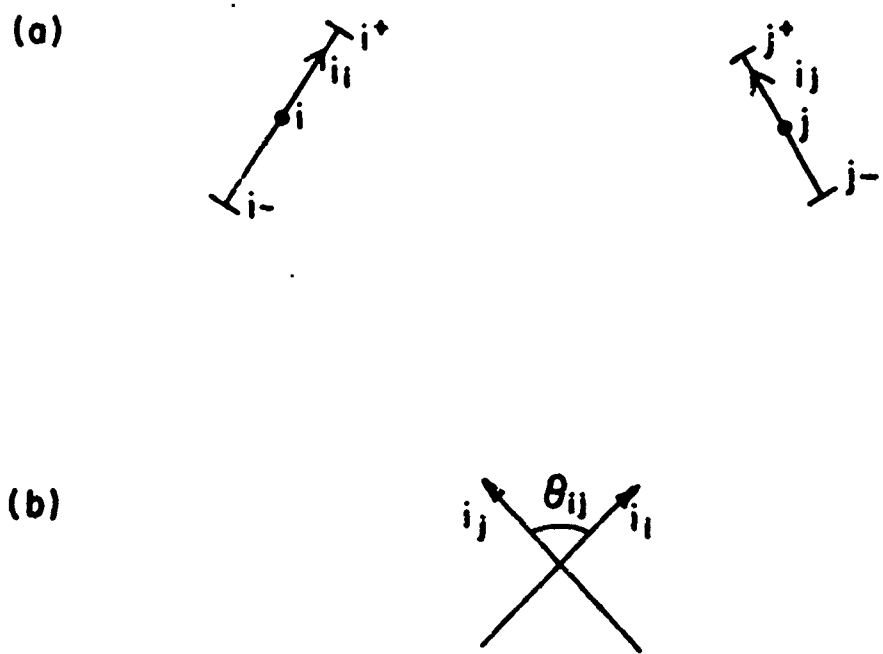


Figure 1-5 Skewed wires (a) typical subsections (b) skew angle

where  $\theta_{ij}$  is the skew angle and  $\psi(+,-)$  represents  $\psi$  of Fig. 1-5a with subsection  $\Delta\ell_j$  shifted  $\Delta\ell_j/2$  towards  $j+$  (so that its center is now at  $j+$ ) and with subsection  $\Delta\ell_i$  shifted  $\Delta\ell_i/2$  towards  $i-$  (so that its center is now at  $i-$ ) etc. The corresponding developments for triangular expansion functions [98], [105] and for sinusoidal expansion functions [125]-[128] are also given in the literature.

## II - LOADING AND EXCITATION IN THE METHOD OF MOMENTS

In this chapter the effects of excitation and loading of subsections are considered. Several different methods for treating loads are outlined.

### 2.1 SUBSECTION (n-PORT) PARAMETERS

Consider a collection of thin-wire antennas such as that shown in Fig. 1-1. The antennas are subsectioned and it is assumed that the subsections are small electrically, i.e.  $\frac{\Delta l}{\lambda} \ll 1$ , where  $\Delta l$  is subsection length. It is assumed that there are  $n$  total subsections, as in Fig. 1-1d, and that  $N$  subsections are excited and/or loaded.

Figure 2-1 shows a typical subsection  $\Delta l_i$  driven with an applied voltage  $v'_i$  and loaded with a lumped impedance element  $z'_{li}$ .  $v'_i$  and  $z'_{li}$  represent the Thevenin's equivalent circuit of the devices and loads attached to subsection  $\Delta l_i$ . Since the subsections are small electrically, the response of the system of antennas to the excitation and loading does not depend on the fine details of the generators and load construction, but only on the values of the applied voltage  $v'_i$  and load  $z'_{li}$ . As far as terminal behavior is concerned, the electromagnetic problem becomes a network problem. The application of boundary conditions leads to the matrix equation

$$[v] = [z][i] \quad (2-1)$$

and the equations of constraint

$$[v] = [v'] - [z_i][i] \quad (2-2)$$

where

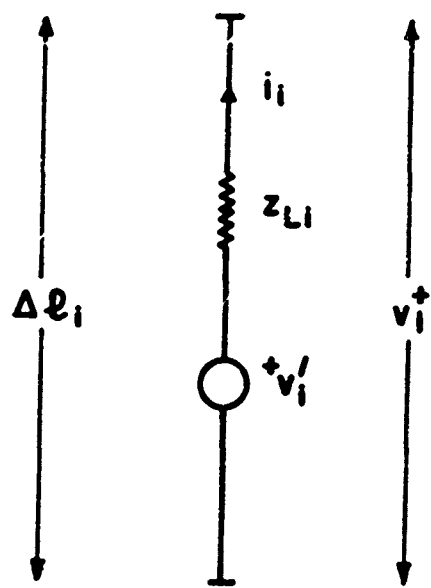


Figure 2-1 A typical driven, loaded subsection (series model)

$$[v] = \begin{bmatrix} v_1 \\ \vdots \\ v_n \end{bmatrix}, \quad [v'] = \begin{bmatrix} v'_1 \\ \vdots \\ v'_n \end{bmatrix}, \quad [i] = \begin{bmatrix} i_1 \\ \vdots \\ i_n \end{bmatrix},$$

$$[z] = \begin{bmatrix} z_{11} & \cdots & z_{1n} \\ \vdots & \ddots & \vdots \\ z_{nl} & \cdots & z_{nn} \end{bmatrix} \quad \text{and} \quad [z_\ell] = \begin{bmatrix} z_{\ell 1} \\ \vdots \\ \text{○} \\ \text{○} \\ \vdots \\ z_{\ell n} \end{bmatrix}$$

Combining (1) and (2):

$$[v] = \begin{bmatrix} v'_1 - z_{\ell 1} & i_1 \\ v'_2 - z_{\ell 2} & i_1 \\ \vdots & \vdots \\ v'_n - z_{\ell n} & i_n \end{bmatrix} = \begin{bmatrix} z_{11} & \cdots & z_{1n} \\ \vdots & \ddots & \vdots \\ z_{nl} & \cdots & z_{nn} \end{bmatrix} \begin{bmatrix} i_1 \\ \vdots \\ i_n \end{bmatrix}$$

transposing terms  $-z_{\ell k} i_k$  yields

$$[v'] = \begin{bmatrix} v'_1 \\ v'_2 \\ \vdots \\ v'_n \end{bmatrix} = \begin{bmatrix} (z_{11} + z_{\ell 1}) & z_{12} & \cdots & z_{1n} \\ z_{21} & (z_{22} + z_{\ell 2}) & \ddots & \vdots \\ \vdots & \vdots & \ddots & \vdots \\ z_{nl} & \cdots & \cdots & (z_{nn} + z_{\ell n}) \end{bmatrix} \begin{bmatrix} i_1 \\ \vdots \\ i_n \end{bmatrix}$$

$$\text{or } [v'] = [[z] + [z_\ell]] [i] = [z'_\ell] [i] \quad (2-3)$$

$$\text{where } [z'_\ell] = [z] + [z_\ell]$$

Solving for the currents:

$$[i] = [z'_\ell]^{-1} [v'] = [y'_\ell] [v'] \quad (2-4)$$

where

$$[y'_\ell] = [z'_\ell]^{-1}$$

and then the total voltages  $[v]$  may be determined by Eq. (2-2). Note that the effect of loading is merely to replace matrix  $[z]$  with  $[[z] + [z_L]]$  and  $[v]$  with  $[v']$ .

In Eq. (2-2), zeros occur on the left hand side if the total voltage across a subsection is zero. In Eq. (2-3), zeros occur on the left hand side only if the applied voltage is zero. Thus, if a subsection is loaded but not driven, a zero would occur in the appropriate element of  $[v']$ . All problems involving loading and excitation may be treated by the above formulation. However, in some cases a simpler matrix equation may be used. These special cases are described in sections 2.2 and 2.3.

## 2.2 N-PORT PARAMETERS OF THE DRIVEN OR LOADED SUBSECTIONS

The addition or changing of a load changes all the currents and, as a result, the near and far fields. In order to determine these quantities, then, we need to invert a new  $n \times n$  matrix as in Eq. (2-4). If, however, we are concerned only with behavior at the  $N$  driven and/or loaded ports, such as port voltages, port currents, coupling from one port to another, etc., then the inversion of an  $N$  by  $N$  matrix is sufficient.

$$\text{Let } [y] = [z]^{-1} \quad (2-5)$$

From the larger  $n \times n$   $[y]$  matrix, the terms corresponding to the  $N$  driven ports are selected to form an  $N$ -port short circuit admittance matrix denoted by  $[Y]$  (see [3], [54], [129]). The  $N$ -Port open circuit impedance matrix, denoted by  $[Z]$ , is the inverse of  $[Y]$ .

$$[Z] = [Y]^{-1} \quad (2-6)$$

and the voltages and currents at the  $N$  driven and/or loaded ports are related by

$$[v] = [Z][I] \quad (2-7)$$

and the appropriate equation of constraint is

$$[V] = [V'] - [Z_\ell][I] \quad (2-8)$$

where

$$[V] = \begin{bmatrix} V_1 \\ \vdots \\ \vdots \\ V_N \end{bmatrix}, \quad [V'] = \begin{bmatrix} V'_1 \\ \vdots \\ \vdots \\ V'_N \end{bmatrix}, \quad [I] = \begin{bmatrix} I_1 \\ \vdots \\ \vdots \\ I_N \end{bmatrix},$$

$$[Z] = \begin{bmatrix} Z_{11} & \cdots & \cdots & Z_{1N} \\ \vdots & & & \vdots \\ \vdots & & & \vdots \\ Z_{N1} & \cdots & \cdots & Z_{NN} \end{bmatrix} \quad \text{and} \quad [Z_\ell] = \begin{bmatrix} Z_{\ell 1} & & & \\ \vdots & \ddots & & \\ \text{O} & & \ddots & \\ \text{O} & & & Z_{\ell N} \end{bmatrix}$$

Note that in Eqs. (2-1) and (2-2), the  $n$ -port parameters are denoted by lower case letters and in Eqs. (2-7) and (2-8) the  $N$ -port parameters of the driven subsections are denoted by upper case letters. Combining Eqs. (2-7) and (2-8) yields

$$[V'] = [[Z] + [Z_\ell]] [I] = [Z'_\ell][I] \quad (2-9)$$

where

$$[Z'_\ell] = [Z] + [Z_\ell]$$

which is solved by matrix inversion

$$[I] = [Z'_\ell]^{-1} [V'] = [Y'_\ell] [V'] \quad (2-10)$$

where

$$[Y'_\ell] = [Z'_\ell]^{-1}$$

The total voltages may then be obtained from Eq. (2-7). Comparing Eqs. (2-4) and (2-10), it is noted that

$$y'_{\ell ij} = y_{\ell ij} \quad (2-11)$$

for those ports  $i, j$  which are loaded and/or driven. Thus the matrix  $[Y_L]$  may be formed by selecting appropriate elements of  $[y_\ell]$ , as is the case with  $[Y]$  and  $[y]$ .

### 2.3 THE DUAL ANALYSIS FOR LOADING

Fig. 2-2 shows the Norton's equivalent circuit of the devices and loads attached to subsection  $\Delta\ell_1$  where  $I'_1$  represents short circuit current and  $y'_{\ell i}$  represents the admittance seen when the current generator is deactivated.

Now we may write the following matrix relationships between currents and voltages at the  $n$  subsections:

$$[i] = [i'] - [y_\ell][v] \quad (2-12)$$

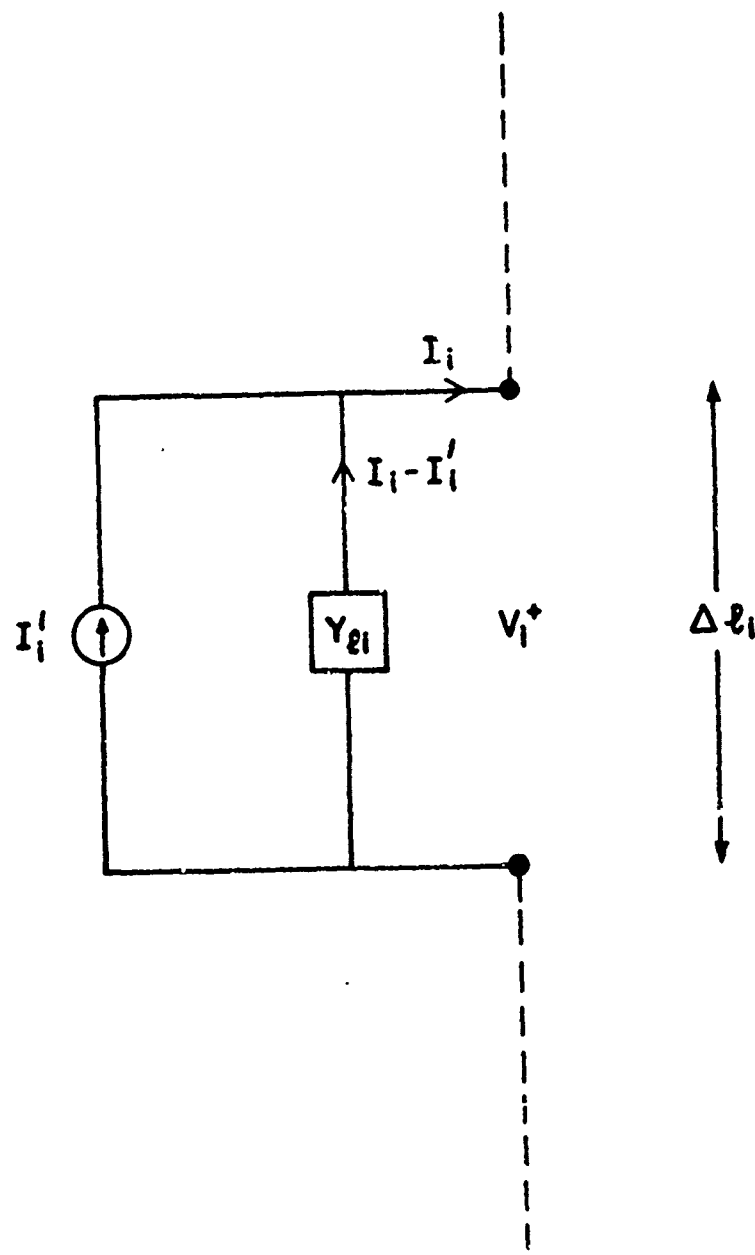
$$[i] = [y][v] \quad (2-13)$$

where

$$[i'] = \begin{bmatrix} v'_1/z_{\ell 1} \\ \vdots \\ \vdots \\ v'_n/z_{\ell n} \end{bmatrix} \quad (2-14)$$

$$[y_\ell] = \begin{bmatrix} y_{\ell 1} & & & \\ & \ddots & & \\ & & y_{\ell 2} & \\ & & & \ddots & \\ & & & & y_{\ell n} \end{bmatrix} = [z_\ell]^{-1} \quad (2-15)$$

and  $[y] = [z]^{-1}$  as in Eq. (2-5)



$$I_i' = V_i' / Z_{si} = Y_{si} V_i'$$

Figure 2-2 A typical driven, loaded subsection (parallel model).

Then, transposing terms in (2-13)

$$[i'] = [[v] + [y_\ell]] [v] = [v'_{\ell D}] [v] \quad (2-16)$$

and

$$[v] = [y'_{\ell D}]^{-1} [i'] = [z'_{\ell D}] [i'] \quad (2-17)$$

where the subscript D indicates a dual quantity. Once the specified driving voltages  $[v']$  are known, then  $[i']$  may be determined from (2-14),  $[v]$  may be determined from (2-17), and  $[i]$  may then be determined from (2-13). Note that  $[y'_{\ell D}]$ ,  $[z'_{\ell D}]$  are not necessarily equal to  $[y'_\ell]$ ,  $[z'_\ell]$ .

Similarly, the following dual relationships may readily be developed for the N-Port analysis:

$$[I'] = [[Y] + [Y_\ell]] [V] = [Y'_{\ell D}] [V] \quad (2-18)$$

$$[V] = [Y'_{\ell D}]^{-1} [I'] = [Z'_{\ell D}] [I'] \quad (2-19)$$

and  $[I] = [I'] - [Y_\ell] [V] \quad (2-20)$

where

$$[I'] = \begin{bmatrix} v'_1/z_{\ell 1} \\ v'_2/z_{\ell 2} \\ \vdots \\ \vdots \\ v'_N/z_{\ell N} \end{bmatrix},$$

$$[Y_\ell] = \begin{bmatrix} Y_{\ell 1} & & & \\ & \ddots & & \\ & & \ddots & \\ & & & Y_{\ell N} \end{bmatrix} = [Z_\ell]^{-1}$$

In chapter two, the effects of loading for a system of n subsections have been considered. Mathematically, the effect is merely to replace the

generalized ( $n \times n$ ) impedance matrix  $[z]$  with  $[z] + [z_L]$  where  $[z_L]$  is a diagonal load matrix, and to replace  $[v]$ , the total voltage excitation matrix, with  $[v']$ , the applied voltage excitation matrix. The terminal behavior (terminal voltages and currents) at driven and/or loaded ports may be described by an  $N \times N$  matrix equation where  $N$  is the total number of such ports. Finally, the dual formulation for loading is described.

### III - SUMMARY OF METHODS FOR THE DETERMINATION OF AUXILIARY QUANTITIES

#### 3.1 INTRODUCTION

In sections one and two, the matrix equation (1-28) and its related forms (1-39), (2-3), (2-16) have been considered as the basic formulation of the radiation or scattering problem, from which the currents may be determined. In this short section, the determination of other quantities of interest is described briefly and references are given for more complete descriptions.

#### 3.2 IMPEDANCE AND ADMITTANCE QUANTITIES

Once the currents and voltages are known for a given system, input impedances at a driven port are given simply by the ratio of voltage to current at that port. The input impedance at any subsection of the system may thus be determined by opening up the subsection and exciting it with a voltage generator. The input impedance may also be determined directly from  $[z]$  and  $[z_g]$ .

Consider an antenna system such as that of Fig. 1d consisting of  $n$  total subsections. Suppose that  $N$  subsections are driven and/or loaded. The open-circuit impedance matrix and the short circuit admittance matrix of the  $N$ -port system can be readily obtained from  $[z]$ . First  $[y]$  is obtained by inverting  $[z]$ . Then the elements  $y_{ij}$  are selected, where both  $i$  and  $j$  are members of the  $N$ -port system (driven and/or loaded ports), to form an  $N \times N$  matrix  $[Y]$  (See [3], [54], [129]). This matrix  $[Y]$  is the short-circuit admittance matrix of the  $N$ -port system, and its inverse  $[Z]$

is the open-circuit impedance matrix. If  $N$  is much smaller than  $n$ , it may be convenient to utilize  $[Y]$  and  $[Z]$  to establish the terminal behavior for different excitations. Any of the other common network parameters, such as the scattering matrix, ABCD parameters, etc., may also, of course, be obtained from  $[Y]$ ,  $[Z]$ .

### 3.3 NEAR AND FAR FIELDS

Once the currents are known, the near and far fields may be obtained by further matrix operations. The near fields are, of course, considerably more complicated than the far fields. At a point in the near field, there are in general three components of  $\underline{E}$  and three components of  $\underline{H}$ . The electric and magnetic vectors at a point trace out independent polarization ellipses in time [130]. However, the basic information is available from the matrix  $[z]$ . Since  $z_{ij}$  is proportional to the electric field (in a given direction) at field point  $i$ , due to the current on subsection  $j$ , one need only sum over all subsections to obtain one component of  $\underline{E}$  at near field point  $i$ . The other components of  $\underline{E}$  are obtained in a like manner and the three components of  $\underline{H}$  are obtained by numerical differentiation of the  $\psi$  functions. Details of the near field procedure are given in [71], [73], [83], [85], [89], [98], [104], [105], [110], [125]-[128], [130]-[134].

The far field computation represents merely a specialization of  $z_{ij}$  to the far field case. The far fields are obtained simply by summing the contributions of all subsections (See [3] for details). Directive gain may be obtained by an integration of the far field beam pattern.

### 3.3.1 Radiation Hazards

Radiation hazards may be evaluated at a point in the near field by considering all complex components of the near fields [130]. The computer program described in [73] has a subroutine which computes radiation hazards in the near field of a collection of thin-wire antennas or scatterers.

### 3.3.2 Near Field Ellipses

Once the six complex components of E and H are known at a near field point, the description of the near field ellipses may readily be obtained [130]. Complete information on the near field E and H ellipses (ellipticity, plane of the ellipse, orientation of the major axis) is provided by a subroutine of the computer program described in [73].

## 3.4 BEAM PATTERN SYNTHESIS

Beam pattern synthesis can be utilized in conjunction with matrix methods. Given an array of  $N$  antennas with  $N$  feed points, one may specify  $N$  points of the far field beam pattern and then determine the required  $N$  voltage excitations at the feed points. One may also specify the beam pattern at more than  $N$  points and find the  $N$  voltage excitations for least square error with respect to the specified pattern. The beam pattern may also be synthesized subject to other constraints. Details on synthesis procedures are given in [46], [87], [151].

## 3.5 OPTIMIZATION OF RADIATION CHARACTERISTICS

Many of the typical performance characteristics of an antenna system, such as gain, efficiency and quality factor, may be optimized with or without constraints. For instance, given a system of  $N$  antennas, with  $N$

feed points, one may readily obtain the value of the maximum gain in a given direction, and the required voltage excitations (at the  $N$  feed points) which produce that gain. Details of the optimization procedures are given in [1], [3], [54], [108].

### 3.6 APERTURE COUPLING

Electromagnetic coupling through apertures in plane screens may be evaluated by the method of moments. Babinet's principle is employed to transform the problem to one of scattering by the complementary disk. For infinitely long slots, the problem simplifies and may be treated accurately for slots of considerable width ( $< 10\lambda$ ). The surface of the complementary disk is modeled exactly in this case. For apertures of arbitrary shape, and of moderate area ( $\leq$  one square wavelength), the complementary disk may be modeled approximately as a wire grid. Then the usual thin-wire methods may be applied to compute such quantities as aperture fields, fields radiated beyond the aperture, transmission coefficient, etc.

### 3.7 ANTENNA-TO-ANTENNA COUPLING

Antenna-to-antenna coupling may, of course, be evaluated directly once all loads have been taken into account and all currents and voltages on the wire structures are known. The power out of a driven section and the power absorbed by a loaded subsection may be evaluated directly in terms of the subsection current and voltage.

### 3.8 ELECTROSTATIC APPLICATIONS

The method of moments may be applied to electrostatic problems. The details of the development for electrostatics are given in [39], [40]. The

excitations are the static voltages applied to a system and the response is, for instance, the unknown induced charge distribution. The charge-bearing surfaces are divided into subsections and appropriate expansion functions for the unknown charge distributions are assumed. A matrix equation of the form

$$[V] = [D][\sigma] \quad (3-1)$$

results, where  $[V]$  is a column matrix representing the voltage excitation,  $[\sigma]$  is a column matrix representing the unknown induced charges, and  $[D]$  is a square matrix representing the interactions among subsections.  $D_{ij}$ , for instance, may represent the potential at subsection  $i$  due to a unit charge on subsection  $j$ . Various electrostatic calculations may be carried out, such as the determination of capacitance and resistance, and the evaluation of electric fields and potentials [49], [39], [40]. The method of moments has been used extensively in connection with the evaluation of the static properties of microstrip transmission lines.

#### IV - SOME APPLICATIONS OF THE METHOD OF MOMENTS FOR THIN WIRES

The method of moments may be applied to a wide variety of antenna and scattering problems. Examples of computed and experimental data for representative problems are presented in this section. Most of the examples presented represent phenomena which could not in the past be adequately treated.

##### 4.1 DIPOLE-TO-DIPOLE COUPLING

One may compute the coupling between any two thin-wire antennas, using the method of moments and the formulation of section two. Coupling is defined here as the ratio of output power to input power.

K. Siarkiewicz has made an extensive theoretical and experimental study of dipole-to-dipole coupling [135]-[137]. Figs. 4-1 to 4-3 show some typical results of this study.\* Fig. 4-1 shows computed and experimental data for the coupling between two resonant parallel dipoles oriented end-to-end as shown in Fig. 4-1. One dipole is centerfed and the other is centerloaded with  $50\Omega$ . Dipole radius is  $0.0119\lambda$  and dipole length is  $0.48\lambda$ . Note that the loaded antenna is located at a beam-pattern null of the driven antenna. Only the radial component  $E_r$  of the electric field, which falls off as  $1/r^2$ , contributes to coupling. Accordingly, the coupling approaches a 12 db/octave asymptote. The experimental data shows reasonably good agreement with the predicted results. There is a small periodic experimental error present, which arises from ground reflections, as explained later. The magnitude of the error increases with spacing  $d$ .

Fig. 4-2 shows computed data for dipole-to-dipole coupling for  $\lambda/4$  dipoles arranged (a) end-to-end and (b) broadside. Dipole radius is

\* The ratio of output to incident power is plotted in Figs. 4-1 to 4-3. This differs from coupling if the input reflection coefficient is nonzero.

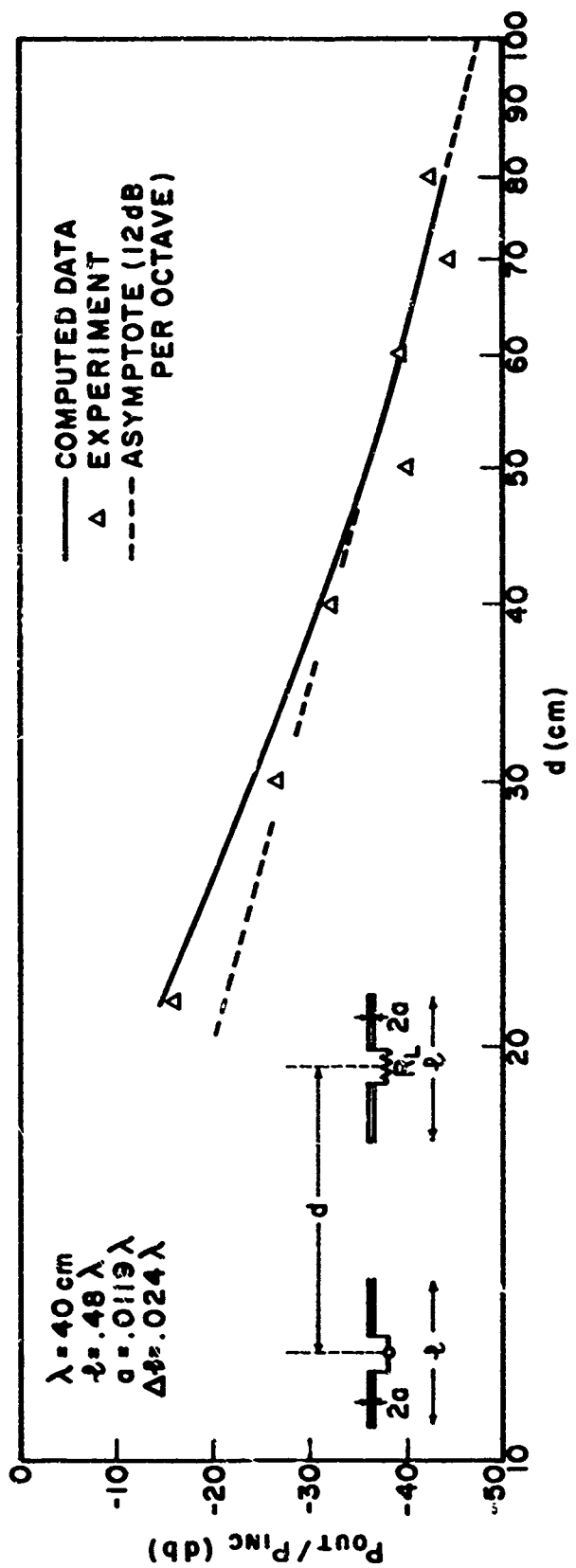


Figure 4-1 Coupling between resonant dipoles oriented end-to-end.

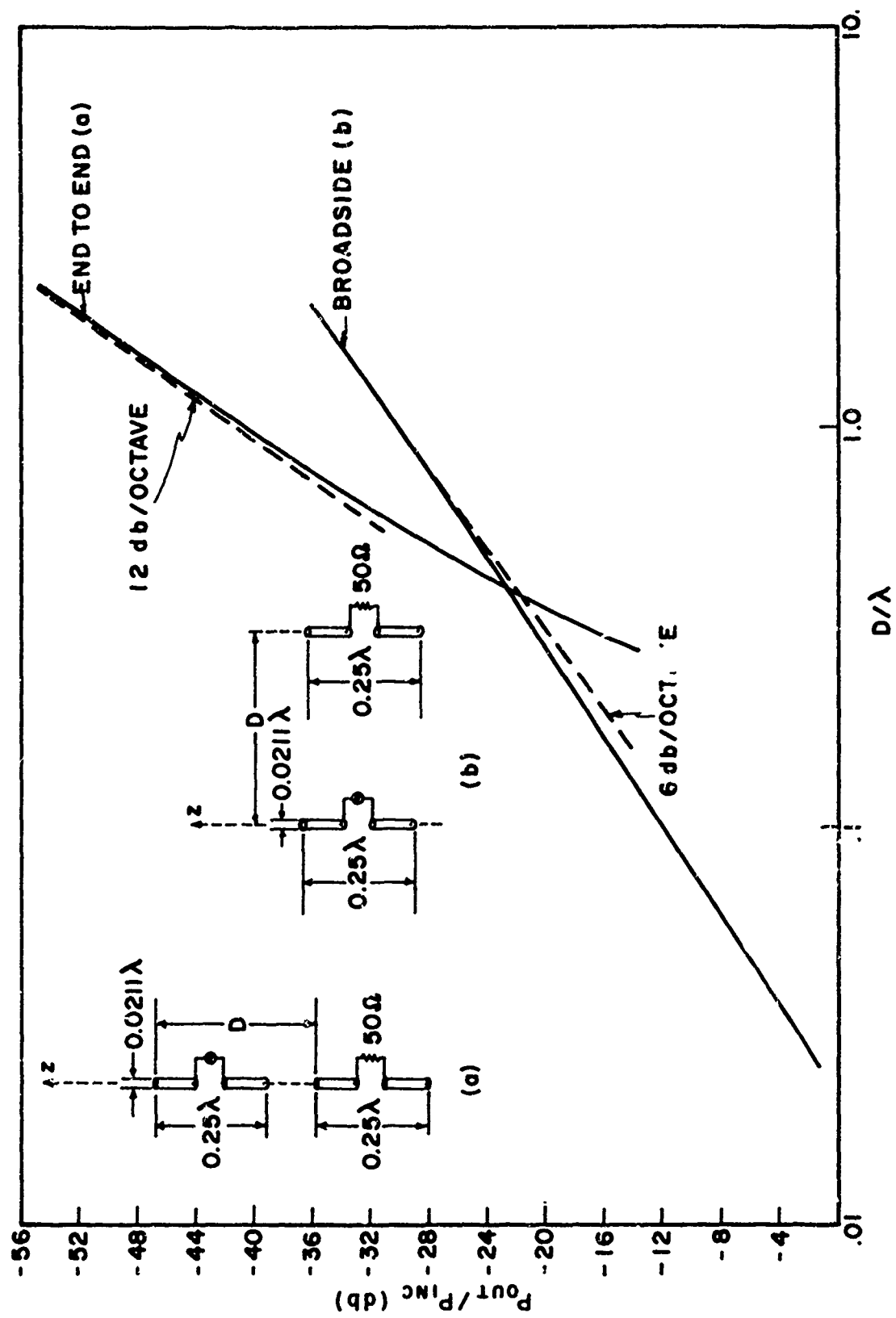


Figure 4-2 Coupling between quarter-wave dipoles oriented end-to-end and broadside.

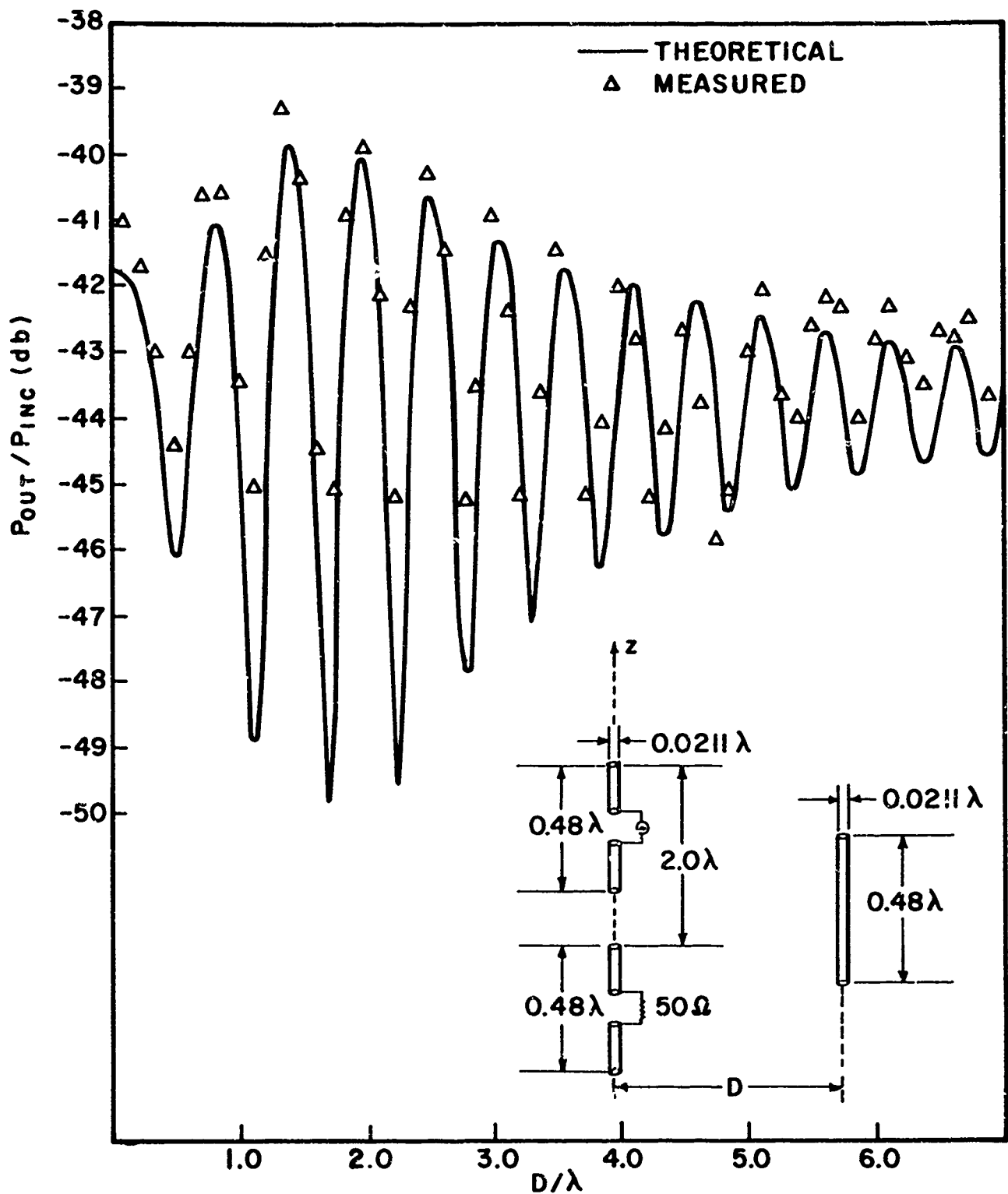


Figure 4-3 Coupling between resonant dipoles oriented end-to-end in the presence of a parasitic wire.

$0.01055\lambda$ . The end-to-end case approaches a 12 db/octave asymptote, whereas the broadside case approaches a 6 db/octave asymptote. Note that for very small values of  $D/\lambda$ , the coupling in the end-to-end case actually exceeds that of the broadside case.

Coupling in the presence of parasitic wires may also be accurately predicted by moment methods. Fig. 4-3 shows two resonant-length dipoles, arranged end-to-end, with a resonant parasitic element located nearby. In effect, there are two coupling paths, one direct and one by way of the parasitic element. Both the currents on the driven element and those on the parasite contribute to coupling. As spacing  $D$  is varied, the two contributions, which are nearly equal in magnitude, add for some spacings and partially cancel for others, giving rise to the oscillatory coupling effect shown in Fig. 4-3. The measured data shows excellent agreement, except near the nulls. Note that both the positions and values of the peaks in coupling are accurately predicted, despite the rapid oscillation as a function of  $D/\lambda$ . A small experimental error due to ground reflections is believed to be responsible for the departure near the nulls. One would not, of course, expect good agreement near the nulls if there were any reflections present. The experimental error caused by ground reflections increases with increasing  $D/\lambda$ .

The experiments for Figs. 4-1 and 4-3 were performed by elevating the dipoles about  $15\lambda$  above a concrete floor. Small reflections from the floor produce interference at the deep nulls of Fig. 4-3 and also give rise to the small periodic experimental error shown in Fig. 4-1. As separation of the dipoles increases, the level of the reflected signal becomes more

significant with respect to the direct signal. Thus experimental errors increase with dipole separation, as indicated in Figs. 4-1 and 4-3.

Siarkiewicz has shown [135] that, for parallel dipoles on a common ground plane, coupling may be accurately predicted by a simple empirical formula. He has also shown that, for electrically small dipoles, coupling cannot be accurately measured (special corrections which utilize theoretical data are required). More complete information on coupling computations is included in references [135]-[137] and in a forthcoming volume of the Method of Moments Applications Series.

#### 4.2 NEAR-FIELD PREDICTION

The study of near fields has been of interest to antenna engineers for many years. It has been a difficult study because of the generally complex nature of the near-field structure. Even for thin-wire antennas, there are only a few specific cases that have been studied in detail. However, interest in such problems is high because of the number of relatively high-power wire and rod antennas and high-gain arrays in use and because of concern over possible associated radiation hazards and compatibility problems.

The near fields of individual dipoles and linear dipole arrays have been studied in some detail and some of the results are shown in Figs. 4-4 to 4-9. Fig. 4-4 shows the near electric and magnetic fields of a center-fed halfwave dipole of a radius  $a = 0.007\lambda$ . Voltage excitation is one volt and frequency is 100 MHz. Fig. 4-4a shows the radial component  $E_r$  of the electric field, as computed by two different techniques of the method of moments. Method 1 uses pulse expansion functions and method 2 uses triangular expansion functions. The computer programs are described respectively

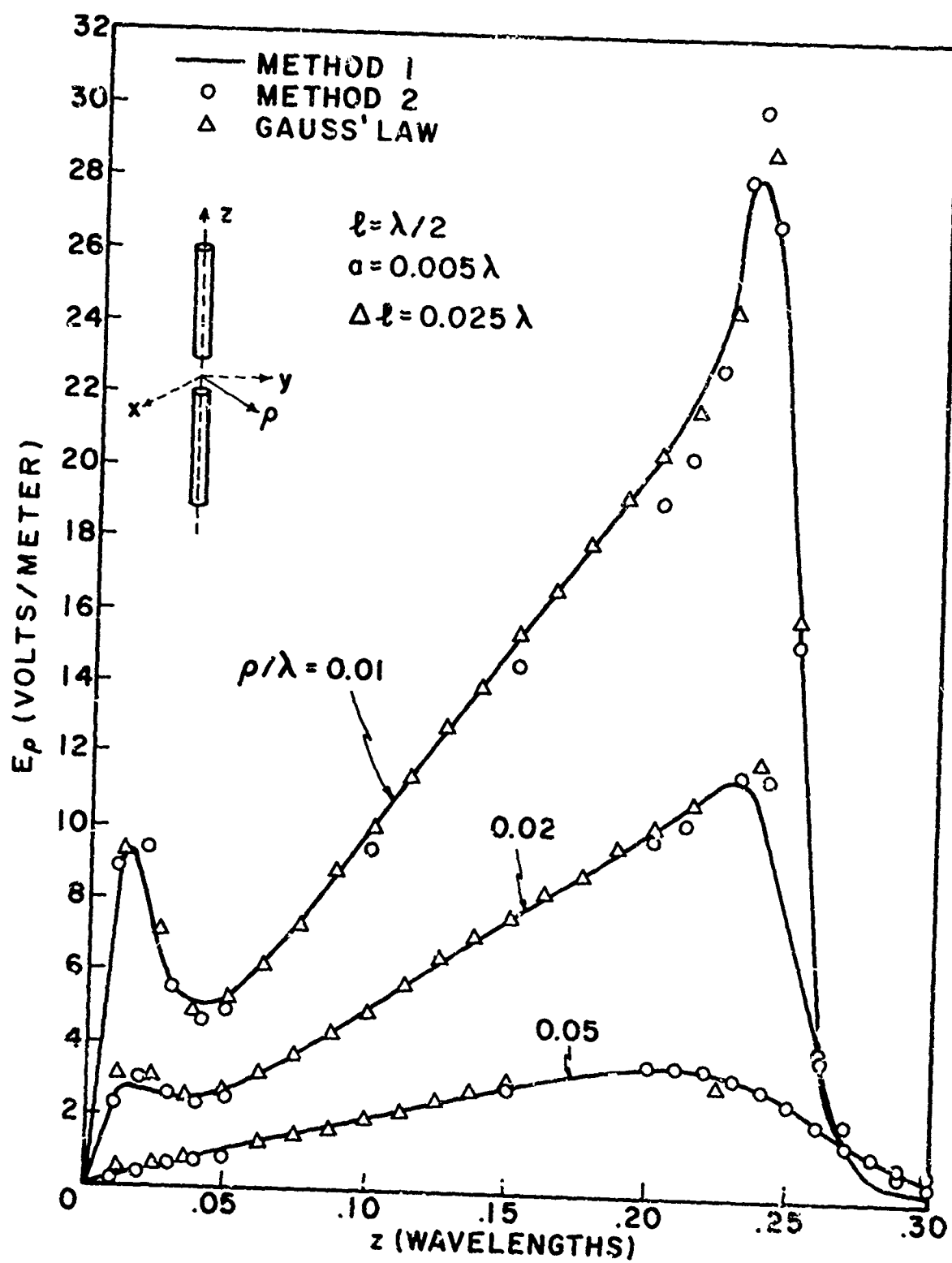


Figure 4-4a Near fields  $E_\rho$  of a halfwave dipole ( $a/\lambda = 0.005$ ,  $\Delta z/\lambda = 0.05$ ,  $V = 1$  volt,  $\lambda = 3$ m).

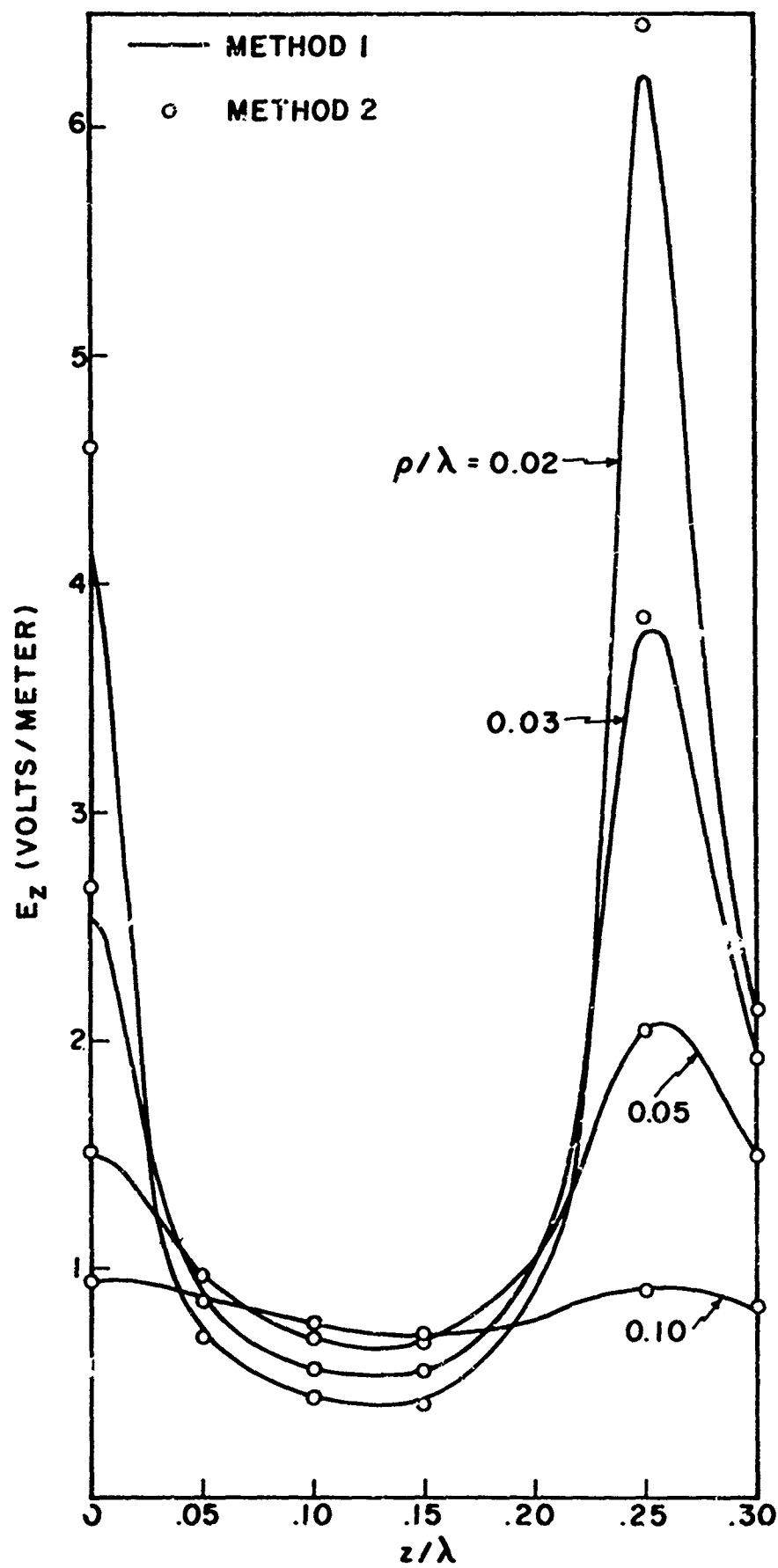


Figure 4-4b Near fields  $E_z$  of a halfwave dipole ( $a/\lambda = 0.005$ ,  $\Delta\ell/\lambda = 0.05$ ,  $V = 1$  volt,  $\lambda = 3$ m).

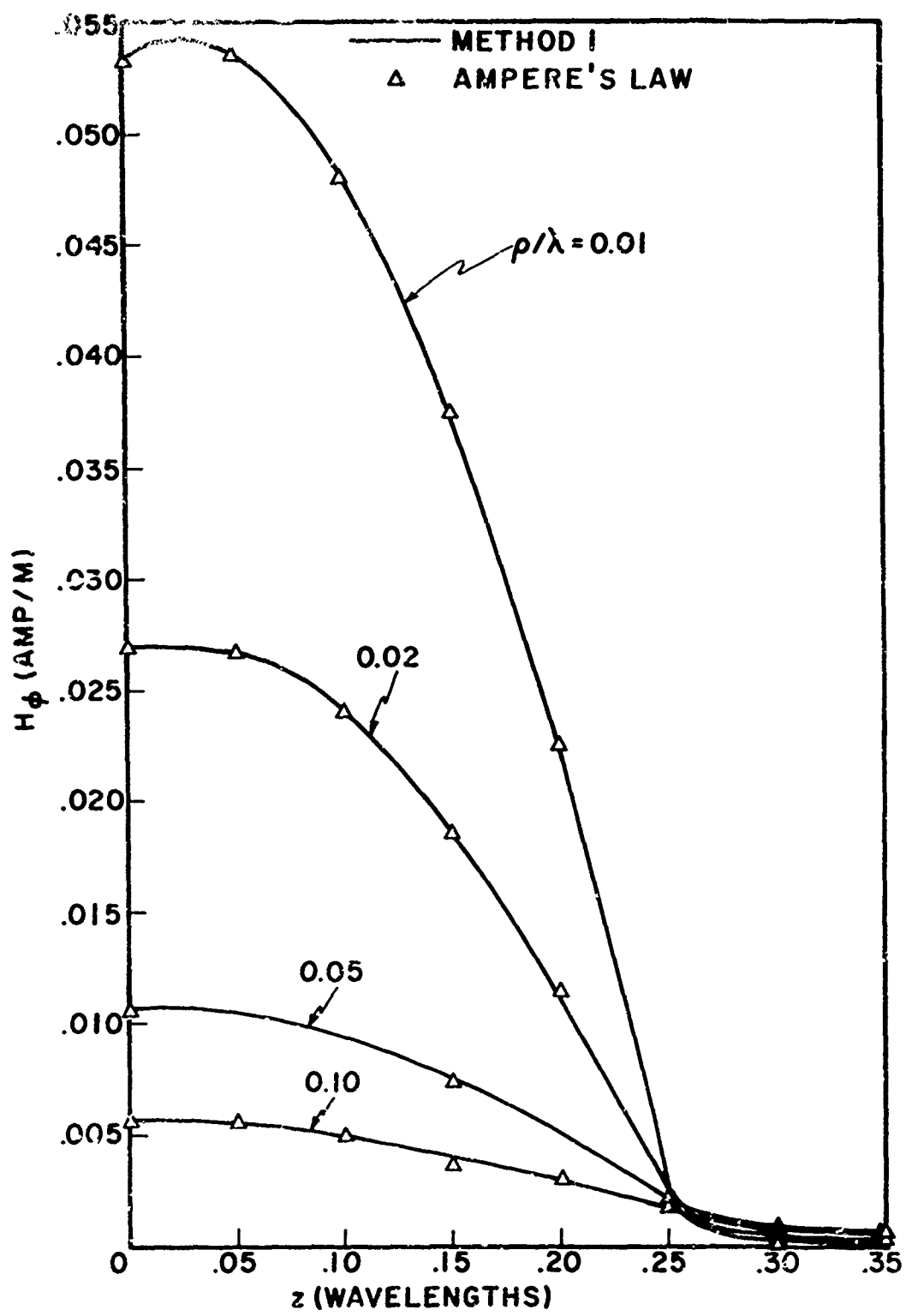


Figure 4-4c Near fields  $H_\phi$  of a halfwave dipole ( $a/\lambda = 0.005$ ,  $\Delta\ell/\lambda = 0.05$ ,  $V = 1$  volt,  $\lambda = 3$ m).

in references [73], [69]. Also shown in Fig. 4-4a is an approximate calculation of near fields from current distributions, based on a generalized Gauss' law formulation [71]. Note the excellent agreement among the three different methods, even at distances as close as  $0.01\lambda$  (for  $a/a = 2$ ).  $E_p$  has peaks near the gaps and near the ends of the dipole. In the central region ( $z \approx 0.125\lambda$ ),  $E_p$  has a  $(1/p)$  dependence on  $p$ . Methods 1 and 2 diverge slightly near the ends of the dipole and this is expected because of the difference in expansion functions. Fig. 4-4b shows the tangential component  $E_z$  of the electric field as computed by methods 1, 2.  $E_z$  has approximately a  $\ln(p/a)$  dependence in the central region ( $z = 0.125\lambda$ ). Fig. 4-4c shows the magnetic field component  $H_p$ , as compared with an approximate calculation of near fields from current distribution, based on a generalized Ampere's law formulation [71].  $H_p$  has approximately a  $1/p$  dependence. The data shown in Fig. 4-4 have also been compared with other results in the literature. The computed data on near fields  $E_p$ ,  $E_z$ ,  $H_p$  show very close agreement with Harrison et al. [138] for  $p = 0.05\lambda$ . The data for  $E_z$  lies between those of King and Wu [139]-[141] and Galejs [142] for  $p < 0.05\lambda$ .

Fig. 4-5 shows a comparison of dipole near-field computation with experimental results. A third technique of the method of moments, that of ref. [127], with sinusoidal expansion functions, is added. Figs. 4-5a, b show data for  $E_p$ ,  $E_z$  respectively at  $p = 0.03\lambda$ . Even at this close spacing, the agreement among computational methods and between theory and experiment is excellent.

Fig. 4-6 shows the near electric field of an eight-element linear array of centered halfwave dipoles with halfwave spacing. Fig. 4-6a shows the

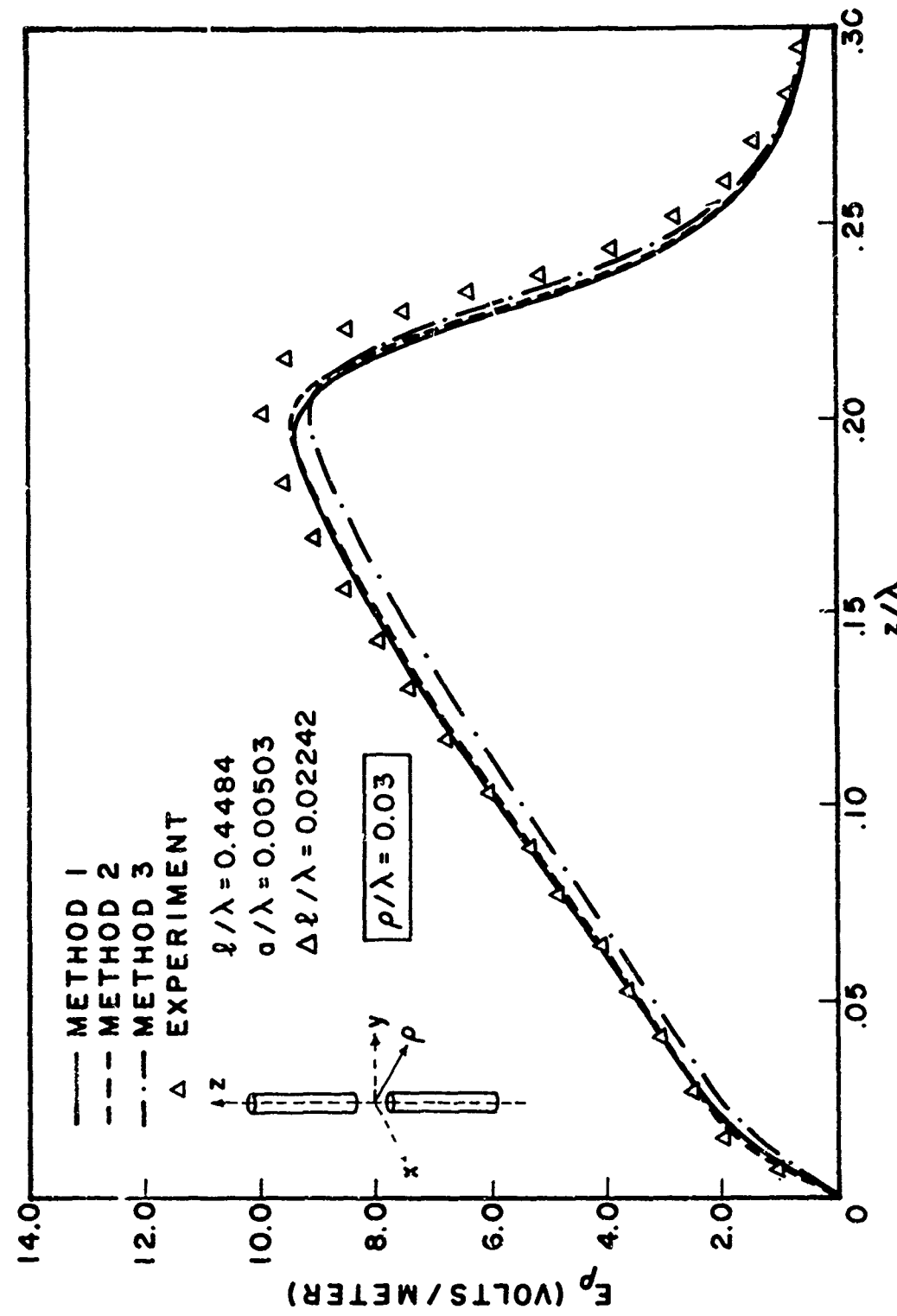


Figure 4-5a Near fields  $E_p$  of a resonant dipole - theory and experiment  
 $(a/\lambda = 0.00503, l/\lambda = 0.04484, \Delta l/\lambda = 0.02242, \lambda = 3\text{m})$ .

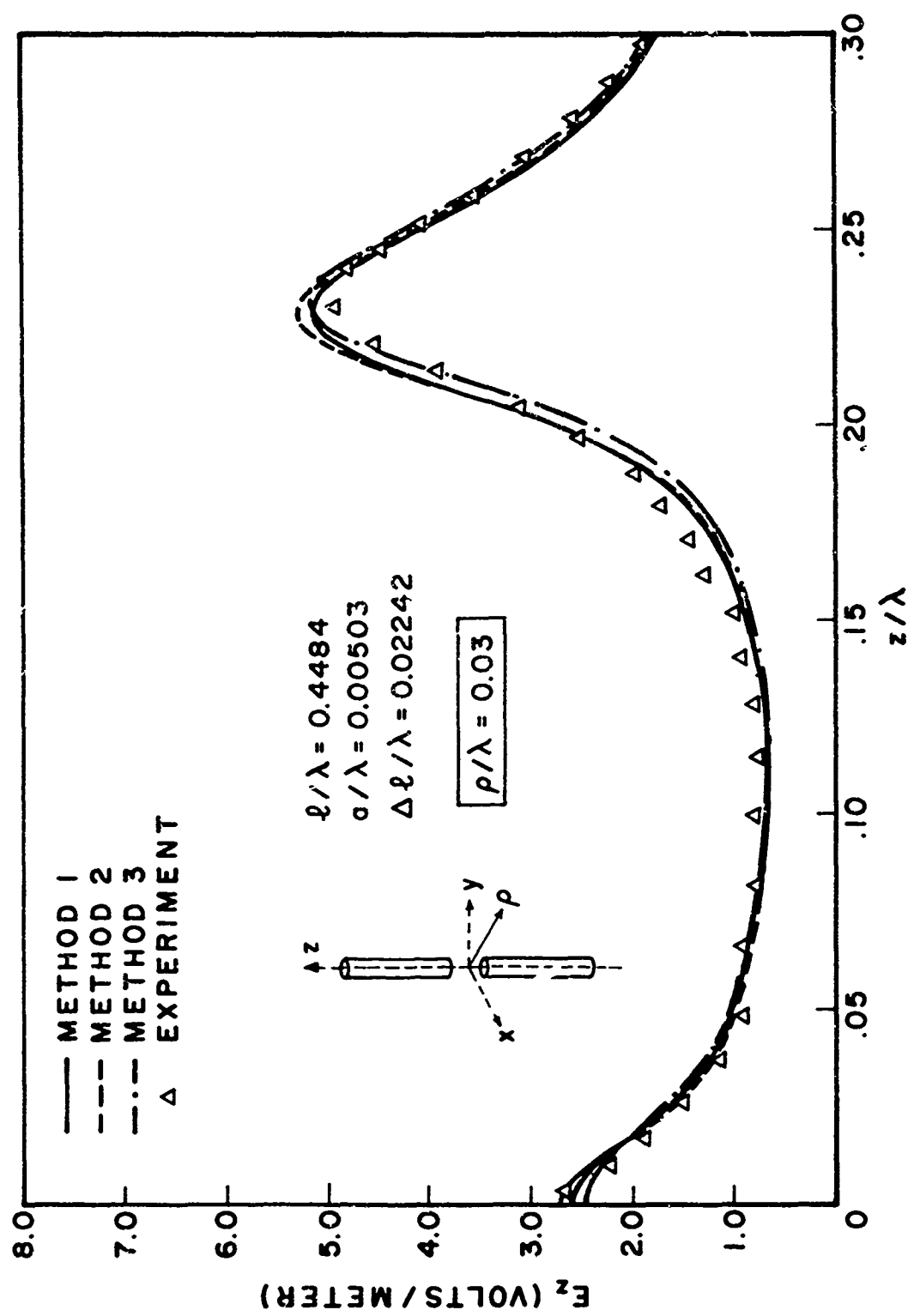


Figure 4-5b Near fields  $E_z$  of a resonant dipole - theory and experiment  
 $(a/\lambda = 0.00503, l/\lambda = 0.4484, \Delta l/\lambda = 0.02242, \lambda = 3m)$ .

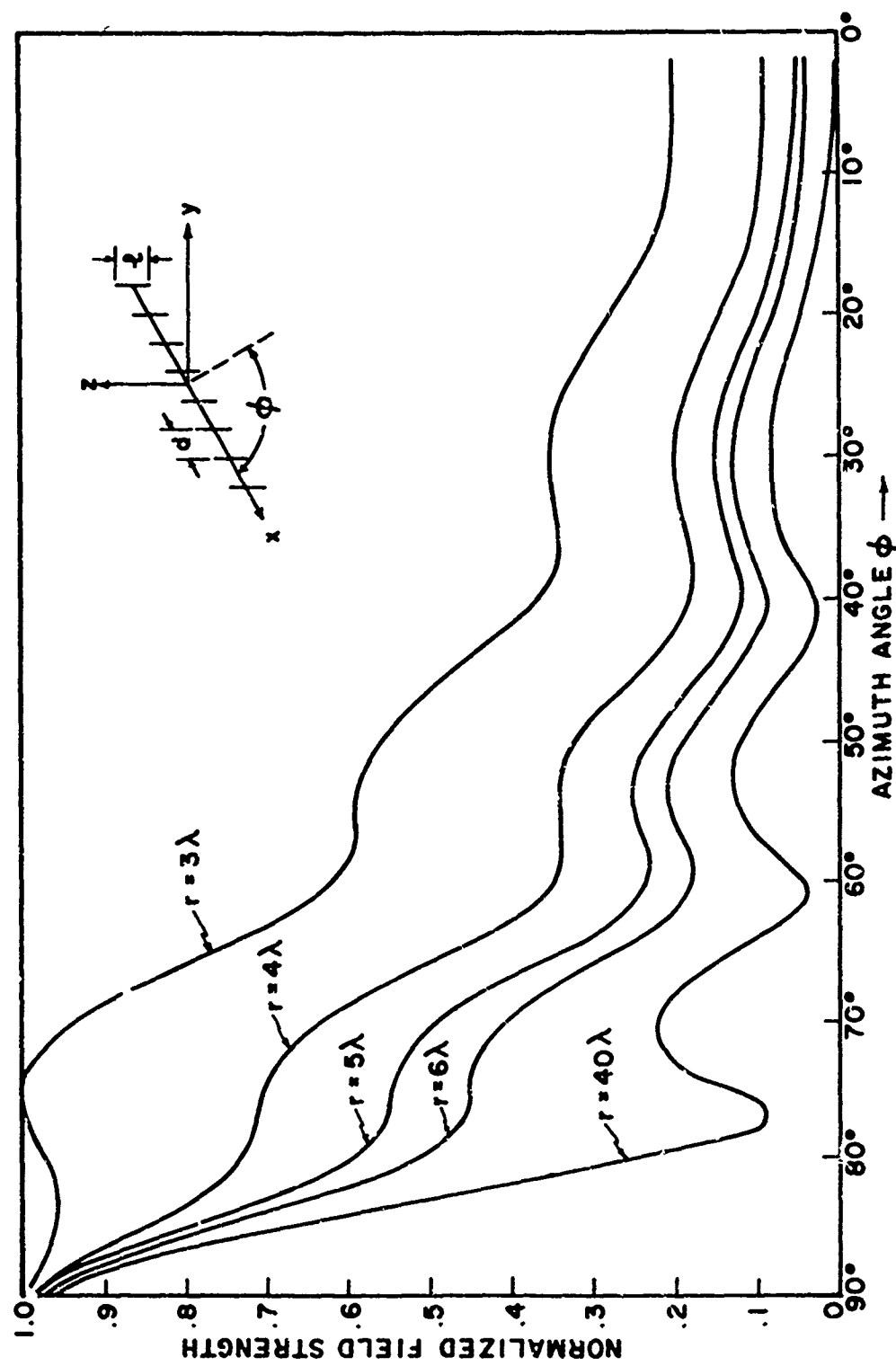


Figure 4-6a Near electric field of an eight-element linear array of dipoles ( $l/\lambda = 0.5$ ,  $d/\lambda = 0.5$ ,  $z = 0$ ). Polar Coordinate plot, broadside excitation.

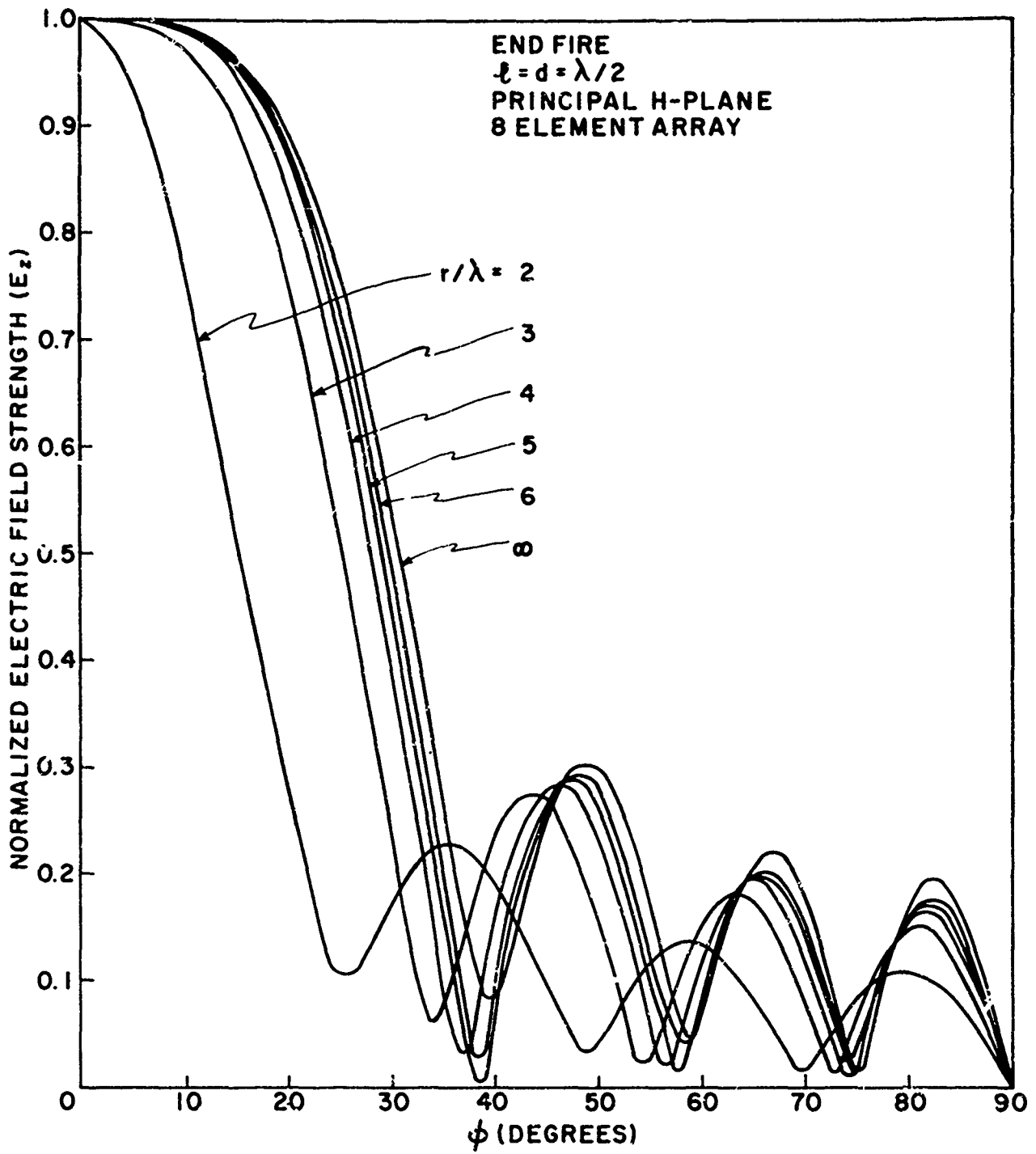


Figure 4-6b Near electric field of an eight-element array of dipoles ( $\ell/\lambda = 0.5$ ,  $d/\lambda = 0.5$ ,  $z = 0$ ) - Polar coordinate plot, endfire excitation.

near electric field, in the principal H-plane, for uniform excitation. Note that the patterns smoothly and gradually approach the far field pattern with the peaks and nulls forming gradually as  $r$  (radial distance to the field point) increases. The pattern for  $r = 40\lambda$  is extremely close to that of the far field. Since mutuals are taken into account, there is some null fill-in and the far field pattern differs slightly from the classical pattern of an array of Hertzian dipoles. Fig. 4-6b shows the near electric field of the eight element array, in the principal H-plane, for endfire excitation. Note that the main beam broadens as radial distance  $r$  increases, in contrast to the broadside case (Fig. 4-6a) which shows main beam narrowing as  $r$  increases.

For points in the "very near" field, the electric and magnetic fields are strongly effected by the mutual interactions among dipoles [71]. Fig. 4-7a shows a plot of electric field strength across the face of the eight-element array, at distances between .05 and  $.25\lambda$ . Fig. 4-7b shows a corresponding plot of the electric field strength of an eight-element array of Hertzian dipoles. Apparently the mutuals have the effect of "smoothing out" the variations of electric field in the "very near" region. The corresponding plot for the Hertzian dipoles in the region  $r = 3 - 40\lambda$  differs only slightly from that of Fig. 4-6a.

The radiation hazards in the near fields may be computed [71], [130] once all the components of the electric field are known. Radiation hazard contours may readily be drawn from the printed output of a so-called "snapshot" routine [73] which prints out radiation hazard values over a given rectangle in space. Fig. 4-8 shows an example of such a plot in the principal H-plane ( $z = 0$ ) of the uniformly excited eight-element array. Each dipole is excited

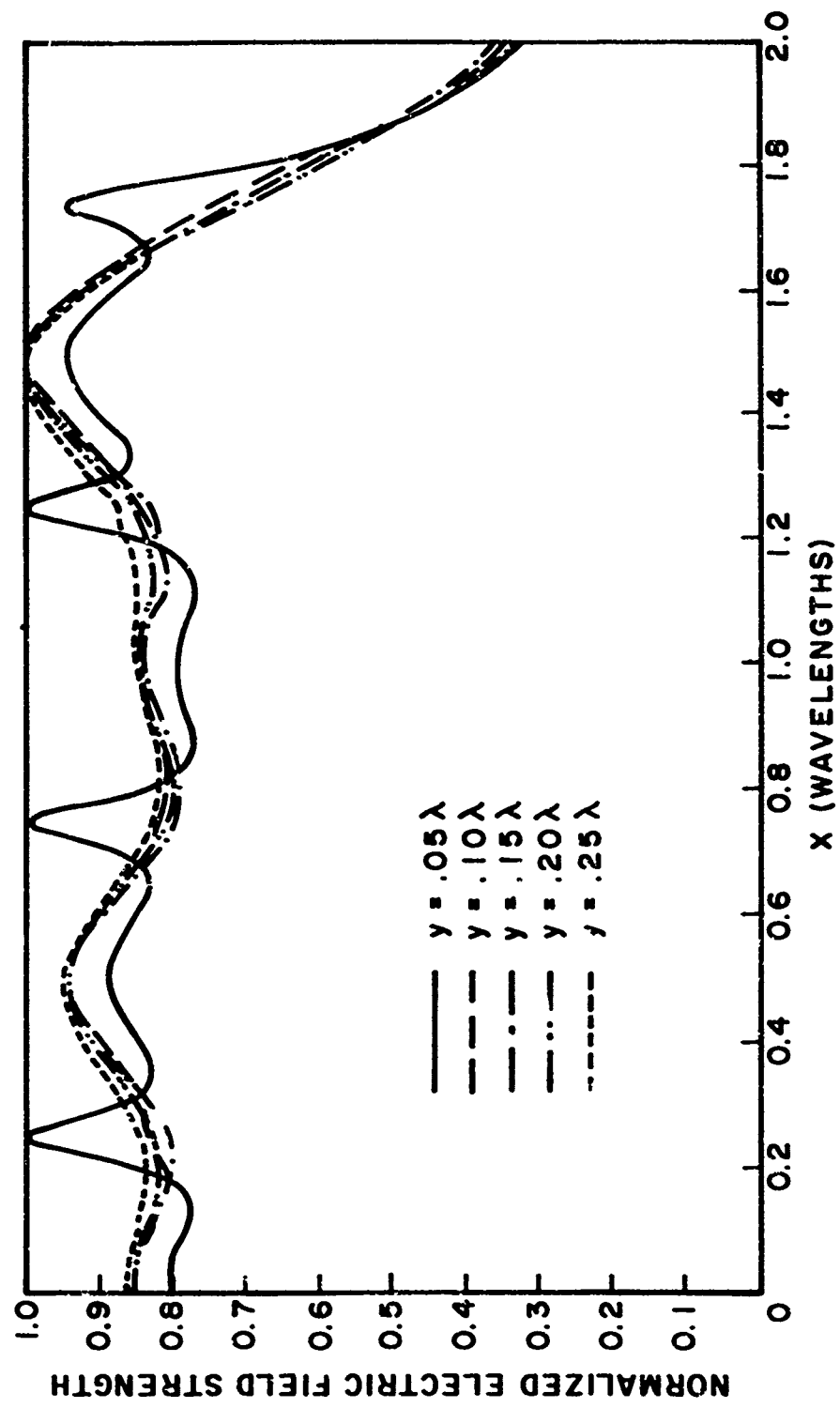


Figure 4-7a Near electric field of a uniformly excited array of dipoles ( $d/\lambda = 0.5$ ,  $z = 0$ ) - Rectangular plot, halfwave dipoles.

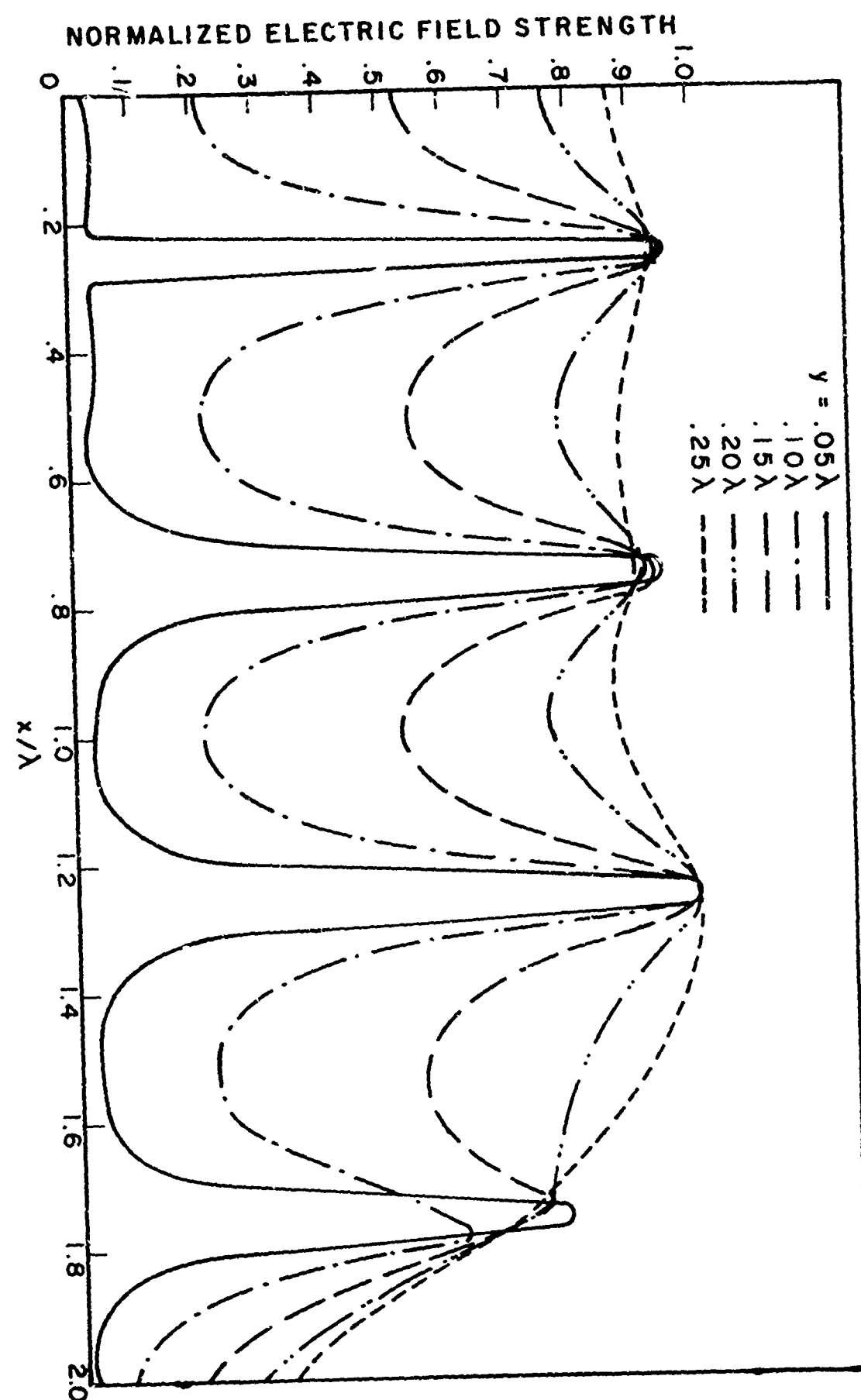


Figure 4-7b Near electric field of a uniformly excited array of dipoles ( $d/\lambda = 0.5$ ,  $z = 0$ ) - Rectangular plot, Hertzian dipoles.

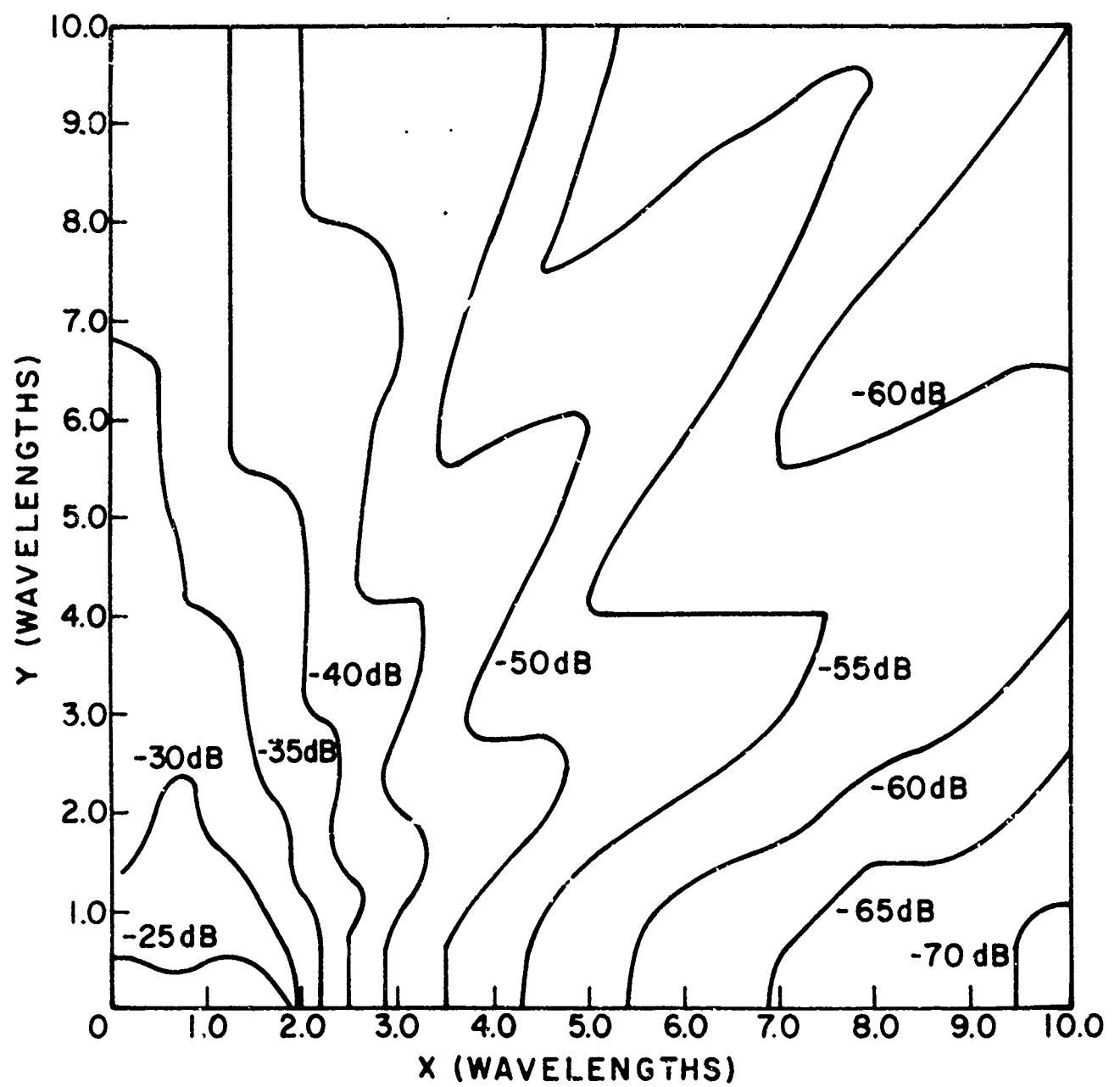


Figure 4-8 Radiation hazard contours in the principal H-plane of a uniformly excited eight-element linear array of dipoles ( $v = 1$  volt,  $\ell/\lambda = 0.5$ ,  $d/\lambda = 0.5$ ,  $z = 0$ ).

with one volt. The assumed radiation hazard criterion is  $10 \text{ mw/cm}^2$  or 194 volts/m. Fig. 4-8 shows decibel levels relative to that criterion. Note that the partially formed peaks and nulls of the near field beam patterns (Fig. 4-6a) show up clearly in the plot of Fig. 4-8, forming progressively (as  $r$  increases) at angles corresponding to peaks and nulls of the far field beam pattern.

Fig. 4-9 shows a comparison of theory and experiment for the near-field component  $E_z$  in the principal H-plane of a two-dipole endfire array of resonant dipoles with halfwave spacing. The agreement between theory and experiment is good except at positions very close to the ends of the dipole.

More complete information on near-field problems is given in references [71], [73], [130]-[133], and in volumes #2, #3, #5 of the RADC Method of Moments Applications Series.

#### 4.3 TRANSMISSION LINE INTERFERENCE WITH DIPOLE PERFORMANCE

Fig. 4-10 shows a transmission line of length  $l_t$ , wire radius "a" and wire center separation  $d$ , connected to a dipole of length  $l$  and wire radius "a". The transmission line interferes with the dipole; it contributes a cross polarized component  $E_\theta$  as well as interfering with the normal dipole pattern.

The characteristics of such thin-wire, finite-gap  $\lambda/2$  and  $\lambda/4$  dipoles fed with a length of two-wire transmission line have been studied using matrix methods [75], [113]. Transmission line length and gap size have been varied obtaining the complete solution (current distributions, impedance and far field beam patterns) in each case. Significant departures from the ideal dipole characteristics are found even for electrically small gap sizes and transmission line lengths. When the departures are small, they can be described

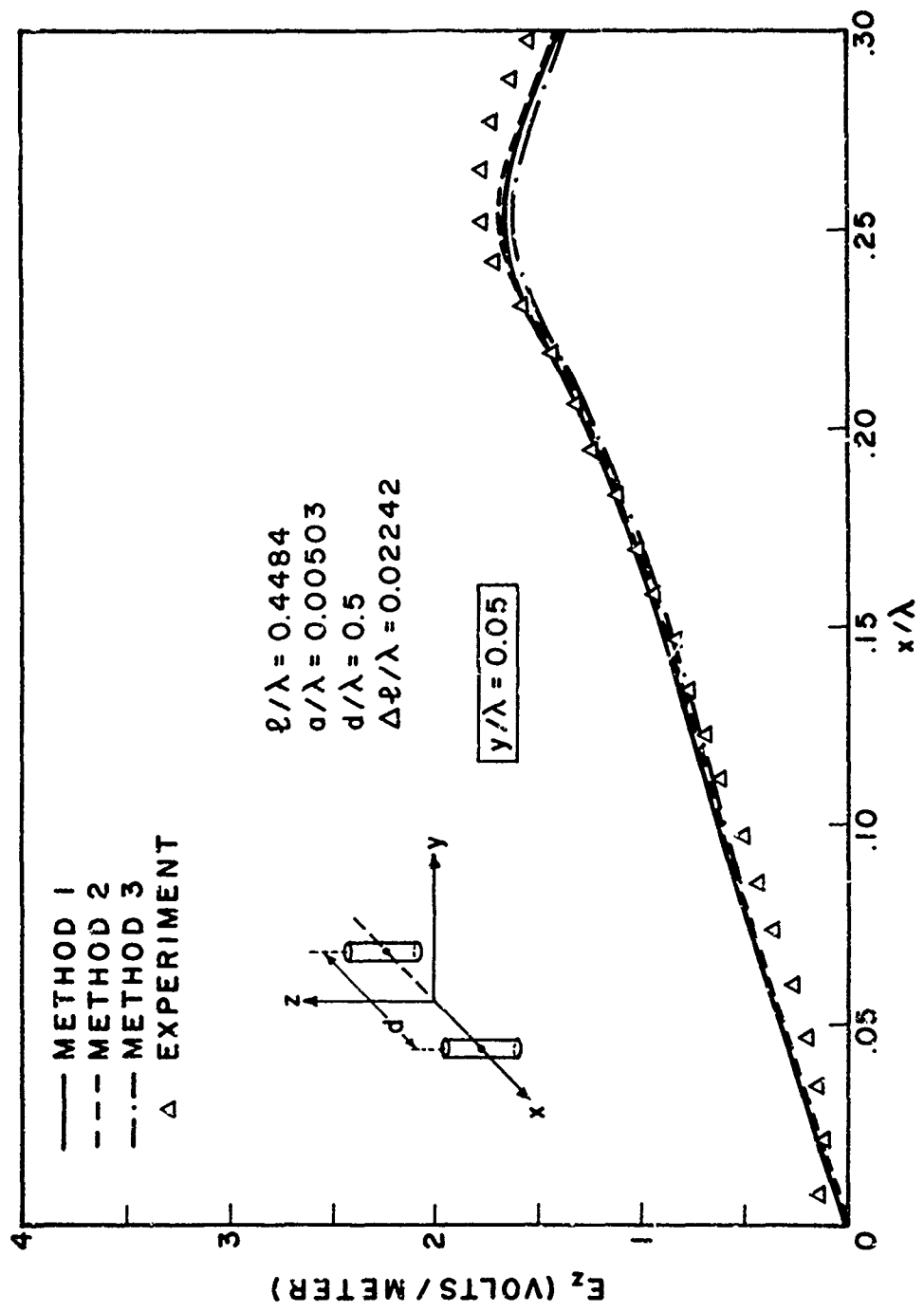


Figure 4-9a Near electric field of a two-element endfire array of resonant dipoles ( $\ell/\lambda = 0.4484$ ,  $d/\lambda = 0.5$ ,  $a/\lambda = 0.00503$ ,  $\Delta\ell/\lambda = 0.02242$ ,  $\lambda = 3\text{m}$ ,  $V = 1\text{ volt}$ ),  $y/\lambda = 0.05$ .

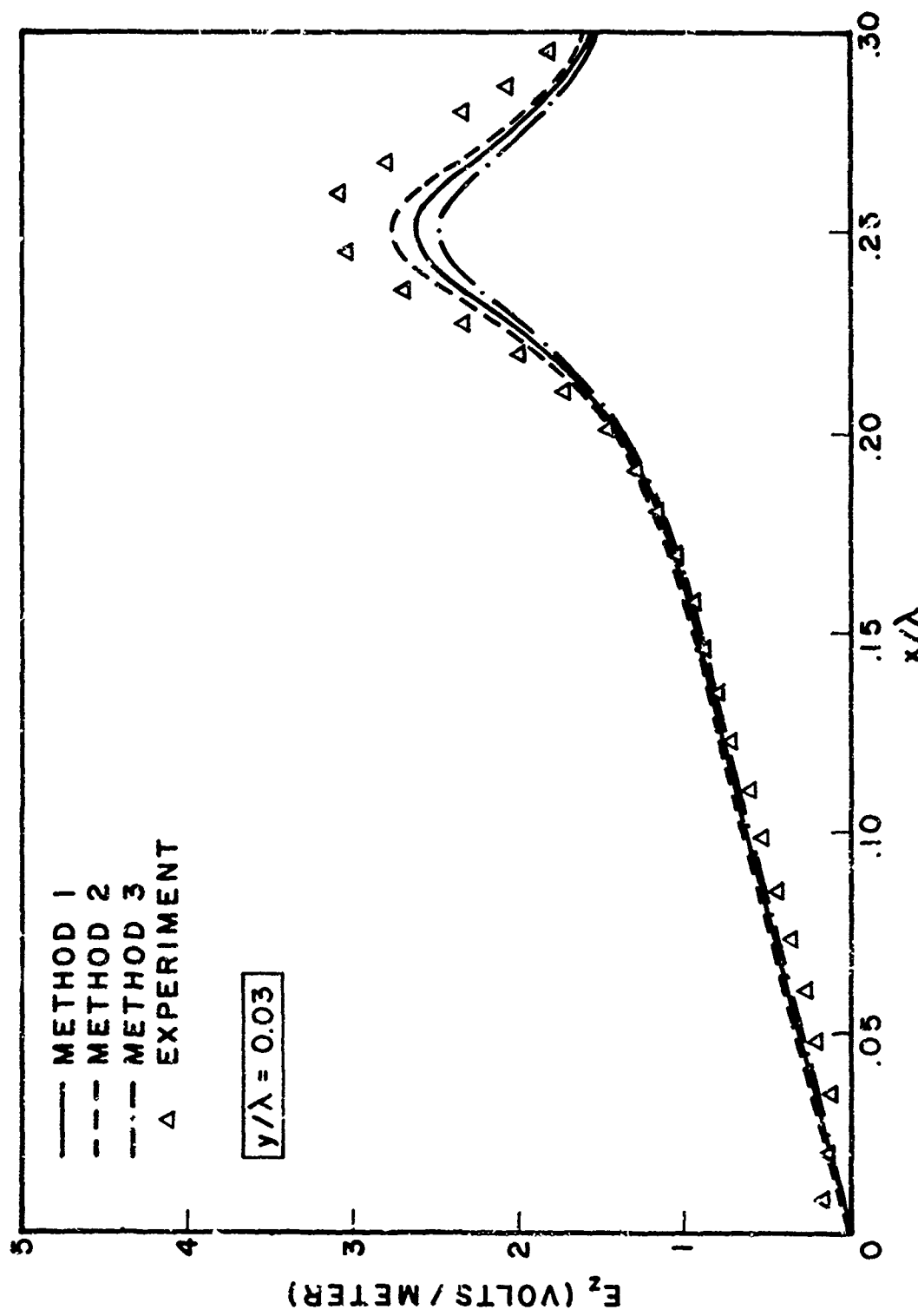


Figure 4-9b Near electric field of a two-element endfire array of resonant dipoles ( $\ell/\lambda = 0.4484$ ,  $d/\lambda = 0.5$ ,  $a/\lambda = 0.00503$ ,  $\Delta\ell/\lambda = 0.02242$ ,  $\lambda = 3\text{m}$ ,  $V = 1\text{ volt}$ ),  $y/\lambda = 0.03$ .

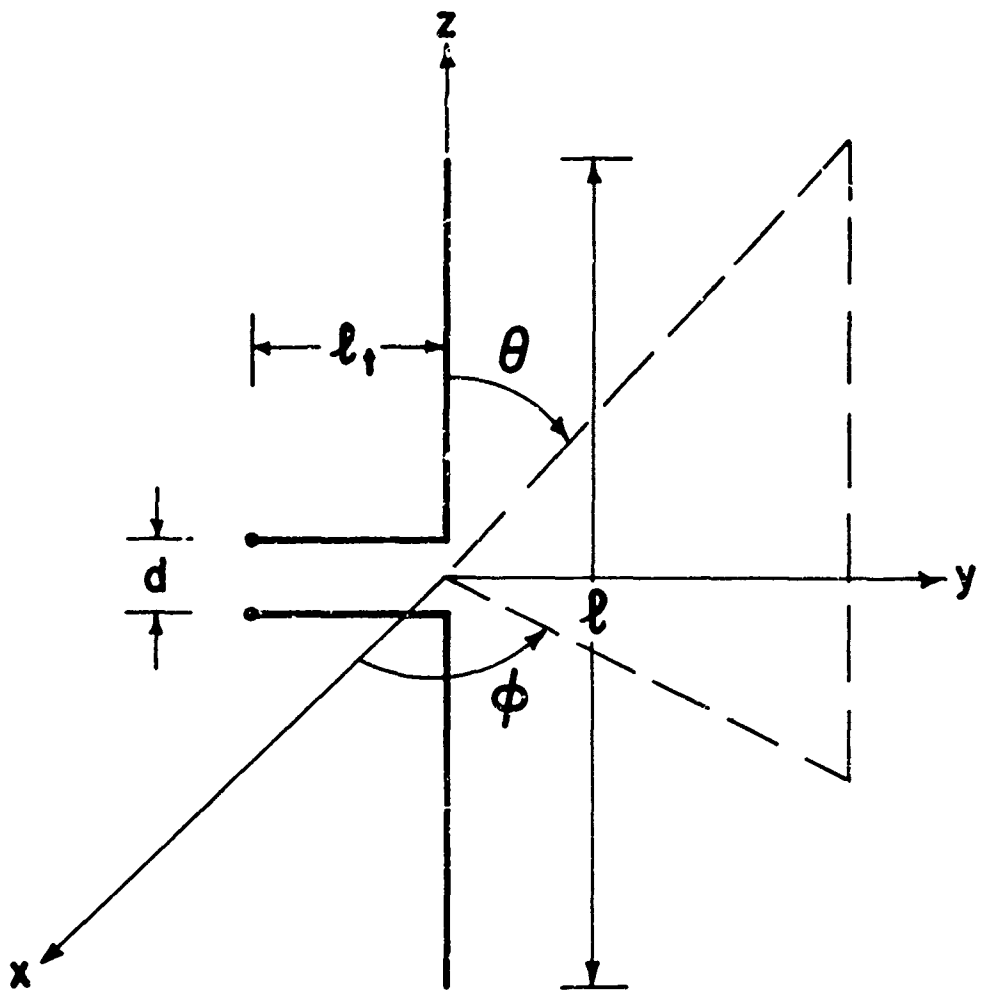


Figure 4-10 Dipole and Transmission line.

adequately by a cross polarization ratio and by null fill-in. These effects are minimized by choosing transmission line length  $l_t$  equal to  $n\lambda$ , where  $n$  is an integer. Departures from ideal dipole performance are significantly increased as dipole length  $l$  decreases, gap length  $d$  increases, transmission line length  $l_t$  increases and current imbalance increases. The cross polarization ratio (defined as  $|E_{\theta \max}| / |E_{\phi \max}|$ ) is minimized by choosing line length  $l_t$  equal to  $n\lambda$  where  $n$  is an integer. Fig. 4-11 shows computed data for the cross polarization ratio and Fig. 4-12 shows a comparison with experimental data. Note the deep null in the cross polarization ratio for  $l_t/\lambda = 1.0$ . More complete information on transmission line interference with dipole performance is given in references [75], [144] and in volume #4 of the RADC Method of Moments Applications Series [113].

#### 4.4 MICROSTRIP APPLICATIONS

Static microstrip problems are ideally suited to treatment by the method of moments and the results may be used for "quasi-TEM" analysis of microstrip. The static capacitance matrix can be computed by three methods associated with the method of moments. In the first, unknown free and bound charges are assumed on all interfaces and simple free-space Green's functions are employed. The basic matrix equation includes boundary conditions on potential over each conductor and boundary conditions on continuity of the normal displacement vector over each dielectric interface. Complex problems involving multiple dielectrics, conductors, and ground planes can be treated by this method. However, the number of unknowns in the matrix equations may be large. This method has been described by Adams and Mautz [49], [40] and was implemented in a computer program by Priebe and Kyle [145].

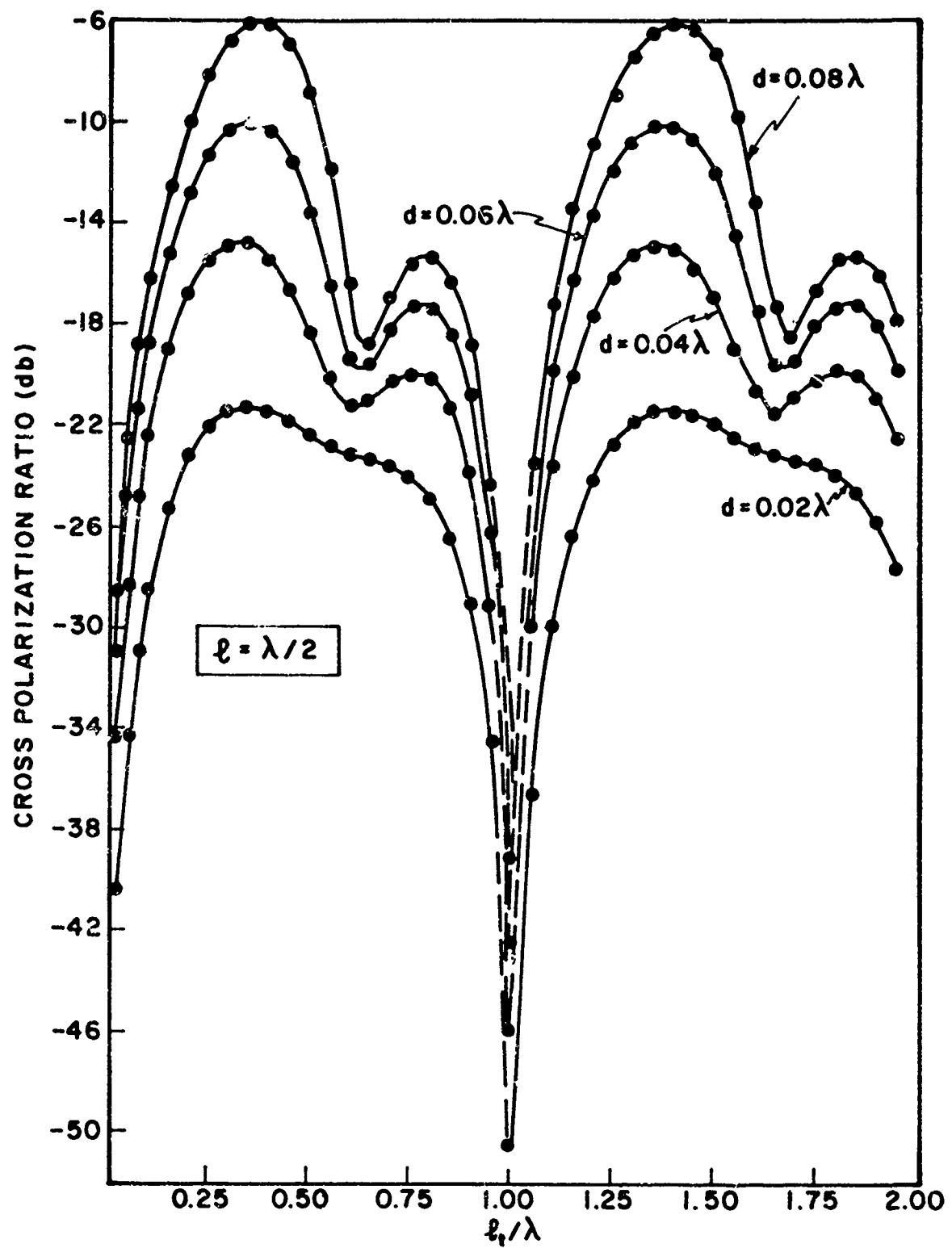


Figure 4-11 Cross polarization ratio of a transmission line and dipole.

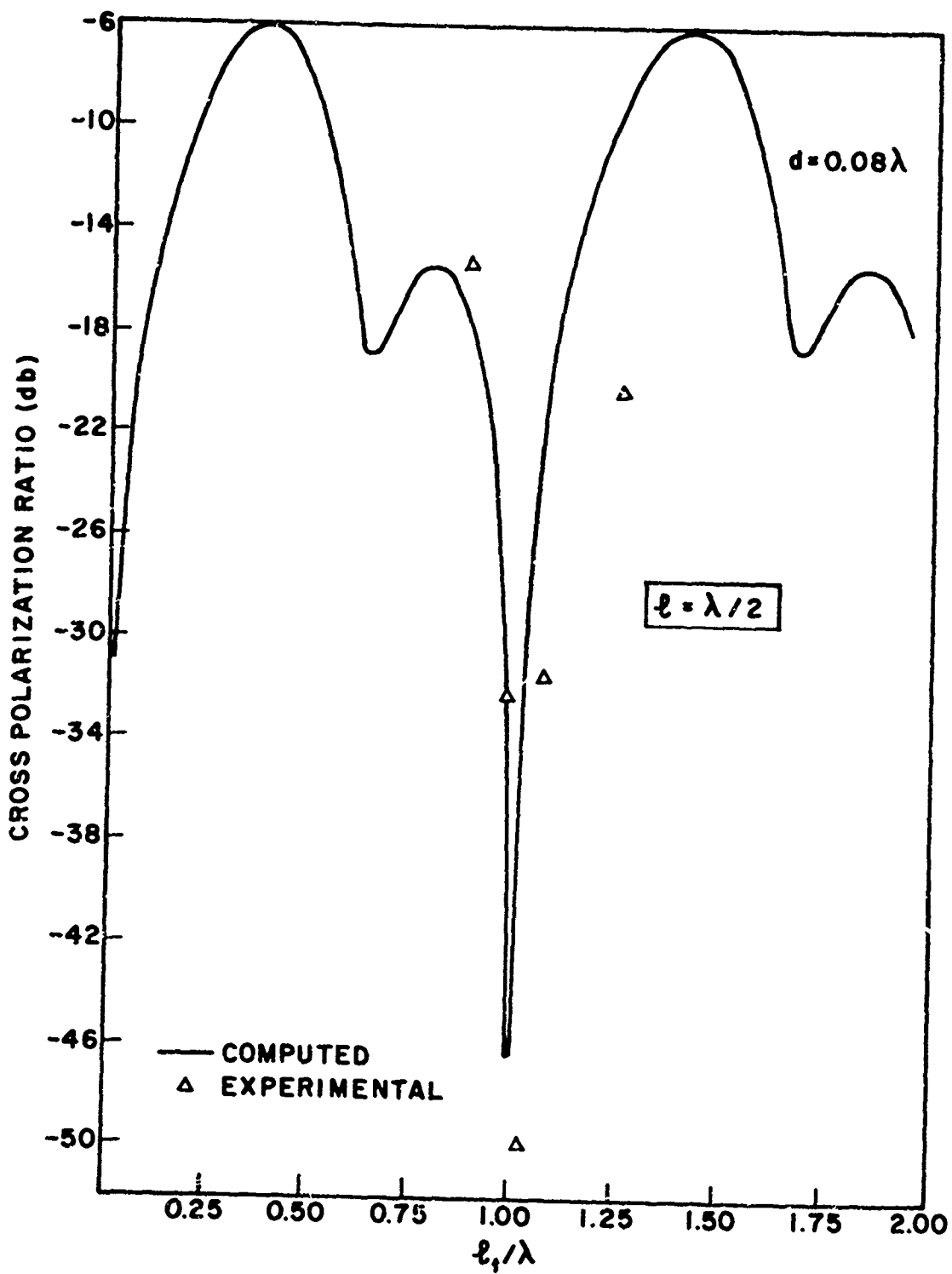


Figure 4-12 Cross polarization ratio of a transmission line and dipole - theory and experiment.

for arbitrary microstrip geometries. Fig. 4-13 shows the capacitance of a dielectric-loaded parallel-plate computed by this method. Results for  $\epsilon_r = 1$  are compared with those of Harrington [1] and Reitan [10].

In the second method, a Green's function for the basic microstrip geometry is obtained by images, leading to a simple matrix equation which includes unknown charges only over each conductor. The number of unknowns is considerably reduced over that of method #1, but the variety of problems which can be treated is more limited. The second method also may be used to obtain the values of discontinuity capacitances in microstrip [56], [65]. Fig. 4-14 shows computed values of discontinuity capacitance for a junction between two microstrip lines of different strip widths.

The third method utilizes an integral solution of the microstrip problem and is applicable to multiple dielectric and multiple ground planes [70], [76]. Computation time is relatively lengthy. Fig. 4-15 shows the capacitance of a three-layer microstrip computed by this third method. More complete information on microstrip applications is covered in references [40], [56], [65], [70], [76], and in volume #6 of the RADC Method of Moments Applications Series [146].

#### 4.5 APERTURE COUPLING

Electromagnetic coupling through an aperture in a plane screen can be treated by the method of moments.\* The aperture is replaced, using Babinet's principle, with the complementary metal disk, which is in turn replaced by a wire grid of appropriate size and shape. The fields in the aperture, and near and far fields beyond the aperture may then be computed by the method

---

\*The method of moments as used here allows one to treat apertures up to about one square wavelength in area.

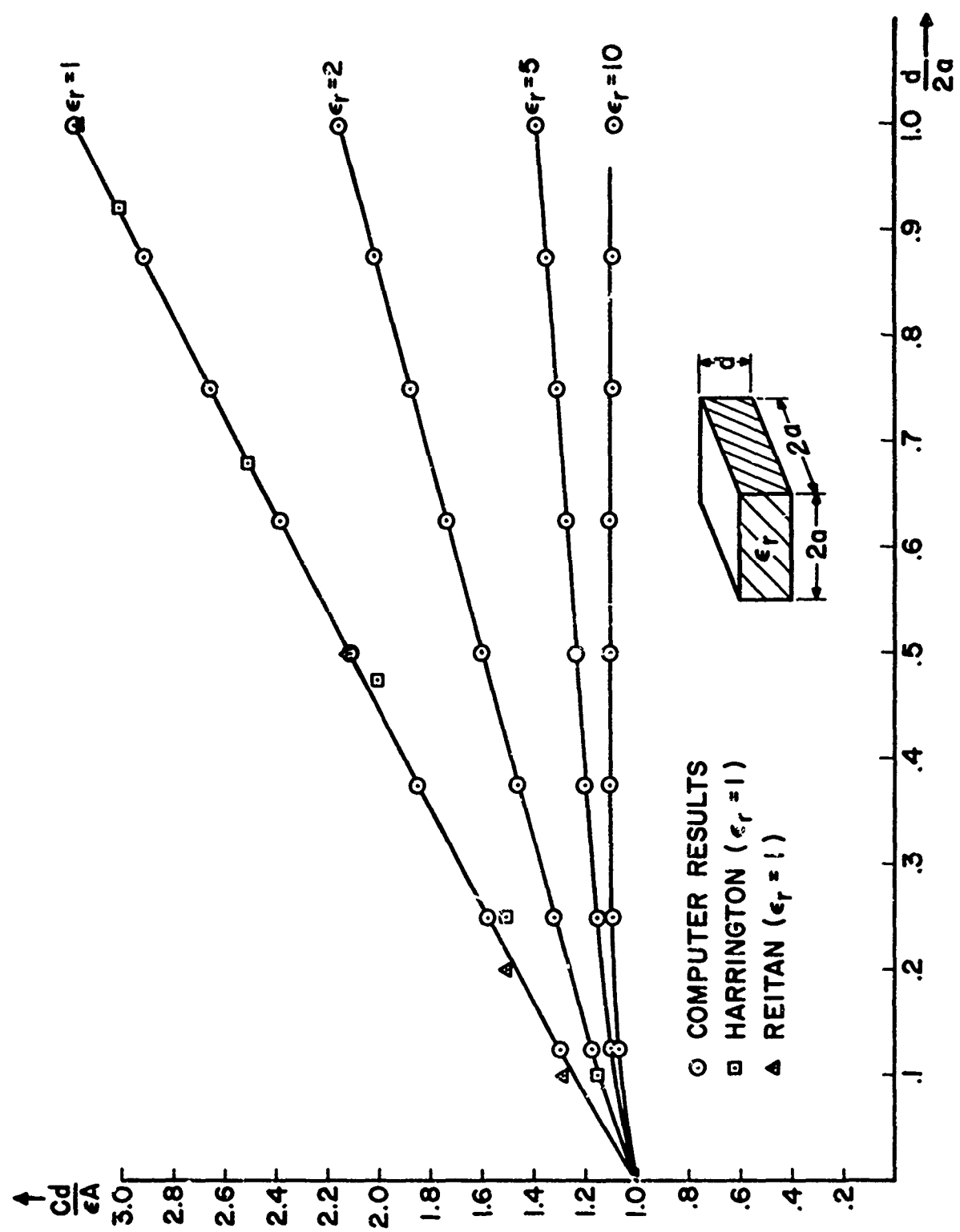


Figure 4-13 Capacitance of a square dielectric-loaded parallel-plate capacitor.

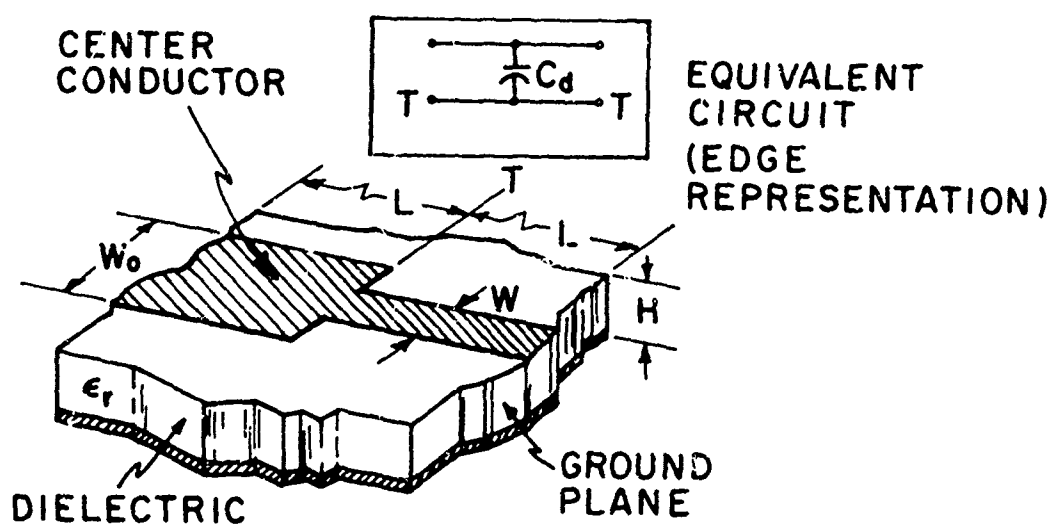


Figure 4-14a A sudden change in width of microstrip.

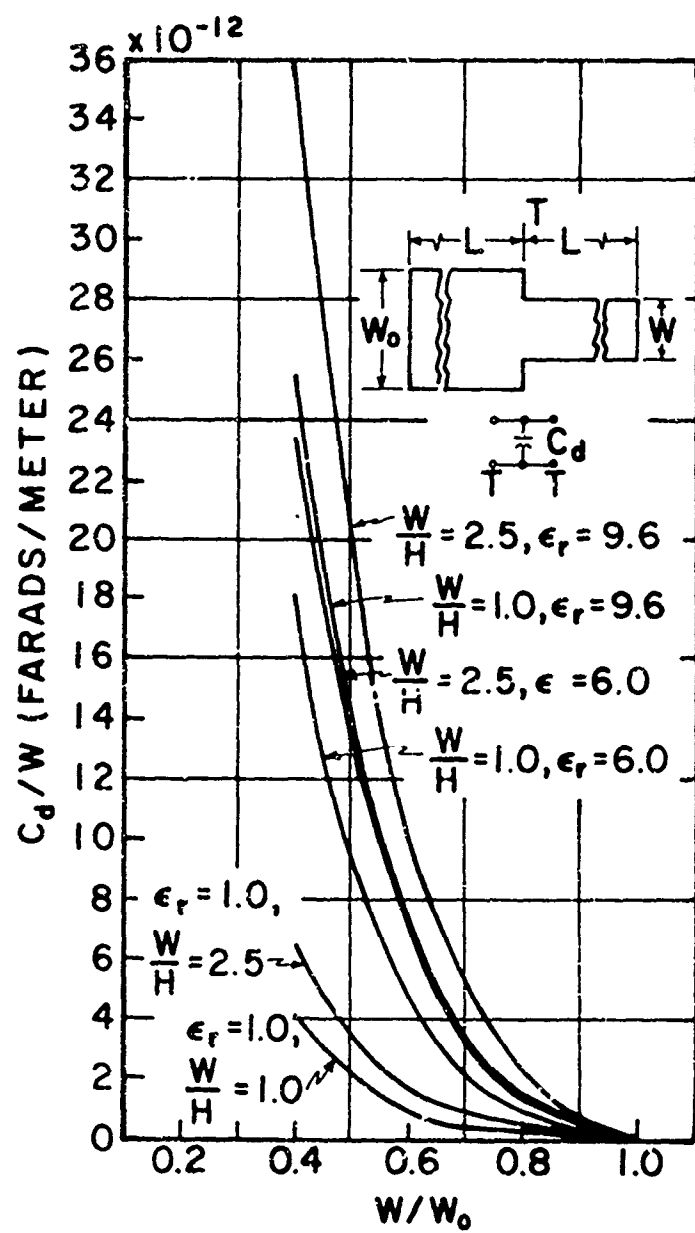


Figure 4-14b Discontinuity capacitance for a sudden change in microstrip width.

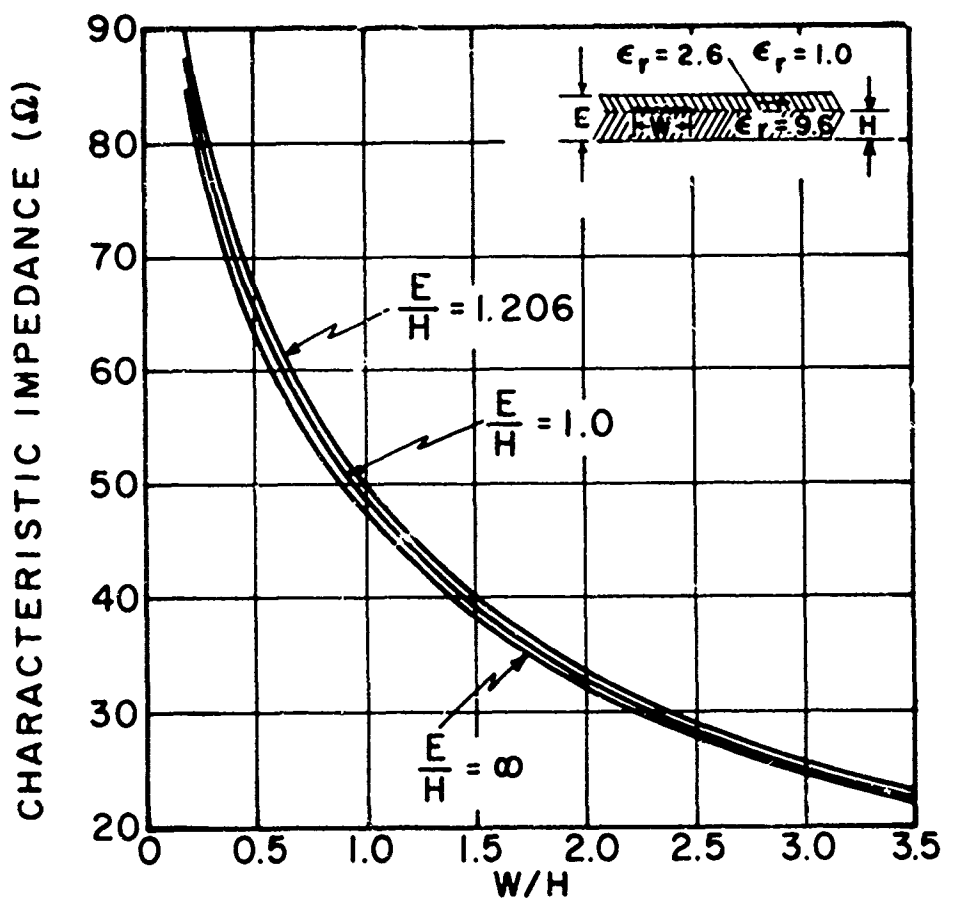


Figure 4-15 Characteristic impedance of a three-layer microstrip.

of moments [147]. Consider a  $\lambda/2$  by  $\lambda/4$  rectangular aperture in a ground plane. This aperture is replaced by a complementary disk which is wire-gridded as shown in Fig. 4-16. A plane wave polarized in the y-direction is incident normally upon the aperture. Incident field intensity is one volt/meter and frequency is 100 MHz. Fig. 4-16 shows resultant disk current  $I_x$  as computed by two different method-of-moments techniques. Fig. 4-17 shows a comparison of computed and experimental data for the y-component of the resultant aperture field. Note that the agreement is very good near the central portion of the aperture. Near the edges the agreement is, of course, less good since fields approach zero or infinity ( $E_y \rightarrow \infty$  at  $y = 0.125\lambda$  and  $E_y \rightarrow 0$  at  $x = 0.25\lambda$ ) and measurement problems arise. Fig. 4-18 shows a near field plot of the electric field in the shadow region beyond the aperture along a circle of radius  $0.5\lambda$  lying in the x-z plane (see Fig. 4-16). A plane wave polarized in the y-direction is normally incident upon the aperture. The experimental data shown in Figs. 4-16 to 4-18 was taken at Sandia Corporation.

In the method-of-moments technique for aperture coupling, arbitrary angles of incidence and arbitrary polarization can be readily treated. Examples are given in reference [147]. In addition, coupling to wires beyond the aperture may also be treated. More complete information on aperture coupling by the method of moments is available in references [147], [148].

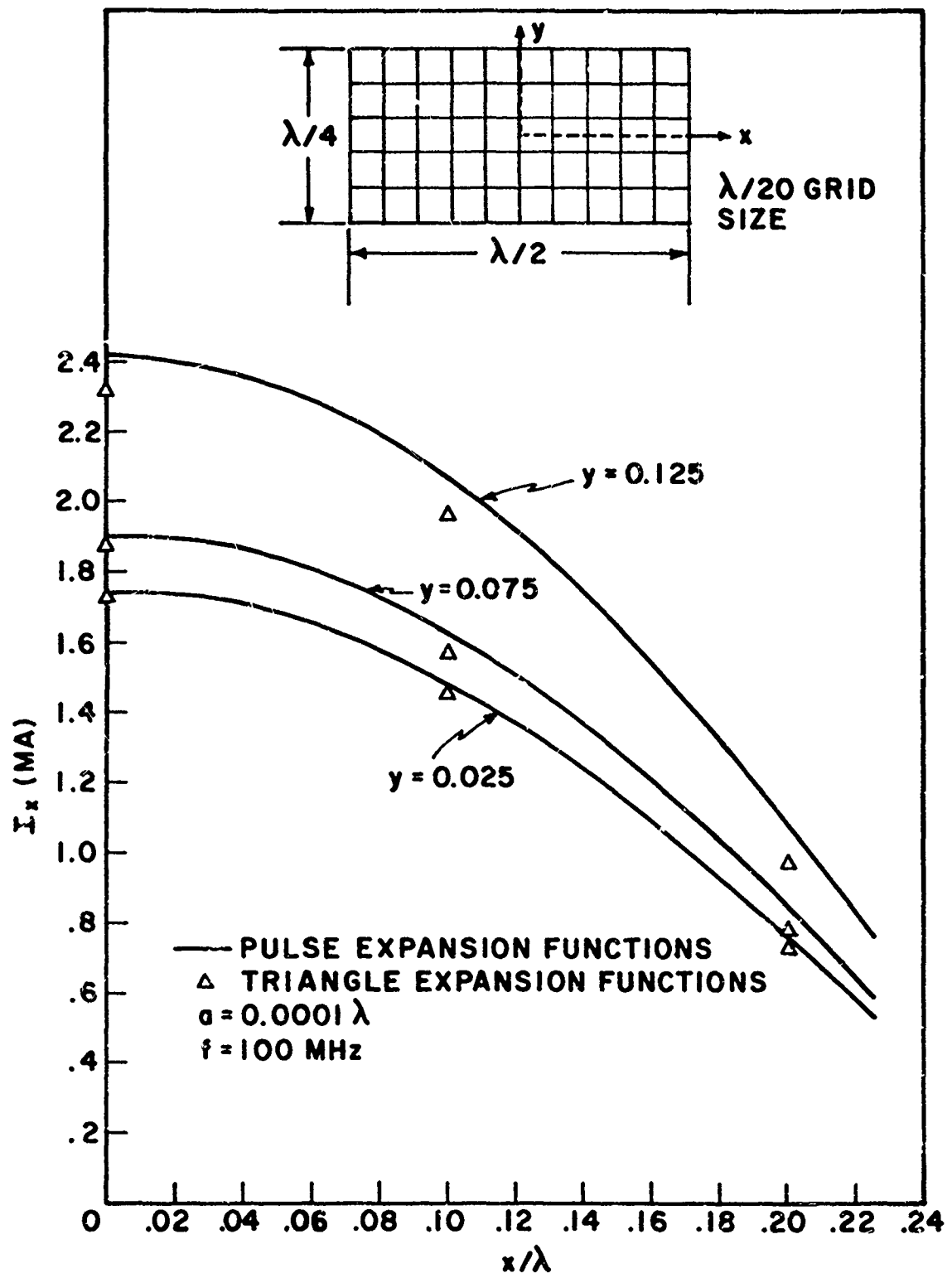


Figure 4-16 Equivalent disk currents on a rectangular grid, due to a plane wave normally incident upon a rectangular aperture in a plane screen, polarized parallel to the short side. ( $E_y^1 = 1 \text{ volt/meter}$ ,  $f = 100 \text{ mhz}$ ).

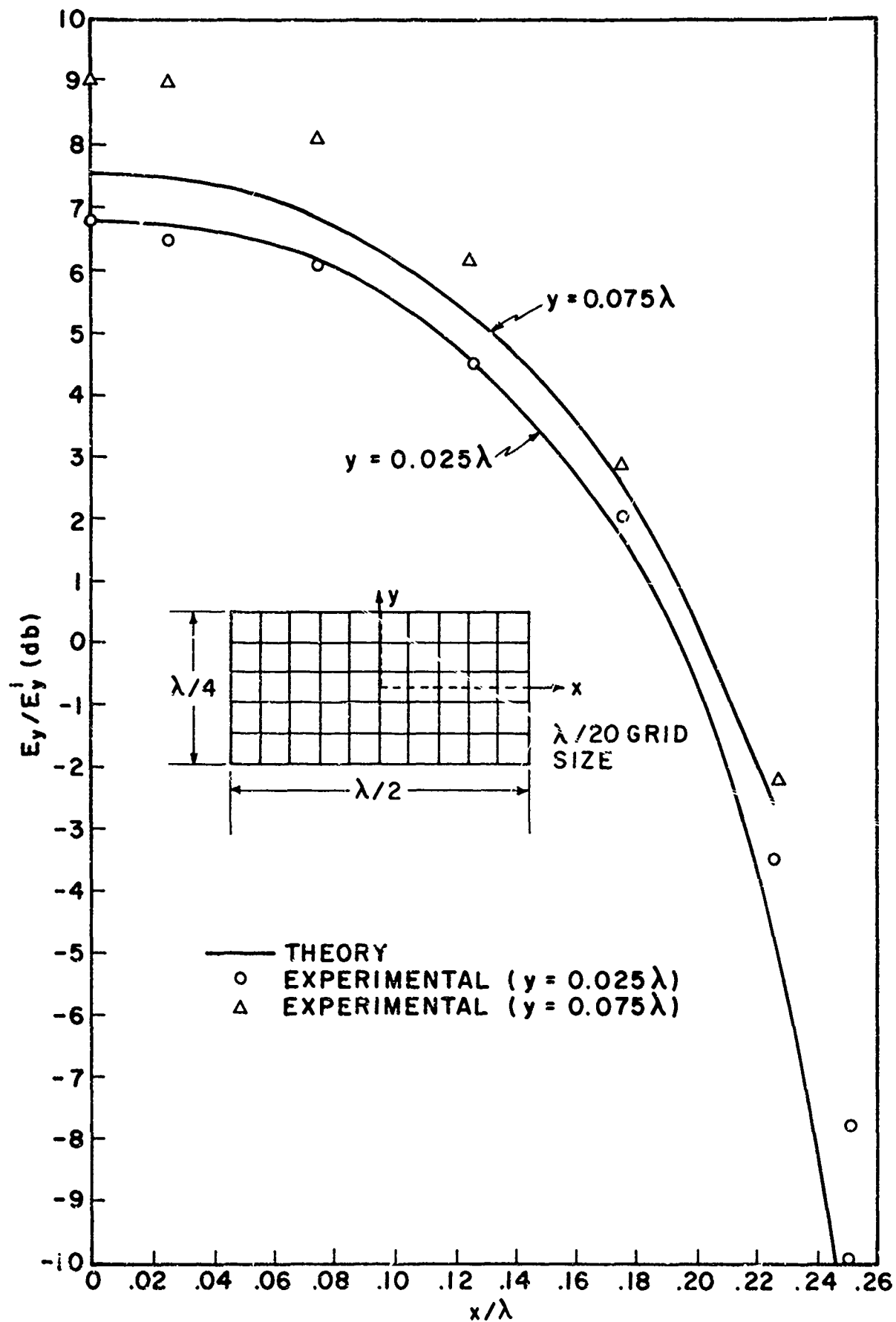


Figure 4-17 Fields in a rectangular aperture in a plane screen, due to a plane wave normally incident, polarized parallel to the short side.

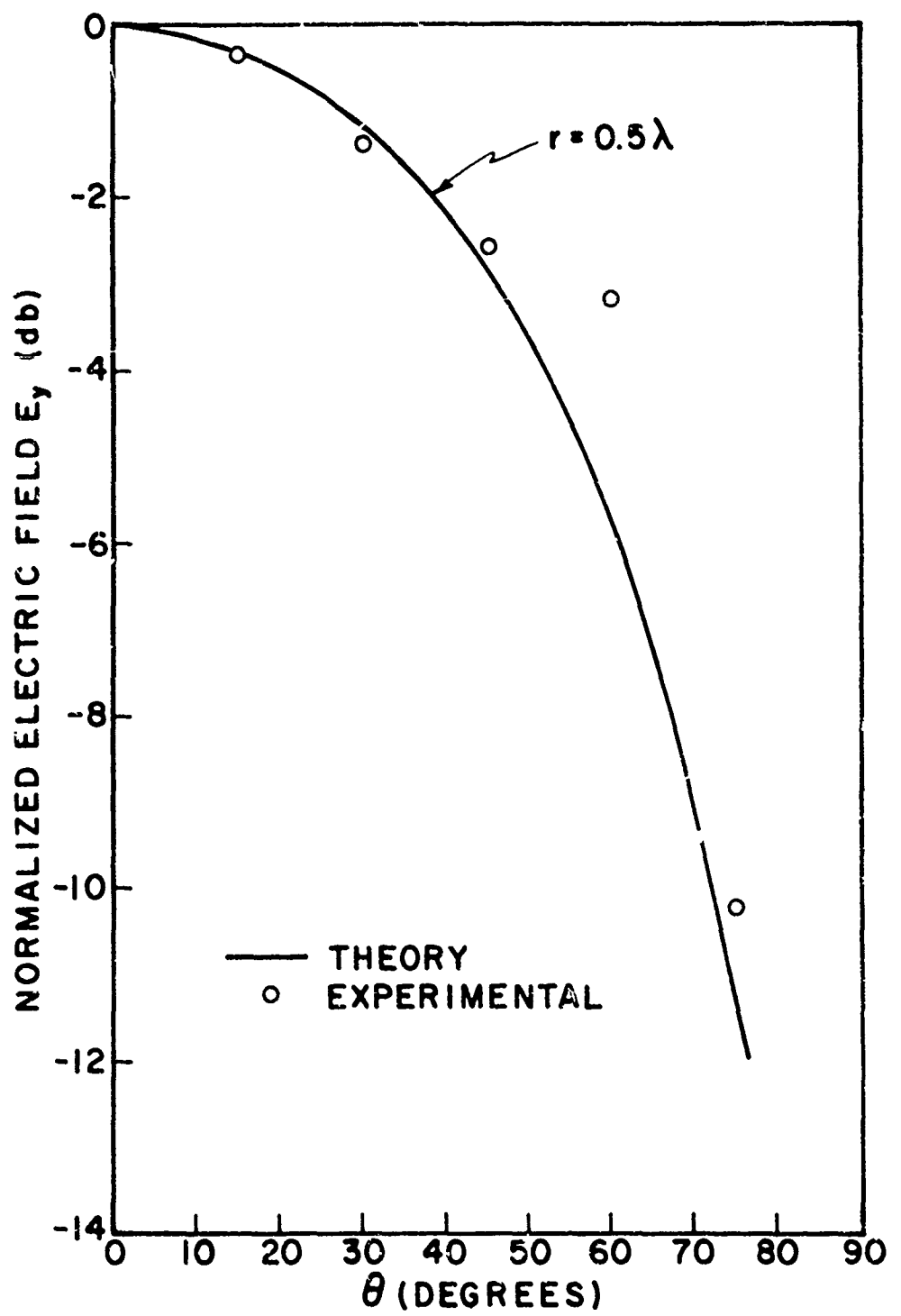


Figure 4-18 Near fields beyond a rectangular aperture in a plane screen, due to a plane wave normally incident, polarized parallel to the short side.

## V - CONCLUSIONS

The method of moments has proven to be a successful method for treating a wide variety of problems, many of which could not be treated heretofore with a high degree of accuracy. Examples of such problems are coupling in the presence of parasitics, near field and radiation hazard prediction, transmission line interference, etc. The basis of its application to thin-wire structures is described in this volume. The method is extremely flexible and conceptually simple, and it is applicable in theory to most problems in electromagnetic theory. Illustrative examples of its application are presented.

## APPENDIX A - JUSTIFICATION OF THE THIN-WIRE MODEL

In this appendix, the effects of finite radius are considered and an attempt is made to justify the filamentary model used in section 1.2. Fig. A-1 shows a fat dipole with surface currents  $J_z$ ,  $J_\phi$ ,  $J_\rho$ . There are several steps that need to be justified: (1) neglect of circumferential currents,  $J_\phi$ , (2) neglect of radial currents,  $J_\rho$ , (3) neglect of  $\phi$  variations in longitudinal currents  $J_z$ , and (4) replacement of  $z$ -directed surface currents with a filamentary model.

The thin-wire model may be explained in several different ways. The results of some classical scattering problems are useful. Consider a plane wave incident upon a conducting cylinder of radius "a" and infinite length (Figure A-2) with its axis parallel to the  $z$ -direction. The incident electric field has intensity  $E_0$  and is polarized in either the  $z$  direction (parallel to the cylinder axis) or in the  $y$  direction (perpendicular to the cylinder axis), as shown in Fig. A-2. The solution of the resultant boundary value problems for the currents and scattered fields are given below [149]:

### I ELECTRIC FIELD PARALLEL TO THE CYLINDER AXIS\*

#### Surface Currents

$$J_z = \frac{-2E_0}{\omega \mu \pi a} \sum_{n=0}^{\infty} \frac{j^{-n} e^{j n \phi}}{H_n^{(2)}(ka)} \quad (A-1)$$

\*In this appendix,  $J(x)$ ,  $H_n^{(2)}(x)$  represent Bessel functions of the first kind and Hankel functions of the second kind, respectively, and  $J'(x)$  and  $H_n^{(2)}(x)$  represent their derivatives with respect to  $x$ .  $n$  represents the order of the respective functions.  $\gamma$  is Euler's constant (1.781).  $k$  is the free space wave number.  $(\rho, \phi, z)$  are the cylindrical coordinates.

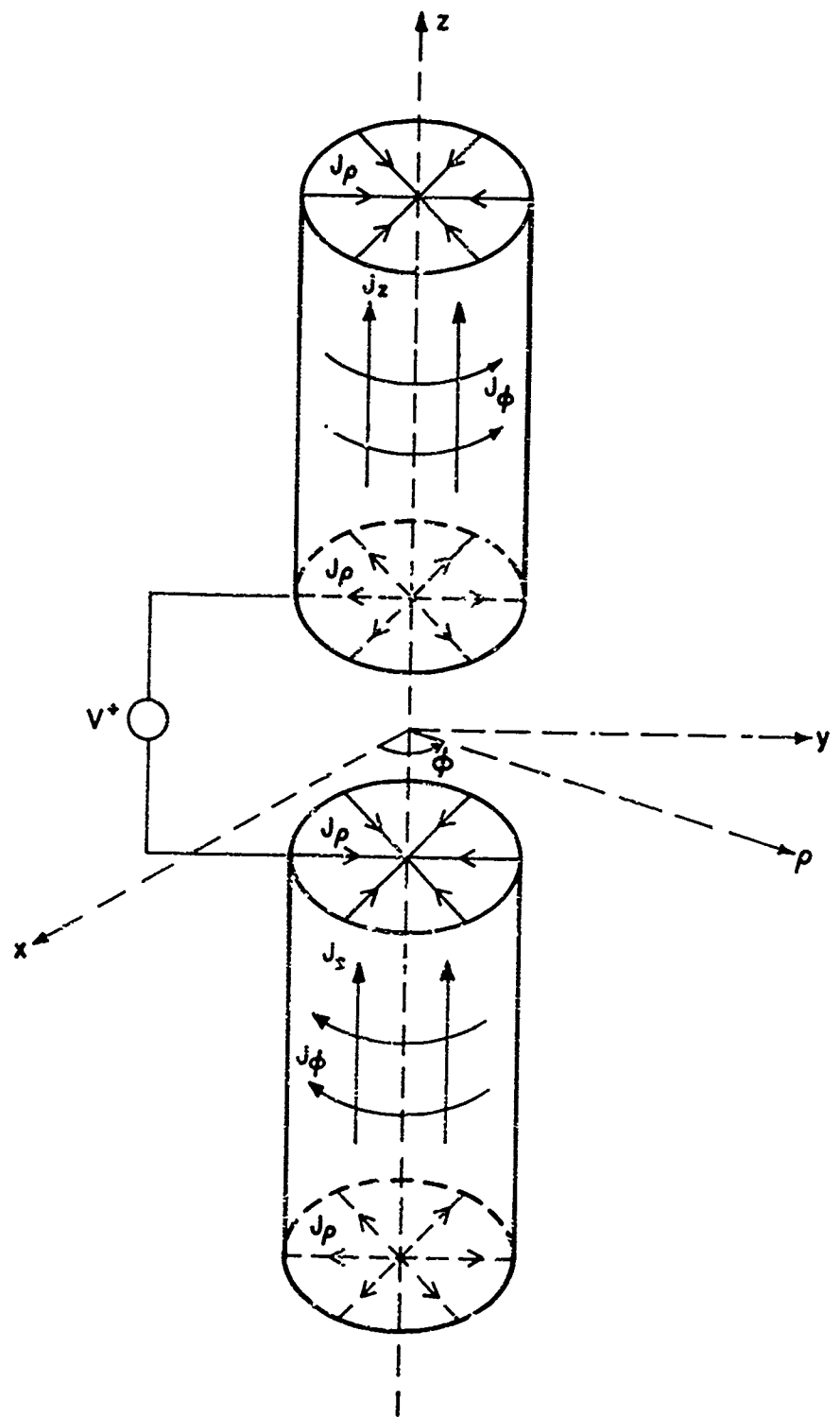


Figure A-1 A fat dipole.

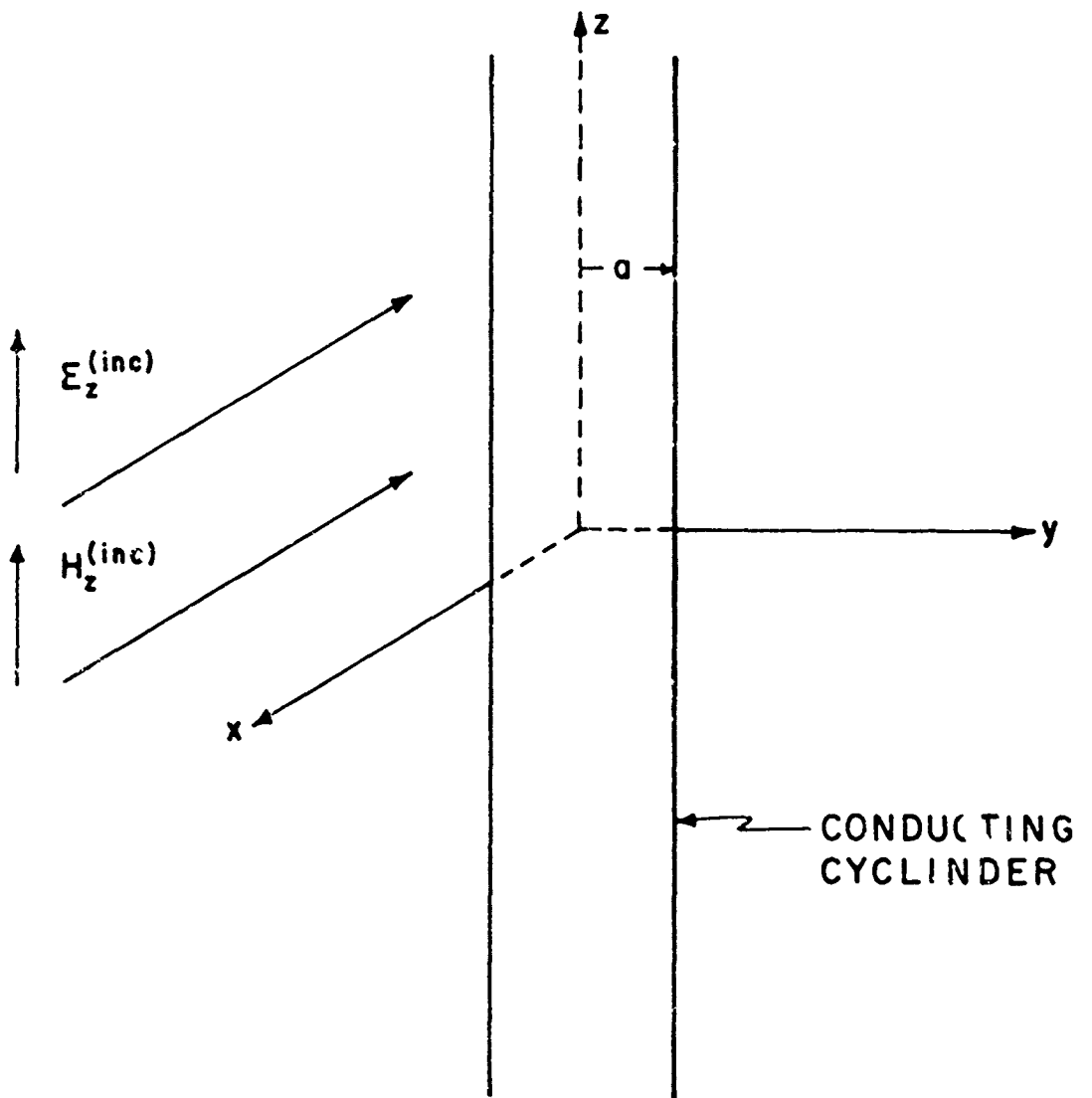


Figure A-2 A plane wave incident upon a conducting cylinder of radius "a" and infinite length.

A study of the small argument forms of  $H_n^{(2)}(ka)$  shows that the  $n = 0$  term of the infinite series dominates for small  $ka$  and thus

$$H_0^{(2)}(ka) \approx 1 - \frac{j2}{\pi} \log(\frac{\gamma ka}{2}) \approx \frac{-j2}{\pi} \log(.8905 ka) \quad \text{for } (ka \ll 1),$$

where  $\log$  indicates the natural logarithm.

$$J_z = -\frac{jE_0}{\omega\mu a} \frac{1}{\log(.8905 ka)} \quad (ka \ll 1) \quad (A-2)$$

$$I_z \text{ (total current)} = 2\pi a J_z = \frac{-j2\pi E_0}{\omega\mu \log(.8905 ka)} \quad (ka \ll 1) \quad (A-3)$$

The  $n = 0$  term of the current, which becomes the total current for small  $ka$ , varies slowly  $[1/(\log(.8905 ka))]$  with  $ka$  for small  $ka$ .

### Scattered Fields

#### Near Fields

$$E_z^s = -E_0 \sum_{n=-\infty}^{\infty} \frac{j^{-n} J_n(ka) e^{jn\phi}}{H_n^{(2)}(ka)} H_n^{(2)}(kp) \quad (A-4)$$

$$\approx \left(\frac{-j\pi}{2}\right) \frac{E_0}{\log(.8905 ka)} H_0^{(2)}(kp) \quad (ka \ll 1) \quad (A-5)$$

#### Far Fields

$$\lim_{p \rightarrow \infty} \left| \frac{E_z(s)}{E_z(\text{inc})} \right| = \sqrt{\frac{2}{\pi kp}} \left| \sum_{n=-\infty}^{\infty} \frac{J_n(ka)}{H_n^{(2)}(ka)} e^{jn\phi} \right| \quad (A-6)$$

$$\approx \sqrt{\frac{\pi}{2kp}} \frac{1}{\log(.8905 ka)} \quad (ka \ll 1) \quad (A-7)$$

Thus, as  $ka \rightarrow 0$ , the  $\phi$ -independent currents dominate and the radiated fields become  $\phi$ -independent. Note especially that the near electric field is

proportional to  $H_o^{(2)}(k\rho)/\log(.8905 ka)$  (see Eq. (A-5)). The term  $H_o^{(2)}(k\rho)$  is proportional to the field of a filament along the z-axis, whereas the term  $1/\log(.8905 ka)$  corresponds to the variation of total longitudinal surface current for small  $ka$  (See Eq.(A-3)). Thus, for small  $ka$ , the radiated fields of a filament are equal to those of the distributed surface current model with the same total current, for  $\rho > a$ . This is the basis for step (4), the replacement of the surface model with a filamentary model.

## II. ELECTRIC FIELD PERPENDICULAR TO THE CYLINDER AXIS

### Surface Currents

$$J_\phi = \frac{j2H_o}{\pi ka} \sum_{n=-\infty}^{\infty} \frac{j^{-n} e^{jn\phi}}{H_n^{(2)'}(ka)} \quad (A-8)$$

where  $H_o = E_o/n =$  incident magnetic intensity.

The current induced has a dipole ( $\cos \phi$ ) term as well as a  $\phi$ -independent ( $n = 0$ ) term. Both are important for small  $ka$ . The  $\phi$ -independent current represents electrically small loops of electric current (for small  $ka$ ). Electrically small loops are equivalent to magnetic dipoles and thus the  $\phi$ -independent electric current is equivalent to a magnetic current filament of infinite length.

### Scattered Fields

### Far Fields

$$\lim_{\rho \rightarrow \infty} \left| \frac{H_z^s}{H_z^i} \right| = \sqrt{\frac{2}{\pi k_o}} \left| \sum_{n=-\infty}^{\infty} \frac{j'(ka)}{H_n^{(2)'}(ka)} e^{jn\phi} \right| \quad (A-9)$$

$$\Rightarrow \frac{\pi(ka)^2}{4} \sqrt{\frac{2}{\pi k_0}} (|1 - 2 \cos \phi|) \quad (A-10)$$

as  $ka \rightarrow 0$

Note that both the dipole ( $\cos \phi$ ) and the magnetic filament contribute as  $ka \rightarrow 0$ . However, the scattered fields are proportional to  $(ka)^2$  in contrast to the scattered fields for the parallel case which are proportional to  $1/(\log.89 ka)$ . In other words, a thin wire may have both longitudinal and circumferential currents. As  $ka$  becomes small, the fields radiated by the circumferential component decrease rapidly with  $ka$ , whereas the fields radiated by the longitudinal component decrease slowly with  $ka$ . This corresponds to the well-known fact that the back-scattering cross section of a thin wire parallel to the incident field varies slowly with wire radius and that it is much greater than that of a thin-wire perpendicular to the incident field.

We can combine the results of the two problems to express the scattering due to arbitrary incident fields with electric field components both parallel and perpendicular to the cylinder axis.

Note that, for arbitrary polarization of the incident fields, both longitudinal and circumferential currents are excited. The fields radiated by the longitudinal currents will always dominate as  $ka \rightarrow 0$ , except for the special case where there is no component of  $\underline{E}^{(inc)}$  parallel to the cylinder. Furthermore, note that because of the dominance of the  $n = 0$  term in (A-1) and (A-4), the variations in  $\phi$  of the longitudinal current are unimportant.

Thus, for plane waves normally incident upon infinite cylinders of small  $ka$ , the scattered fields radiated by the longitudinal currents dominate over those radiated by the circumferential currents. Furthermore, the fields

radiated by the  $\phi$ -independent longitudinal currents dominate over those radiated by the  $\phi$ -dependent longitudinal currents. The above statements are valid in both the near and far fields. The only exception to the above statements is the degenerate case where the incident field is exactly perpendicular to the cylinder axis.

In order to apply the above classical analysis to antenna problems involving thin wires, one must generalize the analysis in several respects. One must consider non-normal (oblique) incidence, near field sources rather than plane waves, wires of finite rather than infinite length. Suffice it to say that none of these generalizations completely invalidate the conclusions reached above. However, some of the conclusions are weakened somewhat. For instance, consider two parallel wires extremely close together (a fraction of a wire radius). One may be considered as a near field source for the other. It is possible, for instance, that a current-carrying wire extremely close to a cylinder may excite significant  $\phi$ -dependent longitudinal currents. Even though these currents radiate less effectively than the  $\phi$ -independent longitudinal currents, there are undoubtedly cases where the radiated fields of the  $\phi$ -dependent currents are significant. For instance, if two wires, both electrically small in radius, are placed in extremely close proximity to each other, then one would expect that (a) the currents would concentrate near the portions of the wires closest to each other and (b) the  $\phi$ -dependent longitudinal current would become significant. How close must the wires be to invalidate the assumptions used in typical thin-wire programs? The results of a static analysis provide some guidelines. Fig. A-3 shows two parallel cylinders of infinite length. A voltage is applied between the cylinders. The

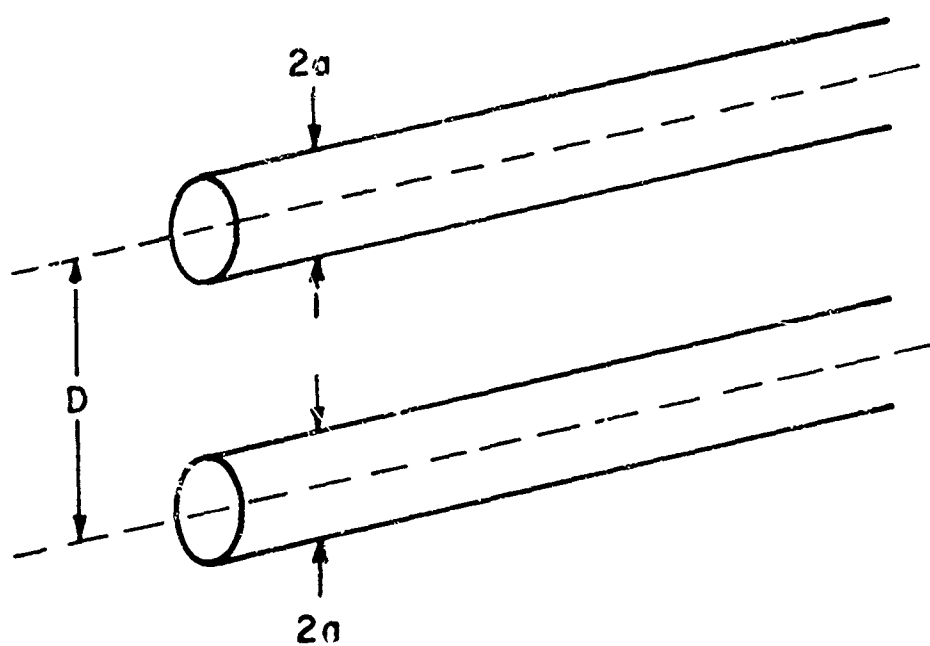


Figure A-3 Two parallel conducting cylinders.

charge distribution on the cylinders is desired. This problem may, of course, be solved by classical methods. For more than two cylinders, or for dielectric-coated cylinders, the method of moments can be used. Clements [150] has treated such problems by the method of moments using sinusoidal expansion functions (i.e., a Fourier series decomposition in  $\phi$ ) for the induced charge distribution. The induced charge is represented as follows:

$$j(\phi) = \sum_{n=0}^N A_n \cos n\phi + B_n \sin n\phi$$

For the case shown in Fig. A-3, the origin of the coordinate system may be chosen such that all the  $B_n$ 's are zero. Fig. A-4 shows the ratio  $A_1/A_0$ , i.e., the ratio of the coefficient of the dipole term to that of the  $\phi$ -independent term, as a function of  $D/2a$ . Figs. A-5a,b,c show the relative magnitudes of the Fourier coefficients for the cases  $D/2a = 1.05, 1.5, 5.0$  respectively. Note that for very close spacing such as  $D/2a = 1.05$  (.1 radius separation), the dipole coefficient exceeds that of the  $\phi$ -independent term. For  $D/2a = 1.5$  (one radius separation between cylinders) the dipole coefficient is comparable to that of the  $\phi$ -independent term. For  $D/2a = 5.0$  (4 diameters separation), the magnitude of the dipole coefficient is less than 1/6 that of the  $\phi$ -independent term.

The TEM transmission line problem is, of course, directly related to the static problem, and, as a result, the ratios  $A_n/A_0$  of Figs. A-5a,b,c are interpreted directly as the Fourier coefficients of the longitudinal surface current density  $J_z$  of the transmission line problem where:

$$J_z = \sum_{n=0}^N A_n \cos n\phi + B_n \sin n\phi$$

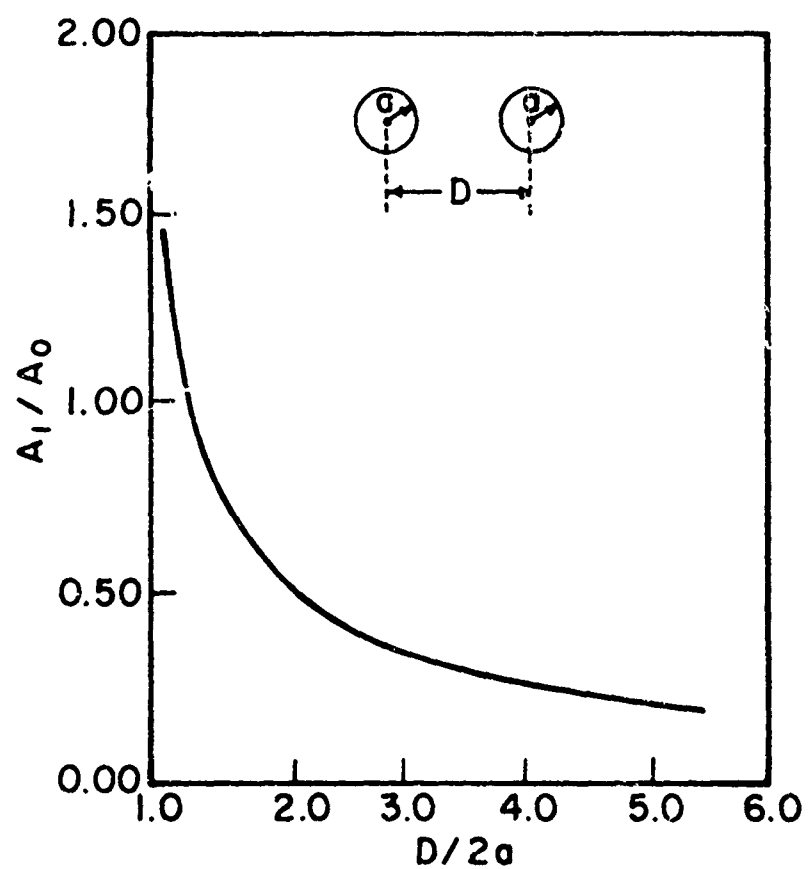


Figure A-4  $A_1/A_0$  for the two wire problem, as a function of spacing.

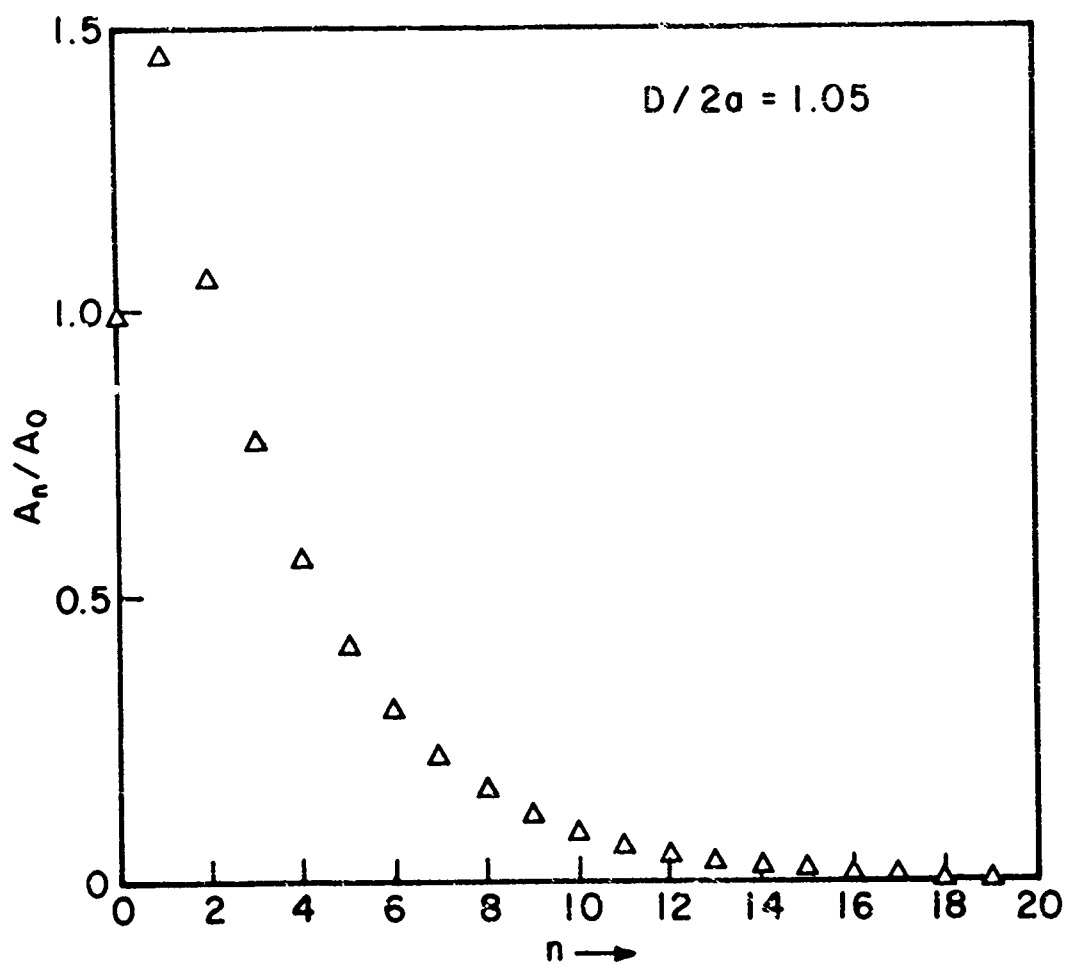


Figure A-5a Fourier coefficients of the two-wire problem ( $D/2a = 1.05$ ).

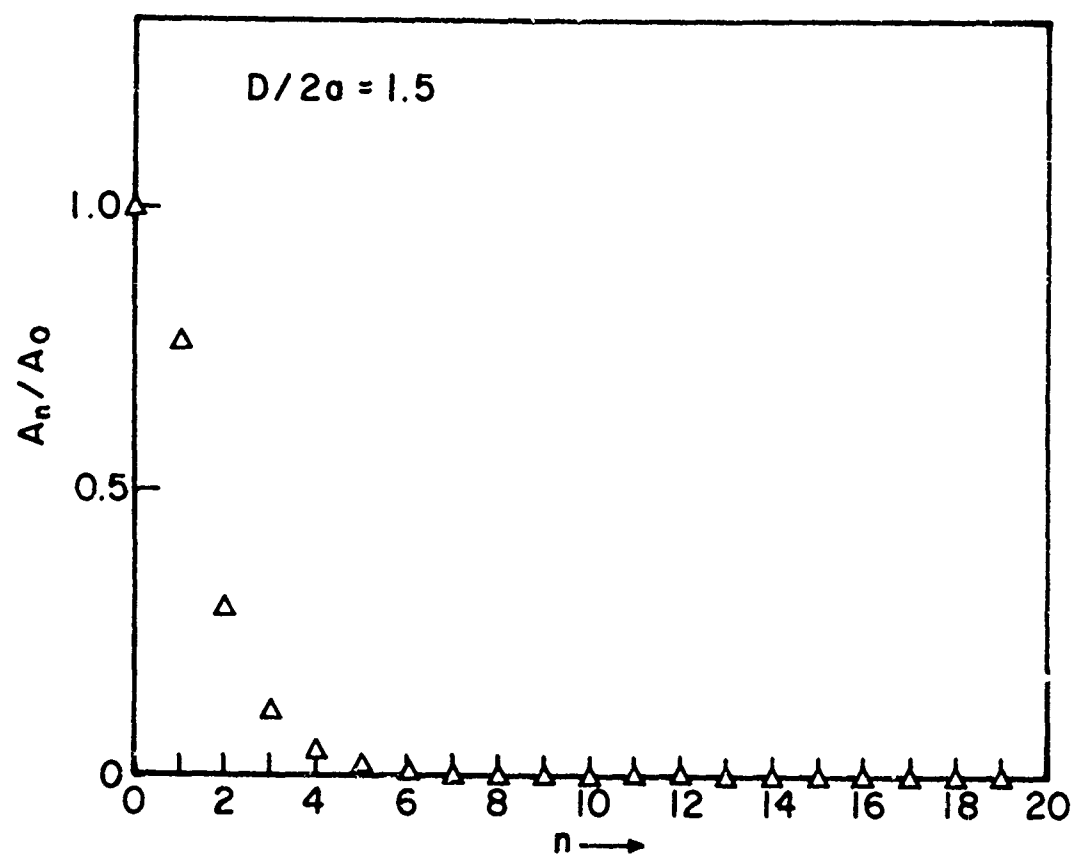


Figure A-5b Fourier coefficients of the two-wire problems ( $D/2a = 1.5$ ).

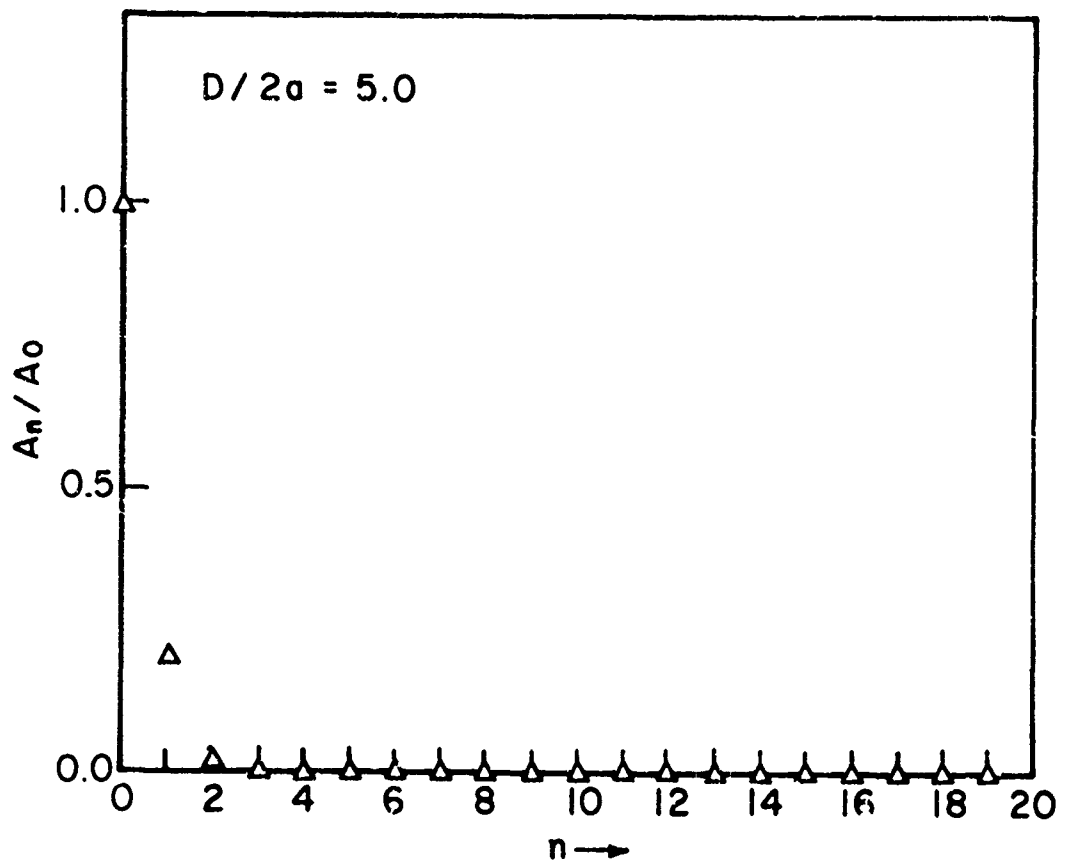


Figure A-5c Fourier coefficients of the two-wire problem ( $D/2a = 5.0$ ).

From this analysis then, one would suspect that the  $\phi$ -variation of the longitudinal current could not be neglected unless the wires were several diameters apart.

In addition to the  $\phi$ -directed and  $\phi$ -dependent currents one must justify the neglect of the  $\rho$ -directed current. Consider the four disks of  $\rho$ -directed currents (two at the gap and two at the ends of the dipole of Fig. A-1). For small  $ka$ , the radial ( $\rho$ -directed) currents are ineffective radiators for several reasons. All of the current elements are electrically short and are ineffective radiators for that reason. Furthermore, the directions of the currents on opposite sides of a disk are such as lead to cancellation. Further, the currents on the two gap disks tend to cancel. The currents on the end disks are considerably smaller than those on the gap disks. Note that very close proximity of parallel wires would upset some but not all of these conclusions. Thus, in most problems, there is a high order of cancellation of the effects of the radial currents and they may, therefore, be neglected.

In summary, for thin-wire antennas ( $ka \ll 1$ ), the surface currents  $J_\phi$  and  $J_\rho$  may be neglected. The circumferential variation of  $J_z$  may be neglected and the resultant uniform surface current  $J_z$  may be replaced by a filament of current along the axis of the wire. These conclusions are based upon a consideration of plane wave scattering by a cylinder. For thin wires very close together (within a few radii of each other), these assumptions may be invalid.

APPENDIX B -  $z_{ij}$  FOR STRAIGHT PARALLEL WIRES WITH PULSE  
EXPANSION FUNCTIONS AND IMPULSIVE WEIGHTS

In this appendix  $z_{ij}$  is expressed in terms of the  $\psi$  function. Fig. B-1a shows the typical subsections  $\Delta\ell_i$ ,  $\Delta\ell_j$  with currents  $i_i$ ,  $i_j$ .  $z_{ij}$  may be expressed as follows (see Eq. (1-26)).

$$z_{ij} = -\frac{\Delta\ell_i}{j\omega\epsilon} \left( \frac{\partial^2}{\partial z_i^2} + k^2 \right) \int_{\Delta\ell_j} \frac{-jk|\underline{r}_i - \underline{r}'|}{4\pi|\underline{r}_i - \underline{r}'|} dz' \quad (B-1)$$

$$= -\frac{\Delta\ell_i \Delta\ell_j}{j\omega\epsilon} \left( \frac{\partial^2}{\partial z_i^2} + k^2 \right) \psi \quad (B-2)$$

$$\text{where } \psi = \frac{1}{\Delta\ell_j} \int_{\Delta\ell_j} \frac{-jk|\underline{r}_i - \underline{r}'|}{4\pi|\underline{r}_i - \underline{r}'|} dz'$$

Note that  $\psi$  is proportional to the tangential magnetic vector potential  $A_z$  at one subsection ( $\Delta\ell_i$ ) due to unit current on another ( $\Delta\ell_j$ ). Fig. B-1a shows the basic geometry.

The origin may be translated to the center of subsection  $\Delta\ell_j$  as in Fig. B-1b without loss of generality. For simplification, coordinates  $(x_i, y_i, z_i)$  of the field point  $i$  are replaced in this appendix with  $(x, y, z)$ ,  $(r, \theta, \phi)$ ,  $(\rho, \phi, z)$  in rectangular, spherical, and cylindrical coordinates as shown in Fig. B-1b. Because of rotational symmetry,  $\psi$  is independent of  $\phi$  and depends only on  $\rho, z$ , and the electrical length  $(k\Delta\ell_j)$  of subsection  $\Delta\ell_j$ . Eq. (B-2) becomes

$$z_{ij} = j\omega\mu\Delta\ell_i \Delta\ell_j \psi - \frac{\Delta\ell_i \Delta\ell_j}{j\omega\epsilon} \frac{\partial^2 \psi}{\partial z^2} \quad (B-3)$$

upon replacing  $z_i$  with  $z$ .

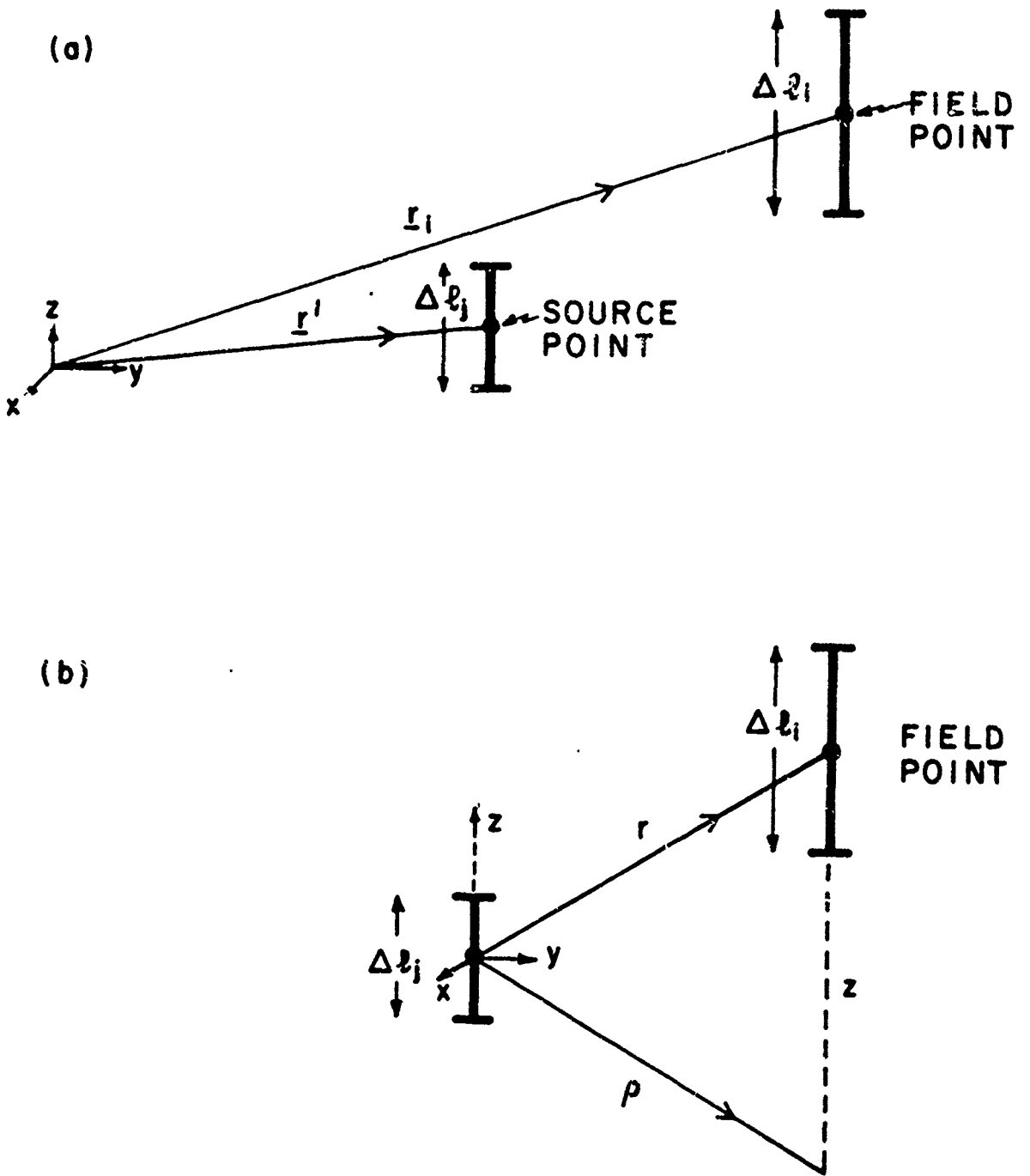


Figure B-1 Typical parallel subsections for thin-wire antenna problems  
 (a) general location (b) translation to the origin.

$\partial\psi/\partial z$  may be approximated by finite differences as follows:

$$\frac{\partial\psi}{\partial z} = \frac{\psi(x, y, z + \frac{\Delta z}{2}) - \psi(x, y, z - \frac{\Delta z}{2})}{\Delta z} \quad (B-4)$$

where  $\Delta z$  is a small length increment - not necessarily equal to  $\Delta l_i$  and where  $\psi(x, y, z + \frac{\Delta z}{2})$  is proportional to the potential at point  $(x, y, z + \frac{\Delta z}{2})$  with the source subsection  $\Delta l_j$  fixed as in Fig. (B-1b) with center at the origin. Equation (B-4) is written in shorthand notation as

$$\frac{\partial\psi}{\partial z} = \frac{\psi(+ \frac{\Delta z}{2}) - \psi(- \frac{\Delta z}{2})}{\Delta z} \quad (B-5)$$

Note that  $\partial\psi/\partial z$  may also be evaluated by keeping the field point fixed and shifting the source subsection  $\Delta l_j$ , ie

$$\frac{\partial\psi}{\partial z} = \frac{-[\psi(+ \frac{\Delta z'}{2}) - \psi(- \frac{\Delta z'}{2})]}{\Delta z'} \quad (B-6)$$

where  $\psi(+ \frac{\Delta z'}{2})$  is proportional to the potential at field point i with the center of the source subsection  $(\Delta l_i)$  shifted to  $(0, 0, \frac{\Delta z'}{2})$  i.e., shifted upwards by an increment  $\frac{\Delta z'}{2}$ .  $\psi(- \frac{\Delta z'}{2})$  indicates a downward shift.

Eqs. (B-5) and (B-6) are related to the identity

$$\frac{\partial r}{\partial z} = - \frac{\partial r}{\partial z'}$$

where  $r = \sqrt{(x-x')^2 + (z-z')^2 + (v-y')^2}$

Now

$$\begin{aligned} \frac{\partial^2 \psi}{\partial z^2} &= \frac{\partial}{\partial z} \left[ \frac{\psi(- \frac{\Delta z'}{2}) - \psi(+ \frac{\Delta z'}{2})}{\Delta z'} \right] \\ &= \left[ \frac{\partial}{\partial z} [\psi(- \frac{\Delta z'}{2})] - \frac{\partial}{\partial z} [\psi(+ \frac{\Delta z'}{2})] \right] \frac{1}{\Delta z'} \end{aligned} \quad (B-7)$$

$\frac{\partial}{\partial z} [\psi(-\frac{\Delta z'}{2})]$  represents the derivative of  $\psi$  with a shifted source subsection; this may be evaluated by shifting the field point by  $\Delta z/2$ :

$$\frac{\partial}{\partial z} [\psi(-\frac{\Delta z'}{2})] = \frac{\psi(-\frac{\Delta z'}{2}, + \frac{\Delta z}{2}) - \psi(-\frac{\Delta z'}{2}, - \frac{\Delta z}{2})}{\Delta z} \quad (B-8)$$

and

$$\frac{\partial}{\partial z} [\psi(\frac{+\Delta z'}{2})] = \frac{\psi(+\frac{\Delta z'}{2}, + \frac{\Delta z}{2}) - \psi(+\frac{\Delta z'}{2}, - \frac{\Delta z}{2})}{\Delta z} \quad (B-9)$$

where  $\psi(+\frac{\Delta z'}{2}, - \frac{\Delta z}{2})$  represents  $\psi$  with  $\Delta \ell_j$  of Fig. B-1b shifted  $\frac{\Delta z'}{2}$  upwards and  $\Delta \ell_i$  shifted  $\frac{\Delta z}{2}$  downwards, etc.

Collecting terms:

$$\begin{aligned} \frac{\partial^2 \psi}{\partial z^2} = & - \frac{1}{\Delta z \Delta z'} [\psi(+\frac{\Delta z'}{2}, + \frac{\Delta z}{2}) - \psi(+\frac{\Delta z'}{2}, - \frac{\Delta z}{2}) \\ & - \psi(-\frac{\Delta z'}{2}, + \frac{\Delta z}{2}) + \psi(-\frac{\Delta z'}{2}, - \frac{\Delta z}{2})] \end{aligned} \quad (B-10)$$

Substituting in Eq. (B-3) yields

$$\begin{aligned} z_{ij} = & j\omega\mu\Delta\ell_i\Delta\ell_j\psi + \frac{1}{j\omega\epsilon} \frac{\Delta\ell_i\Delta\ell_j}{\Delta z \Delta z'} [\psi(+\frac{\Delta z'}{2}, + \frac{\Delta z}{2}) - \psi(\frac{\Delta z'}{2}, - \frac{\Delta z}{2}) \\ & - \psi(-\frac{\Delta z'}{2}, + \frac{\Delta z}{2}) + \psi(-\frac{\Delta z'}{2}, - \frac{\Delta z}{2})] \end{aligned} \quad (B-11)$$

Note that Eq. (B-11) involves the evaluation of five different  $\psi$  functions with vectors  $\underline{r}_{ij}$ ,  $\underline{r}_{ij}(+ +)$ ,  $\underline{r}_{ij}(+ -)$ , etc. as shown in Fig. B-2, and corresponding terms  $z_{ij}(+ -)$ ,  $z_{ij}(+ +)$  where  $z_{ij}(+ -)$  represents the distance from shifted field point  $i$  to the perpendicular bisector plane of shifted source subsection  $\Delta\ell_j$ , etc. Each of the different  $\psi$  functions may be evaluated by the methods outlined by Harrington [1], [2].

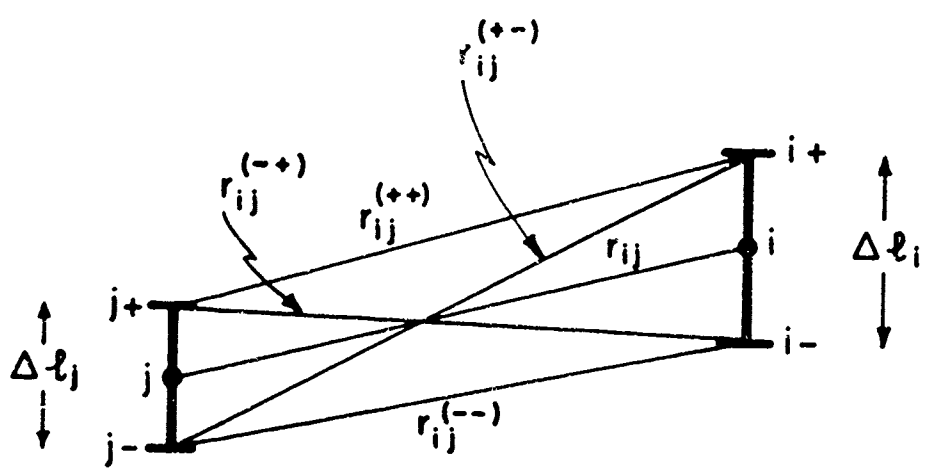


Figure B-2 Distance elements for parallel subsections.

Eq. (B-11) has been derived under a consideration of current distribution alone; the charge distribution is determined by the equation of continuity. Thus pulse current expansion functions lead to impulsive charges at the ends of each subsection.

It is interesting to compare the foregoing result based on Eq. (1-19) and assuming pulse currents and impulsive charges, with one based on Eq. (1-12) and derived under the assumption of pulse expansion functions for both currents and charge [3]. This latter combination is inconsistent mathematically but represents a more realistic charge distribution.

If  $\Delta z = \Delta \ell_i$ ,  $\Delta z' = \Delta \ell_j$ , then Eq. (B-11) becomes

$$z_{ij} = j\omega\mu\Delta\ell_i\Delta\ell_j\psi + \frac{1}{j\omega\epsilon} [\psi(++) - \psi(+-) - \psi(-+) + \psi(--)] \quad (B-12)$$

which agrees with Eq. (22) of [3]. Thus the two methods (pulse currents and impulsive charges - pulse currents and pulse charges) lead to identical results if the increments  $\frac{\Delta z}{2}$ ,  $\frac{\Delta z'}{2}$  used for finite differences are half subsections.

## APPENDIX C - SYMMETRY ABOUT THE MAIN DIAGONAL FOR THE MATRICES [z] AND [D]

In general, for the method of moments, the matrices [z] and [D] are not symmetric about the main diagonal, i.e.

$$z_{ij} \neq z_{ji}$$

$$D_{ij} \neq D_{ji}$$

where  $z_{ij}$  is the voltage at subsection i due to unit current density on subsection j (in time-harmonic problems) and  $D_{ij}$  is the potential at subsection i due to unit charge/unit charge density\* on subsection j [40].

If the weighting and expansion functions are identical (Galerkin's method, a variational solution), then the matrices [z] or [D] are symmetrical about the main diagonal.

For parallel current segments  $\Delta l_i$ ,  $\Delta l_j$  of equal length,  $z_{ij} = z_{ji}$ .

For parallel segments of unequal length, or for skewed segments,  $z_{ij}$  is not necessarily equal to  $z_{ji}$ . Similar distinctions apply to charge filaments  $\Delta l_i$ ,  $\Delta l_j$  and  $D_{ij}$ ,  $D_{ji}$  functions.

Consider an example from electrostatics consisting of two perpendicular, thin, charged wires, two typical subsections of which are shown in Fig. C-1. Subsections  $\Delta l_i$  and  $\Delta l_j$  are shown with line charge densities  $\lambda_i$  and  $\lambda_j$  and subsection centers i and j respectively. Subsection lengths differ:

$$\Delta l_i = c$$

$$\Delta l_j = b$$

and the separation of subsections is equal to "a".  $D_{ij}$  is the potential at

---

\*  $D_{ij}$  may be defined as potential due to unit charge or unit charge density. The former definition is used here.

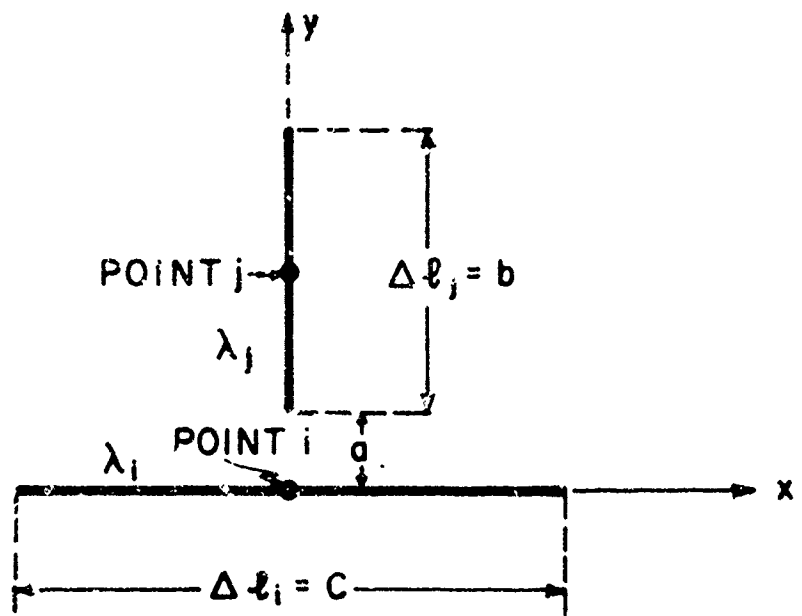


Figure C-7 Two perpendicular, thin, charged wires.

point  $i$  due to unit charge on subsection  $\Delta \lambda_j$  and  $D_{ji}$  is the potential at point  $j$  due to unit charge on subsection  $\Delta \lambda_i$ .

$$D_{ij} = \frac{V_i}{(\lambda_j b)} = \left(\frac{1}{\lambda_j b}\right) \frac{1}{4\pi\epsilon_0} \int_a^{a+b} \frac{\lambda_j dy'}{y'} = \frac{1}{4\pi\epsilon_0 b} \log\left(1 + \frac{b}{a}\right) \quad (C-1)$$

where  $V_i$  is the potential at point  $i$  due to  $\lambda_j$ .

$$D_{ji} = \frac{1}{4\pi\epsilon_0 c} \int_{-c/2}^{c/2} \frac{dx'}{\sqrt{(x')^2 + (a + \frac{b}{2})^2}} = \frac{1}{4\pi\epsilon_0 c} \log \frac{\frac{c}{2} + \sqrt{\frac{c^2}{4} + (a + \frac{b}{2})^2}}{-\frac{c}{2} + \sqrt{\frac{c^2}{4} + (a + \frac{b}{2})^2}} \quad (C-2)$$

where  $\log$  indicates the natural logarithm.

If  $b = c$ , then Eq. (C-2) becomes

$$D_{ji} = \frac{1}{4\pi\epsilon_0 b} \log \frac{\frac{b}{2} + \sqrt{a^2 + ab + \frac{b^2}{2}}}{-\frac{b}{2} + \sqrt{a^2 + ab + \frac{b^2}{2}}} \quad (C-3)$$

Clearly  $D_{ij}$  is not equal to  $D_{ji}$ , even for  $b = c$ . However, as the separation increases ( $b/a$  and  $c/a$  approach zero),  $D_{ij}$  approaches  $D_{ji}$ :

$$D_{ij} = \frac{1}{4\pi\epsilon_0 b} \log (1 + b/a) \approx \frac{1}{4\pi\epsilon_0 a} \quad (\because a \ll 1) \quad (C-4)$$

$$\begin{aligned} D_{ji} &= \frac{1}{4\pi\epsilon_0 c} \log \frac{\frac{c}{2} + a\sqrt{1 + \frac{b^2 + c^2}{4a^2} + \frac{b}{a}}}{-\frac{c}{2} + a\sqrt{1 + \frac{b^2 + c^2}{4a^2} + \frac{b}{a}}} \approx \frac{1}{4\pi\epsilon_0 c} \log \frac{\frac{c}{2} + a(1 + \frac{b}{2a})}{-\frac{c}{2} + a(1 + \frac{b}{2a})} \\ &= \frac{1}{4\pi\epsilon_0 c} \log \frac{1 + c/(2a + b)}{1 - c/(2a + b)} \approx \frac{1}{4\pi\epsilon_0 c} \log [1 + 2c/(2a + b)] \\ &\approx \frac{1}{4\pi\epsilon_0 a} \quad (b/a \ll 1, \quad c/a \ll 1) \end{aligned} \quad (C-5)$$

Fig. C-2 shows a plot of  $R$  (where  $R = D_{ij}/D_{ji}$ ), as a function of  $b/a$ , for the special case  $b = c$ . Note that the matrix  $[D]$  is highly asymmetric about the main diagonal for large  $b/a$ , and that  $D_{ij}$  is indistinguishable from  $D_{ji}$  for  $b/a < 0.3$ . Stewart [128] has shown explicitly that, if pulse weighting and expansion functions are used in this problem,  $D_{ij} = D_{ji}$ . This is true in general; the Galerkin method always yields matrices symmetric about the main diagonal.

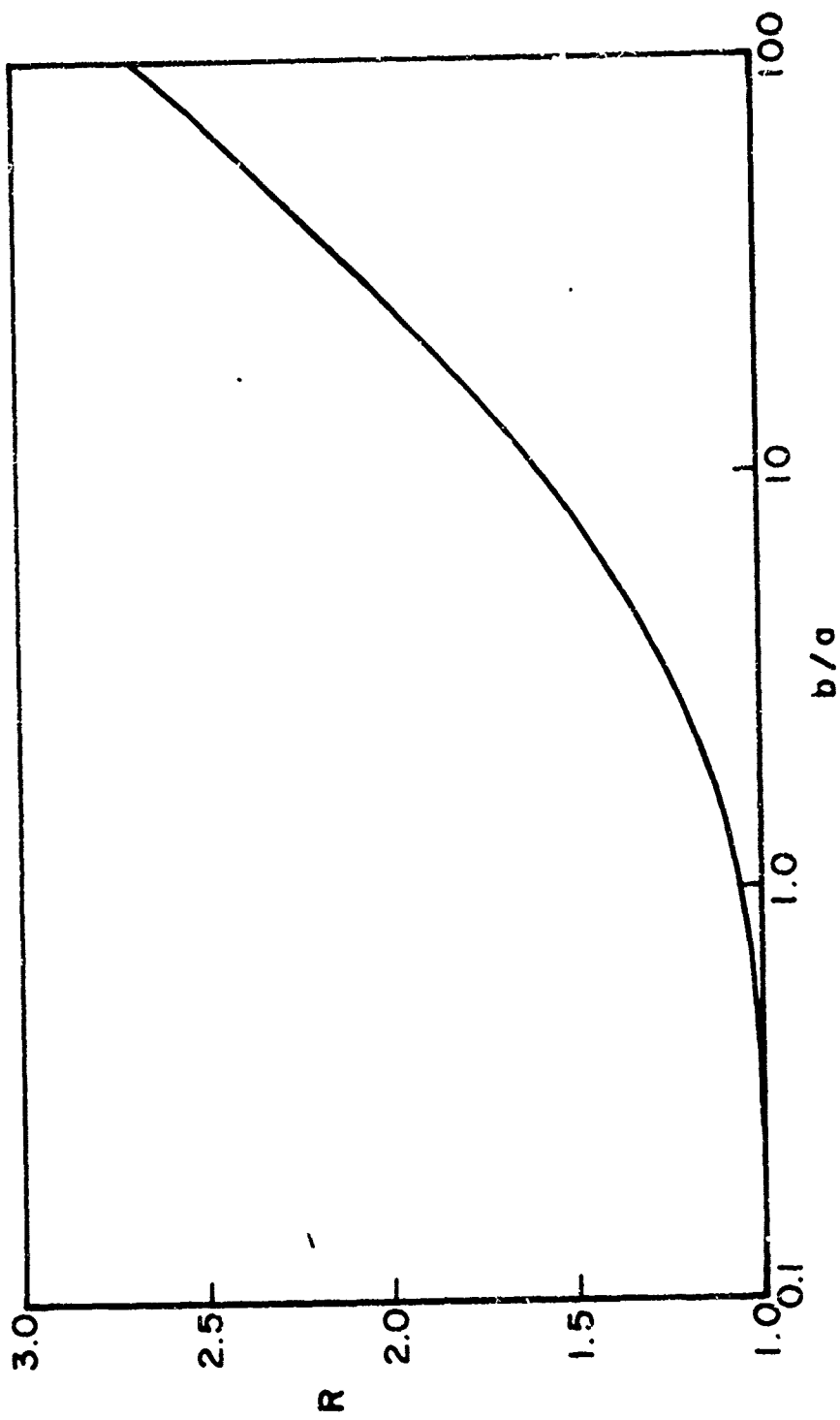


Figure C-2 Ratio  $R$  ( $D_{ij}/D_{j1}$ ) as a function of  $b/a$ .

#### ACKNOWLEDGMENT

The author wishes to acknowledge the contributions of Thomas E. Baldwin, Jr., Joseph Clements, Andrew Farrar, James Logan, Ephraim Mendelovicz, Ada Mendelovicz, Kenneth Siarkiewicz, C. Bruce Varnado, and Daniel Warren to the studies described in this volume and to Drs. Bradley J. Strait, J.R. Mautz and R.F. Harrington for useful conversation and advice.

## REFERENCES

- [ 1] R.F. Harrington, Field Computation by Moment Methods, Macmillan Co., New York, 1968.
- [ 2] R.F. Harrington, "Matrix Methods for Field Problems", Proc. IEEE, vol. 55, pp. 136-149, Feb. 1967.
- [ 3] B.J. Strait and A.T. Adams, "Analysis and Design of Wire Antennas with Applications to EMC", IEEE Trans. on Electromagnetic Compatibility, vol. EMC-12, No. 2, May 1970, pp. 45-54.
- [ 4] A.T. Adams and B.J. Strait, "Modern Analysis Methods for EMC", 1970 IEEE-EMC Symposium Record, July 1970, pp. 383-393.
- [ 5] H. Cavendish, Electrical Researches, Cambridge Univ. Press, Cambridge, England, 1879, pp. 394, 424.
- [ 6] T. Higgins and D.K. Reitan, "Calculation of the Capacitance of a Circular Annulus by the Method of Subareas", AIEE Trans. vol. 70, 1951, pp. 926-933.
- [ 7] D. Reitan and T. Higgins, "Calculation of the Electrical Capacitance of a Cube", J. Appl. Phys., vol. 22, No. 2, Feb. 1951, pp. 223-226.
- [ 8] J.J. Stiles and T.J. Higgins, "Determination of the Characteristic Impedance of UHF Coaxial Rectangular Transmission Lines", Proc. N.E.C., Chicago, Ill., vol. 10, Oct. 1954, pp. 97-108.
- [ 9] D. Reitan and T. Higgins, "Accurate Determination of the Capacitance of a Thin Conducting Plate", AIEE Trans., vo'. 75, Part I, Jan. 1957, pp. 761-766.
- [10] D.K. Reitan, "Accurate Determination of the Capacitance of Rectangular Parallel-Plate Capacitors", J. Appl. Phys., vol. 30, No. 2, Feb. 1959, pp. 172-176.
- [11] K.K. Mei and J.G. Van Biadel, "Scattering by Perfectly Conducting Rectangular Cylinders", IEEE Trans. on Antennas and Propagation, vol. AP-11, March 1963, pp. 185-192.
- [12] C.H. Tang, "Input Impedances of Arc Antennas and Short Helical Radiators", IEEE Trans. on Antennas and Propagation, vol. AP-12, Jan. 1964, pp. 2-9.
- [13] M.C. Andreasen and R.L. Tanner, "Radiation from a Generalized Antenna in a Stratified Medium", IEEE Trans. on Antennas and Propagation, vol. AP-12, No. 5, Sept. 1964, pp. 522-530.
- [14] M.G. Andreasen, "Scattering from Parallel Metallic Cylinders with Arbitrary Cross Sections", IEEE Trans. on Antennas and Propagation, vol. AP-12, Nov. 1964, pp. 746-754.

- [15] H.Y. Yee, "Scattering of Electromagnetic Waves by Circular Dielectric-Coated Conducting Cylinders with Arbitrary Cross Section", IEEE Trans. on Antennas and Propagation, vol. AP-13, Jan. 1965, pp. 141-149.
- [16] R.F. Harrington, "On the Calculation of Scattering by Conducting Cylinders", IEEE Trans. on Antennas and Propagation, vol. AP-13, Sept. 1965, pp. 812-813.
- [17] P.A. Laura, "Determination of Cutoff Frequencies of Waveguides with Arbitrary Cross Sections by Point-Matching", Proc. IEEE, vol. 53, No. 10, Oct. 1965, pp. 1660-1661.
- [18] H.Y. Yee and N.F. Audeh, "Cutoff Frequencies of Waveguides with Arbitrary Cross Sections", Proc. IEEE, vol. 53, No. 6, June 1965, pp. 637-638.
- [19] A. Baghdasarian and D.J. Angelacos, "Scattering from Conducting Loops and Solution of Circular Loop Antennas by Numerical Methods", Proc. IEEE, vol. 53, No. 8, August 1965, pp. 818-822.
- [20] Jack H. Richmond, "Digital Computer Solutions of the Rigorous Equations for Scattering Problems", Proc. IEEE, vol. 53, No. 8, Aug. 1965, pp. 796-800.
- [21] Jack H. Richmond, "Scattering by an Arbitrary Array of Parallel Wires", IEEE Trans. on Microwave Theory and Techniques, vol. MTT-13, July 1965, pp. 408-412.
- [22] H.Y. Yee and N.F. Audeh, "Uniform Waveguides with Arbitrary Cross Section Considered by the Point Matching Technique", IEEE Trans. on Microwave Theory and Techniques, MIT-13, Nov. 1965, pp. 847-851.
- [23] M.G. Andreasen, "Scattering from Cylinders with Arbitrary Surface Impedance", Proc. IEEE, vol. 53, No. 8, Aug. 1965, pp. 812-817.
- [24] J.H. Richmond, "Scattering by a Dielectric Cylinder of Arbitrary Cross Section Shape", IEEE Trans. on Antennas and Propagation, vol. AP-13, No. 3, May 1965, pp. 334-342.
- [25] K.K. Mei, "On the Integral Equations of Thin Wire Antennas", IEEE Trans. on Antennas and Propagation, vol. AP-13, No. 3, May 1965, pp. 374-378.
- [26] M.G. Andreasen, "Scattering from Bodies of Revolution", IEEE Trans. on Antennas and Propagation, vol. AP-13, March 1965, pp. 303-310.
- [27] H.Y. Yee and N.F. Audeh, "Cutoff Frequencies of Eccentric Waveguides", IEEE Trans. on Microwave Theory and Techniques, vol. MTT-14, Oct. 1966, pp. 487-493.
- [28] P.A. Laura, "Application of the Point-Matching Method in Waveguide Problems", IEEE Trans. on Microwave Theory and Techniques, vol. MTT-14, No. 5, May 1966, p. 251.

- [29] H.Y. Yee and N.F. Audeh, "Attenuation Constants of Waveguides with General Cross Sections", IEEE Trans. on Microwave Theory and Techniques, vol. MTT-14, May 1966, pp. 252-253.
- [30] H.Y. Yee, "On Determination of Cutoff Frequencies of Waveguides with Arbitrary Cross Section", Proc. IEEE, vol. 54, Jan. 1966, p. 64.
- [31] J.H. Richmond, "TE Scattering by a Dielectric Cylinder of Arbitrary Cross Section Shape", IEEE Trans. on Antennas and Propagation, vol. AP-14, No. 4, July 1966, pp. 460-465.
- [32] J.H. Richmond, "A Wire Grid Model for Scattering by Conducting Bodies", IEEE Trans. on Antennas and Propagation, vol. AP-14, Nov. 1966, pp. 782-786.
- [33] A. Wexler, "Solution of Waveguide Discontinuities by Modal Analysis", IEEE Trans. on Microwave Theory and Techniques, vol. MTT-15, No. 9, Sept. 1967, pp. 508-517.
- [34] R.L. Brooke and J.E. Cruz, "Current Distribution and Impedance of Lossless Conductor Systems", IEEE Trans. on Microwave Theory and Techniques, vol. MTT-15, No. 6, June 1967, pp. 358-364.
- [35] R.H.T. Bates, "The Point-Matching Method for Interior and Exterior Two-Dimensional Boundary Value Problems", IEEE Trans. on Microwave Theory and Techniques, vol. MTT-15, No. 3, March 1967, pp. 185-187.
- [36] J.H. Richmond, "Scattering by Imperfectly Conducting Wires", IEEE Trans. on Antennas and Propagation, vol. AP-15, No. 6, Nov. 1967, pp. 802-806.
- [37] R.F. Harrington and J.R. Mautz, "Straight Wires with Arbitrary Excitation and Loading", IEEE Trans. on Antennas and Propagation, vol. AP-15, No. 4, July 1967, pp. 502-515.
- [38] Y.S. Yeh and K.K. Mei, "Theory of Conical Equiangular-Spiral Antennas: Part I - Numerical Techniques", IEEE Trans. on Antennas and Propagation, Vol. AP-15, No. 5, Sept. 1967, pp. 634-639.

#### Syracuse University Bibliography

- [39] R.F. Harrington, Moment Methods for Field Computation, Macmillan Company, 1968.
- [40] A.T. Adams, Electromagnetics for Engineers, Ronald Press Co, New York, 1971, Chapters 8 and 9.
- [41] R.F. Harrington, "Matrix Methods for Field Problems", Proc. IEEE, vol. 55, No. 2, Feb. 1967, pp. 136-149.
- [42] R.F. Harrington, "Generalized Network Parameters in Field Theory", Proc. Symp. on Generalized Networks, MRI Symp. Series vol. XIV, Polytechnic Press, Brooklyn, N.Y., 1966, pp. 51-67.

- [43] R.F. Harrington and J.R. Mautz, "Straight Wires with Arbitrary Excitation and Loading", IEEE Trans. on Antennas and Propagation, vol. AP-15, No. 4, July 1967, pp. 502-515.
- [44] R.F. Harrington and J.R. Mautz, "Electromagnetic Behavior of Circular Wire Loops with Arbitrary Excitation and Loading", Proc. IEE (London), vol. 115, No. 1, Jan. 1968, pp. 68-77.
- [45] R.F. Wallenberg and R.F. Harrington, "Two-dimensional Radiation and Scattering from Conducting Cylinders of Arbitrary Shape", IEEE Trans. on Antennas and Propagation, vol. AP-17, No. 1, Jan. 1969, pp. 56-62.
- [46] B.J. Strait and K. Hirasawa, "Array Design for a Specified Pattern by Matrix Methods," IEEE Trans. on Antennas and Propagation, vol. AP-17, No. 2, March 1969, also reprinted in the book Significant Phased Array Papers by R.C. Hansen, Artech House, 1973.
- [47] J.R. Mautz and R.F. Harrington, "Radiation and Scattering from Bodies of Revolution", Appl. Sci. Res., vol. 20, June 1969, pp. 405-435.
- [48] R.F. Harrington, K. Pontoppidan, P. Abrahamsen, and N.C. Albertson, "Computation of Laplacian Potentials by an Equivalent Source Method", Proc. IEE (London), vol. 116, No. 10, Oct. 1969, pp. 1715-1720.
- [49] A.T. Adams and J.R. Mautz, "Computer Solution of Electrostatic Problems by Matrix Inversion", Proc. N.E.C., vol. 25, Dec. 1969.
- [50] B.J. Strait and K. Hirasawa, "On Radiation and Scattering from Arrays of Wire Antennas", Proc. NEC, vol. 25, Dec. 1969, pp. 242-247.
- [51] J.R. Mautz and R.F. Harrington, "Computation of Rotationally Symmetric Laplacian Potentials", Proc. IEE (London), vol. 117, No. 4, April 1970, pp. 850-851.
- [52] B.J. Strait and A.T. Adams, "Analysis and Design of Wire Antennas with Applications to EMC", IEEE Trans. on Electromagnetic Compatibility, vol. EMC-12, No. 2, May 1970, pp. 45-54.
- [53] B.J. Strait and K. Hirasawa, "On Long Wire Antennas with Multiple Excitation", IEEE Trans. on Antennas and Propagation, vol. AP-18, No. 5, September 1970.
- [54] A.T. Adams and B.J. Strait, "Modern Analysis Methods for EMC", 1970 EMC Symposium Record, July 1970, pp. 383-393.
- [55] K. Hirasawa and B.J. Strait, "On a Method for Array Design by Matrix Inversion", IEEE Trans. on Antennas and Propagation, vol. AP-19, No. 3, May 1971, pp. 446-447.

- [56] A. Farrar and A.T. Adams, "Computation of Lumped Microstrip Capacities by Matrix Methods - Rectangular Sections and End Effect", IEEE Trans. on Microwave Theory and Techniques, MTT-19, No. 5, May 1971, pp. 495-497, also reprinted in Microwave Integrated Circuits by J. Frey, Artech House, 1974.
- [57] H.H. Chao and B.J. Strait, "Radiation and Scattering by Configurations of Bent Wires with Junctions", IEEE Trans. on Antennas and Propagation, vol. AP-19, No. 5, Sept. 1971, pp. 701-702.
- [58] R.F. Harrington and J.R. Mautz, "Theory of Characteristic Modes for Conducting Bodies", IEEE Trans. on Antennas and Propagation, vol. AP-19, No. 5, Sept. 1971, pp. 622-628.
- [59] R.F. Harrington and J.R. Mautz, "Computation of Characteristic Modes for Conducting Bodies", IEEE Trans. on Antennas and Propagation, vol. AP-19, No. 5, Sept. 1971, pp. 629-639.
- [60] B.J. Strait and R.F. Harrington, "Computer-Aided Antenna Design", Proc. IEEE Fall Electronics Conference, Oct. 1971, pp. 474-479.
- [61] R.F. Harrington, J.R. Mautz, Y. Chang, "Characteristic Modes for Dielectric and Magnetic Bodies", IEEE Trans. on Antennas and Propagation, vol. AP-20, No. 2, March 1972, pp. 194-198.
- [62] E.P. Savre and R.F. Harrington, "Time Domain Radiation and Scattering by Thin Wires", Appl. Sci. Res., vol. 27, April 1972.
- [63] R.F. Harrington and J.R. Mautz, "Green's Functions for Surfaces of Revolution", Radio Science, vol. 7, No. 5, May 1972, pp. 603-611.
- [64] R.F. Harrington and J.R. Mautz, "Control of Radar Scattering by Reactive Loading", IEEE Trans. on Antennas and Propagation, vol. AP-20, No. 4, July 1972, pp. 446-454.
- [65] A. Farrar and A.T. Adams, "Matrix Methods for Microstrip Three-Dimensional Problems", IEEE Trans. on Microwave Theory and Techniques, vol. MTT-20, No. 8, Aug. 1972, pp. 497-504; also reprinted in part in the 1974 Microwave Engineers Handbook, Microwave Journal, Jan. 1974, p. 81.
- [66] B.E. Spielman and R.F. Harrington, "Waveguides of Arbitrary Cross Section by Solution of a Nonlinear Integral Eigenvalue Equation", IEEE Trans. on Microwave Theory and Techniques, vol. MTT-20, No. 9, Sept. 1972, pp. 578-585.
- [67] B.J. Strait and K. Hirasawa, "Constrained Optimization of the Gain of an Array of Thin Wire Antennas", IEEE Trans. on Antennas and Propagation, vol. AP-20, No. 5, Sept. 1972, pp. 665-666.
- [68] K. Hirasawa and D.H. Sinnott, "On the Relationship Between Classical and Matrix Design Methods for Arrays of Wire Antennas", IEEE Trans. on Antennas and Propagation, vol. AP-20, No. 5, Sept. 1972, pp. 661-663.

- [69] D.C. Kuo, H.H. Chao, J.R. Mautz, B.J. Strait, and R.F. Harrington, "Analysis of Radiation and Scattering by Arbitrary Configurations of Thin Wires", (Program Description) IEEE Trans. on Antennas and Propagation, vol. AP-20, No. 6, Nov. 1972, pp. 814-815.
- [70] A. Farrar and A.T. Adams, "A Potential Theory Method for Covered Micro-strip", IEEE Trans. on Microwave Theory and Techniques, vol. MTT-21, No. 7, July 1973, pp. 494-496.
- [71] A.T. Adams, B.J. Strait, D.W. Warren, D.C. Kuo, and T.E. Baldwin, Jr., "Near Fields of Wire Antennas by Matrix Methods", IEEE Trans. on Antennas and Propagation, vol. AP-21, No. 5, Sept. 1973, pp. 602-610.
- [72] J.R. Mautz and R.F. Harrington, "Modal Analysis of Loaded N-port Scatterers", IEEE Trans. on Antennas and Propagation, vol. AP-21, March 1973, pp. 188-199.
- [73] D.E. Warren, T.E. Baldwin, and A.T. Adams, "Near Electric and Magnetic Fields of Wire Antennas", IEEE Trans. on Antennas and Propagation, vol. AP-22 No. 2, March 1974, p. 364. Program and description on deposit: ASIS-NAPS Document No. NAPS-02221.
- [74] A.T. Adams, R. Greenough, R. Wallenberg, A. Mendelovitz, and C. Lumjiaak, "The Quadrifilar Helix Antenna", IEEE Trans. on Antennas and Propagation, vol. AP-22, No. 2, March 1974, pp. 173-178.
- [75] E. Mendelovitz, A.T. Adams, K. Siarkiewicz and A. Mendelovitz, "Feedline Interference with Dipole Performance - Theory and Experiment", IEEE Trans. on Antennas and Propagation, vol. AP-15, No. 2, May 1974, pp. 90-97.
- [76] A. Farrar and A.T. Adams, "Multilayer Microstrip Transmission Lines", IEEE Trans. on Microwave Theory and Techniques, October 1974.
- [77] I.W. Bristol, "Waveguides of Arbitrary Cross Section", Ph.D. Dissertation, Syracuse University, Nov. 1967.
- [78] R.F. Wallenberg, "Two-dimensional Scattering and Radiation from Perfectly Conducting Cylinders of Arbitrary Shape", Ph.D. Dissertation, Syracuse University, March 1968.
- [79] J.R. Mautz, "Radiation and Scattering from Bodies of Revolution", Ph.D. Dissertation, Syracuse University, June 1968.
- [80] R.H. Kyle, "Mutual Coupling Between Log-Periodic Dipole Antennas", Ph.D. Dissertation, Syracuse University, December 1968.
- [81] J.A. Cummins, "Analysis of a Circular Array of Antennas by Matrix Methods", Ph.D. Dissertation, Syracuse University, December 1968.
- [82] E.P. Sayre, "Transient Response of Wire Antennas and Scatterers", Ph.D. Dissertation, Syracuse University, May 1969.
- [83] T.E. Baldwin, "Near Field Analysis of Arrays", M.S. Thesis, Syracuse University, May 1970.

- [84] A. Mendelovicz, "Numerical Solution for Scattering and Radiation of a Quadrifilar Helix", M.S. Thesis, Syracuse University, June 1970.
- [85] H.H. Chao, "Computer Programs for Radiation and Scattering by Arbitrary Configurations of Bent Wires", M.S. Thesis, Syracuse University, Sept. 1970.
- [86] R. Spielman, "Waveguides of Arbitrary Cross Section by Solution of a Nonlinear Integral Eigenvalue Equation", Ph.D. Dissertation, Syracuse University, January 1971.
- [87] K. Hirasawa, "Analysis and Design of Arrays of Loaded Thin Wires by Matrix Methods", Ph.D. Dissertation, Syracuse University, May 1971.
- [88] R. Joseph, "Effects of Matrix Thinning in Analyzing Dipole Arrays by the Method of Moments", M.S. Thesis, Syracuse University, June 1971.
- [89] D.C. Kuo, "Analysis of the Electromagnetic Behaviour of Thin-Wire Antennas and Scatterers with Emphasis upon the Near Fields", M.S. Thesis, Syracuse University, April 1972.
- [90] D. Sinnott, "Analysis and Design of Circular Arrays by Matrix Methods", Ph.D. Dissertation, Syracuse University, January 1972.
- [91] W.E. Cramer, "Inversion of Block Toeplitz Matrices for Electrostatic Problems", M.S. Thesis, Syracuse University, May 1973.
- [92] J.C. Logan, "A Comparison of Techniques for Treating Radiation and Scattering by Wire Configurations with Junctions", M.S. Thesis, Syracuse University, August 1973.
- [93] R.F. Harrington and J.R. Mautz, "Radiation and Scattering from Bodies of Revolution", Report AFCRL 69-0305, July 1969 (AD 895 670).
- [94] B.J. Strait and K. Hirasawa, "Computer Programs for Radiation, Reception and Scattering by Loaded Straight Wires", Report AFCRL-69-0440, Oct. 1969 (AD 697 481).
- [95] B.J. Strait and K. Hirasawa, "Computer Programs for Analysis and Design of Linear Arrays of Loaded Wire Antennas", Report AFCRL-70-0108, Feb. 1970 (AD 702 925).
- [96] R.F. Harrington and J.R. Mautz, "Computation of Radiation and Scattering from Loaded Bodies of Revolution", Report AFCRL-70-0046, Jan. 1970 (AD 701 744).
- [97] R.F. Harrington and J.R. Mautz, "Computation of Green's Functions for Bodies of Revolution", Report AFCRL-70-0393, July 1970 (AD 711 099).
- [98] H.H. Chao and B.J. Strait, "Computer Programs for Radiation and Scattering by Arbitrary Configurations of Bent Wires", Report AFCRL-70-0374, Sept. 1970 (AD 713 156).

- [ 99] R.F. Harrington and J.R. Mautz, "Theory and Computation of Characteristic Modes for Conducting Bodies", Report AFCRL-70-0657, Dec. 1970 (AD 716 494).
- [100] J.R. Mautz and R.F. Harrington, "Computer Programs for Characteristic Modes for Bodies of Revolution", Report AFCRL-71-0014, Jan. 1971 (AD 718 969).
- [101] J.R. Mautz and R.F. Harrington, "Computer Programs for Characteristic Modes of Wire Objects", Report AFCRL-71-0174, March 1971 (AD 722 62).
- [102] K. Hirasawa and B.J. Strait, "Analysis and Design of Arrays of Loaded Thin Wires by Matrix Methods", Report AFCRL-71-0296, May 1971 (AD 725 767).
- [103] J.R. Mautz and R.F. Harrington, "Control of Radar Scattering by Reactive Loading", Report AFCRL-71-0429, August 1971 (AD 729 926).
- [104] D.C. Kuo and B.J. Strait, "A Program for Computation of Near Fields of Thin Wire Antennas", Report AFCRL-71-0463, Sept. 1971 (AD 731 178).
- [105] D.C. Kuo and B.J. Strait, "Improved Programs for Analysis of Radiation and Scattering by Configurations of Arbitrarily Bent Thin Wires", Report AFCRL-72-0051, Jan. 1972.
- [106] R.F. Harrington and J.R. Mautz, "Modal Analysis of Loaded N-port Scatterers", Report AFCRL-72-0179, March 1972.
- [107] R.F. Harrington and J.R. Mautz, "Synthesis of Loaded N-port Scatterers", Report AFCRL-72-0665, October 1972.
- [108] B.J. Strait and D.C. Kuo, "Optimization Methods for Arrays of Parallel Wire Antennas", AFCRL-72-0725, Dec. 1972.
- [109] B.J. Strait, T. Sarkar, and D.C. Kuo, "Special Programs for Analysis of Radiation by Wire Antennas", AFCRL-TR-73-0399, June 1973.
- [110] A.T. Adams, T.E. Baldwin, D.E. Warren and E. Mendelovicz, "Near Fields of Thin-Wire Antennas", RADC TR-73-217, vol. II, August 1973, AD767 909/5
- [111] J.R. Mautz and R.F. Harrington, "Computational Methods for Antenna Pattern Synthesis", AFCRL-TR-73-0500, August 1973.
- [112] J.R. Mautz and R.F. Harrington, "Computer Programs for Antenna Pattern Synthesis", AFCRL-73-0654, Oct. 1973.
- [113] E. Mendelovicz, A.T. Adams, K. Siarkiewicz, and A. Mendelovicz, "Feedline Interference with Dipole Performance - Theory and Experiment", RADC TR-73-217, vol. IV, Jan. 1974, AD773 173/0GI
- [114] B.J. Strait, T. Sarkar, and D.C. Kuo, "Programs for Analysis of Radiation by Linear Arrays of Vertical Wire Antennas over Imperfect Ground", AFCRL Scientific Report, January 1974.
- [115] A.T. Adams, "An Introduction to the Method of Moments", RADC TR-73-217, vol. I, Aug. 1974.

End of Syracuse University Bibliography

- [116] A Short Course in Electromagnetic Theory on Wire Antennas and Scatterers, vols. 1 and 2, University of Mississippi Short Course, University, Mississippi, April 24-28, 1972.
- [117] The Application of Moment Methods to Field Problems, University of Mississippi short course, University, Mississippi, May 8-11, 1973.
- [118] Computer Techniques for Electronics and Antennas, University of Illinois short course, Urbana, Illinois, March 1970.
- [119] The Application of GT and Numerical Techniques to the Analysis of Electromagnetic and Acoustic Radiation and Scattering, vols. 1 - 2, Ohio State University short course, Columbus, Ohio, Sept. 10-14, 1973.
- [120] Numerical Techniques for Antennas and Electromagnetics, vols. 1-6, UCLA short course, Los Angeles, California, June 25-29, 1973.
- [121] Computer Electromagnetics Course, vols. 1-5, University of Naples short course, Sorrento, Italy, Sept. 5-8, 1972.
- [122] Numerical and Asymptotic Techniques for Electromagnetics, University of Trondheim short course, Trondheim, Norway, July 1-5, 1974.
- [123] Computer Techniques for Electronics and Antennas, R. Mittra (Ed.), Pergamon Press, 1972.
- [124] J.R. Mautz, "Radiation and Scattering from Two Perfectly Conducting Surfaces of Revolution whose Axes are Parallel", Internal Memorandum, Dept. of Electrical and Computer Engineering, Syracuse University, Sept. 1973.
- [125] J.H. Richmond, "Radiation and Scattering by Thin-Wire Structures in the Complex Frequency Domain", Report 2902, The Ohio State University Electromagnetic Laboratory, July 1973.
- [126] J.H. Richmond, "Radiation and Scattering by Thin Wire Structures in a Homogeneous Conducting Medium", IEEE Trans. on Antennas and Propagation, vol. AP-22, No. 2, March 1974, p. 365. Program and description of deposit: ASIS-NAPS Document No. NAPS-02223.
- [127] Antenna Modeling Program: Engineering Manual (Report IS-R-72/10 , July 1972) User Manual (Report IS-R-72/15, July 1973), Systems Manual (Report IS-R-72/10) of April 1973). Information Systems Division of MB Associates, Menlo Park, California.
- [128] J.R. Stewart, "Application of Optimization Theory to Electromagnetic Radiation and Scattering", Ph.D. Thesis, Syracuse University, Jan. 1974.
- [129] W.W. Everett, Ed. Topics in Intersystem Electromagnetic Compatibility, Holt, Rinehart and Winston, New York, 1972, chapter 15.
- [130] A.T. Adams and E. Mendelovicz, "The Near Field Polarization Ellipse", IEEE Trans. on Antennas and Propagation, vol. AP-21, No. 1, Jan. 1973, pp.124-126.

- [131] T.E. Baldwin and A.T. Adams, "Near Field Prediction for Antenna Arrays", 1971 IEEE-EMC Symposium Record, July 1971, pp. 137-142.
- [132] A.T. Adams and T.E. Baldwin, "Near Field Analysis by Matrix Methods", Proc. of the 1972 Purdue Symposium on Electromagnetic Hazards, Pollution, and Environmental Quality, May 1972, pp. 61-73.
- [133] A.T. Adams, T.E. Baldwin and Daniel Warren, "Electric and Magnetic Fields of Arrays of Straight Skewed Wires", 1972 IEEE-EMC Symposium Record, July 1972, pp. 337-342.
- [134] T.E. Baldwin, Jr., "Thin Wire Analysis Program (TWAP) User Manual" RADC TR-73-217, vol. III, Oct. 1973.
- [135] K. Siarkiewicz and A.T. Adams, "Analysis and Prediction of Coupling between Co-located Antennas", 1972 IEEE-EMC Symposium Record, July 1972, pp. 315-320.
- [136] K. Siarkiewicz, A.T. Adams, and D.E. Warren, "Prediction of Near Field Coupling for Straight-wire Antennas", 1973 IEEE-EMC Symposium Record, June 1973, pp. 226-240.
- [137] K. Siarkiewicz, "Antenna Near Field Coupling" NATO Allied Radio Frequency Agency 2nd Biennial Symposium, Brussels, Belgium, Nov. 26-28, 1973.
- [138] C.W. Harrison, C.D. Taylor, E.A. Aronson, and M.L. Houston, "An Accurate Representation of the Complete Electromagnetic Field in the Vicinity of a Base-driven Cylindrical Monopole", IEEE Trans. on Electromagnetic Compatibility, vol. EMC-12, Nov. 1970, pp. 164-173.
- [139] R.W.P. King and T.T. Wu, "The Electric Field Very Near a Driven Cylindrical Antenna", Radio Science, vol. 1, March 1966, pp. 353-359.
- [140] R.W.P. King and T.T. Wu, "Currents, Charges and Near Fields of Cylindrical Receiving and Scattering Antennas", IEEE Trans. on Antennas and Propagation, vol. AP-13, Nov. 1965, pp. 978-979.
- [141] R.W.P. King and T.T. Wu, "Electromagnetic Field Near a Parasitic Cylindrical Antenna", Proc. IEE (London), vol. 113, 1966, pp. 35-40.
- [142] J. Galejs, "Near Fields of a Cylindrical Antenna", Radio Science, vol. 3, Sept. 1968, pp. 893-901.
- [143] T.E. Baldwin, Jr., "Thin-wire Antenna Analysis Computer Codes Compared with Measured Data", RADC-TR-73-217, vol. V, July 1974.
- [144] E. Mendelovicz and A.T. Adams, "Feedline Interference with Dipole Performance", 1972 International IEEE/G-AP Symposium Digest, Williamsburg, Virginia, December 1972, pp. 73-76.

- [145] Donald A. Priebe and Robert H. Kyle, "ATLAB - A Computer Program for the Analysis of Transmission Lines with Arbitrary Boundaries", G.E.T.I.S. R-70-ELS-6 of Nov. 1970.
- [146] A.T. Adams and A. Farrar, "Matrix Methods for Static Microstrip Applications", RADC-TR-73-217, vol. VI.
- [147] A.T. Adams, C. Bruce Varnado, and Daniel E. Warren, "Aperture Coupling by Matrix Methods", 1973 IEEE-EMC Symposium Record, June 1973, pp. 226-240.
- [148] J.L. Lin, W.L. Curtis and M.C. Vincent, "On the Field Distribution of an Aperture", IEEE Trans. on Antennas and Propagation, vol. AP-22, No. 3, May 1974, pp. 467-471.
- [149] R.F. Harrington, Time-Harmonic Electromagnetic Fields, McGraw-Hill, New York, 1961, section 5.9.
- [150] J.C. Clements, "Computation of the Capacitance Matrix for Dielectric-Coated Wires", M.S. Thesis, University of Kentucky, April 1973.
- [151] J. Perini and M.H. Idselis, "Radiation Pattern Synthesis for Broadcast Antennas", IEEE Trans. on Broadcasting, vol. BC-18, No. 3, September 1973, pp. 53-62.

MISSION  
of  
*Rome Air Development Center*

RADC is the principal AFSC organization charged with planning and executing the USAF exploratory and advanced development programs for electromagnetic intelligence techniques, reliability and compatibility techniques for electronic systems, electromagnetic transmission and reception, ground based surveillance, ground communications, information displays and information processing. This Center provides technical or management assistance in support of studies, analyses, development planning activities, acquisition, test, evaluation, modification, and operation of aerospace systems and related equipment.

Source AFSCR 23-56, 11 May 70